The role of Transient Receptor Potential Melastanin 7 (TRPM7) channels in epilepsy

Aytakin Khalil

Department of Clinical and Experimental Epilepsy

Institute of Neurology, UCL

Queen Square, London, WC1N 3BG

A thesis submitted to University College London for the degree of

Doctor of Philosophy

September 2015

Declaration

I, Aytakin Khalil confirm that the work presented here is my original research and was conducted only by me.

The project and study design was agreed with Professor Matthew Walker. Data collection, Data analysis and writing up were conducted by me with guidance from Professor Matthew Walker.

Abstract

Drug-resistance occurs in about 30% of patients with epilepsy and is associated with increased mortality and morbidity and cognitive decline. Furthermore, present AEDs treat the symptom (seizures) but do not modify the disease or associated cognitive comorbidities and do not prevent the development of epilepsy following brain injury. Transient receptor potential melastanin 7 (TRPM7) is a ubiquitous, stress-activated channel, that plays essential roles in cell viability and Mg^{2+} homeostasis, and opening of the channel depolarises neurons. Inhibiting TRPM7 channels is neuroprotective in brain ischemia. Conditions that activate the channel, such as low intracellular Mg^{2+} concentrations, oxidative stress, and decreased intracellular pH occur during seizure activity.

This thesis aimed to assess the role of blocking TRPM7 channel in preventing: 1) seizure occurrence, 2) seizure induced cell death, 3) the development of epilepsy after brain damage induced by status epilepticus (SE) and 4) cognitive comorbidity in epilepsy.

The low Mg^{2+} and pentylenetetrazol (PTZ) *in vitro* seizure models were used in entorhinal-hippocampal slices to assess the effect of TRPM7 inhibitors carvacrol and Waxiencin A (a recent more specific inhibitor) on seizure-like activity. The perforant path stimulation (PPS) model of epilepsy was used to investigate the effect of carvacrol on status epilepticus (SE), chronic epilepsy and memory dysfunction in epilepsy *in vivo*.

TRPM7 inhibitors abolished (carvacrol) or significantly reduced (Waxiencin A) seizure-like activity *in vitro* indicating that TRPM7 channels contribute to seizure generation. Status epilepticus resulted in cell loss in CA1 area and hilus in the PPS model of epilepsy, and this was rescued by treatment with carvacrol, suggesting that TRPM7 channels contribute to status epilepticus induced cell death. Blocking TRPM7 channels *in vivo* prevented the occurrence of recurrent SE and early seizures following induced SE but did not affect chronic seizures. Lastly, TRPM7 channel inhibition by carvacrol significantly prevented memory impairment as measured by rewarded T-maze alternation in chronic epilepsy.

These findings suggest that *in vitro* seizure-like activity and the sequelae of status epilepticus and chronic epilepsy such as neuronal death and memory dysfunction can be effectively treated by blocking TRPM7 channels.

Table of Contents

List of figures

List of tables

Abbrevations

2-APB - 2-aminoethyl-diphenylborinate

4-AP - 4-Aminopyridine

ACSF - Artificial cerebrospinal fluid

ACSF – artificial cerebro-spinal fluid

AEDs - antiepileptic drugs

ANOVA - analysis of variance

ATP - adenosine triphosphate

BSA - Bovine Serum Albumin

CA -Cornu Ammonis’

cAMP - adenosine 3,5 -monophosphate

CAP - compound action potentials

CNS - central nervous system

CRAC - calcium release activated channels

DAPI -4',6-diamidino-2-phenylindole

DG- dentate gyrus

EEG - electroencephalogram

EEG – electroencephalography

fEPSP - field excitatory postsynaptic potential

GABA-γ-aminobutyric acid

Gd^{3+} - gadolinium

GTCS - generalised tonic-clonic seizures

HICAP cells - hilar commissural-associational pathway related cells

HIPP cells - hilar perforant path-associated cell

HVA - high voltage activated

I.P. - intraperitoneal

IQR - interquartile range

La^{3+} - Lanthanum

LTRPC7 - long TRP channel 7

LWDAQ - Long-wire-data acquisition

MES - maximal electroshock seizures

MRI - magnetic resonance imaging

MTLE - mesial temporal lobe epilepsy

NM - Nafamostat mesilate

NMDA - N-methyl-D-aspartate

Normal Goat Serum (NGS

PBS - phosphate-buffer saline

PFA - paraformaldehyde

PIP2 - Phosphatidylinositol 4,5-bisphosphate

PKA - protein kinase A

PPS - perforant path stimulation

PTZ - pentylenetetrazol

ROS - reactive oxygen species

SD - standard deviation

SE - Status epilepticus

SEM - standard error of the mean

SSSE - self sustained status epilepticus

TLE - Temporal lobe epilepsy

TLE- temporal lobe epilepsy

TRP - Transient receptor potential

TRPM7 - Transient receptor potential melastanin 7

Acknowledgment

I would like to dedicate this thesis to my family: to memory of my father and to my mother who always encouraged me to follow my dreams, provided me the best education, taught me to be the best in whatever career path I choose, to be a good person, to see positive sides in every difficult situation in life and to be always thankful; to my brother, who is the best brother in the world and the best friend, for his help, support and encouragement in every success in my life; and of course to my daughter, for spiritual support, for her patience and love. I am thankful to them for who I am today and my little contribution to science was possible thanks to their immense encouragement, support and love.

I would like to express my deepest gratitude to my primary supervisor Professor Matthew Walker, for his immense support and guidance in every step throughout my PhD.

I am grateful to Dr Rob Wykes for the guidance with all in vivo experiments; to Dr Elodie Chabrol for giving me hand with some animal experiments; to Dr Dennis Kaetzel for explaining and providing behavioural protocol and to Dr Marife Cano-Jaimez for introducing me to immunostaining techniques.

I would like to thank Dr Stjepana Kovac for her scientific advice and guidance and for spiritual support; Dr Yamina Bakiri for her spiritual support and for always being there for me. I am also thankful to my PhD fellows, Sophie, Amy and Ramona for their warm company, friendship and support. I am thankful to everyone in the lab who has been helpful and supportive during these years. I am thankful to people in my life, who made me the better person, the better scientist.

And of course, I am very grateful to Azerbaijan Ministry of Education for fully funding my studies for four years.

Chapter 1. Introduction

1. Overview

Epilepsy affects over 50 million people worldwide and is the commonest serious neurological disorder, (Neligan et al., 2012) and second in terms of disease burden after stroke. Epilepsy is associated with a high mortality and morbidity, amongst which are psychiatric comorbidity and cognitive decline. Seizure-induced cell loss may contribute to the latter. Moreover, epilepsy significantly affects patients' quality of life. The disease can occur at any age, however, higher prevalence is reported in young children and in the elderly. The lowest incidence was reported between ages of 20 and 40; the incidence then rises significantly after 50 years (Rugg-Gunn and Smalls, 2013). In respect to seizure origin, epilepsy is broadly divided into generalised and partial (focal) epilepsy. Although there are many drugs available that control the symptoms - seizures - none of the presently available drugs modify the course of the disease (Walker et al., 2002). Idiopathic generalised epilepsy syndromes which compromise about 92% of all generalised epilepsies have better treatment outcome, the majority of patients recover fully , whereas patients with symptomatic focal epilepsy respond poorly to treatment and temporal lobe epilepsy was the most drug resistant (Semah et al., 1998). Up to 60% of all active epilepsies in the general population comprise partial epilepsies and nearly 60-70% of these are of temporal lobe origin (Frampton, 2015; Téllez-Zenteno et al., 2011). Identifying new targets for better seizure control, preventing epileptogenesis and neuronal loss are questions that need to be urgently addressed. This thesis is concerned with disease modification in temporal lobe epilepsy following status epilepticus.

2. Temporal lobe epilepsy

Temporal lobe epilepsy (TLE) is divided into mesial and neocortical TLE, however, spread from one to another is common. Among partial epilepsies mesial temporal lobe epilepsy (MTLE) comprises the majority and is the most drug-resistant type. Cognitive involvement is present in majority of cases, ranging from mood changes, memory impairment to psychosis.

Seizures in TLE can be simple partial or complex partial. The former can manifest as aura without objective signs. Typical MTLE complex partial seizures evolve slowly and last longer than other partial seizures (2-10 min). They have three stages: aura, blank spells (motor arrest) and automatism. Postictal confusion and headache are common (Rugg-Gunn and Smalls, 2013). While the commonest causes of neocortical TLE are malformations of cortical development and tumours such as glioma, cavernous angioma, hamartoma etc., (Tassi et al., 2009), the most common pathology found in patients with MTLE is hippocampal sclerosis.

2.1 Psychiatric comorbidity and cognitive decline in epilepsy

Epilepsy is associated with an increased prevalence of mental health disorders. Psychiatric comorbidity varies between 19 and 80% in different patient groups and epilepsy syndromes; it is most common in TLE (80%) (Swinkels et al., 2005). Increased rates of major depression, anxiety and suicidal ideation were reported in patients with epilepsy (Agrawal and Govender, 2011). Furthermore, memory difficulties have been frequently reported by patients. Abnormal mood such as depressed affect, aggressive behaviour as well as manic symptoms (grandiose delusions, religiosity) occur often post-ictally (Nadkarni et al., 2007). Several potential risk factors that can contribute to the development of psychiatric problems in epilepsy have been identified, including seizure type,

age of onset, duration, laterality and others iatrogenic factors (eg antiepileptic drugs, surgery) (Agrawal and Govender, 2011).

The prevalence of psychosis in epilepsy is also high and occurs more commonly in TLE (Devinsky, 2003). Ictal psychosis is rare and comprises visual or auditory hallucinations together with affective changes, whereas postictal psychosis has clinical features similar to schizophrenia-like psychoses and is present in 2-9% of epilepsy patients (Elliott et al., 2009; Nadkarni et al., 2007). This is characterised by hallucinations, delusions, and gross abnormalities of behaviour lasting up to seven days after a seizure (Nadkarni et al., 2007).

Chronic interictal psychosis also occurs more commonly in TLE (Elliott et al., 2009). The interictal psychosis resembles primary schizophrenia; persecutory auditory hallucinations are common and religiosity also can occur (Nadkarni et al. 2007; Elliott et al. 2009). Short recurrent or sometimes continuous subclinical electrographic activity during psychotic symptoms has been reported. Therefore, it is unclear whether the psychosis is caused by such activity or is a result of functional change provoked by such activity (Elliott et al., 2009).

Patients with epilepsy ranked cognitive and memory problem as being their primary concern (Fisher et al., 2000; Thompson and Corcoran, 1992). This is particularly worse in TLE. Short term memory loss is well known in epilepsy. The memory impairment correlates positively with the degree of brain damage in humans demonstrated with histology (Rausch and Babb, 1993; Pauli et al., 2006) and atrophy observed in MRI (Lencz et al., 1992). Moreover, age of onset, seizure frequency and lifetime number of seizures have also been shown to play a role (Butler and Zeman, 2008). The site of seizure focus determines the type of memory loss i.e. left TLE causes predominantly verbal memory loss, whereas non-verbal memory impairment is more prominent in right TLE (Hermann et al., 1997; Gleissner et al., 1998; Baxendale et al., 1998).

However, memory problems reported by patients are often undetectable by objective memory tests, which do not always correlate with the severity of subjective complains. Three other distinct types of memory impairment have been described in epilepsy:

- *transient epileptic amnesia*, which is itself the primary manifestation of seizures, is a form of TLE.
- *accelerated long-term forgetting*, when memory for recently learned information vanish over days to weeks
- *remote memory impairment*, which is a loss of memory for events of the distant past (Butler and Zeman, 2008).

2.2 Pathogenesis of epilepsy

Epilepsy syndromes are divided into two broad categories: idiopathic and symptomatic. Different factors contribute to the aetiology of various epilepsy types. Genetic components possibly play a role in all epilepsy syndromes (Ottman et al., 1996). A strong genetic contribution has been shown in idiopathic generalised epilepsies (Johnson et al. 2001), whereas the aetiology of acquired partial epilepsies (amongst the commonest epilepsy syndromes) is often attributed to a brain insult. The development of epilepsy following brain damage is termed epileptogenesis. Any major brain disorder or injuries that disrupt neuronal connectivity may initiate epileptogenesis (Theodore and Porter, 1995).

A cascade of structural and functional changes occurring in the brain following brain insults such as head trauma, cerebrovascular disease, brain tumours, neurosurgical procedures, neurodegenerative conditions, status epilepticus (SE), febrile convulsions may lead to the development of epilepsy in susceptible individuals (Walker et al. 2002; Löscher, 2012). About 40% of epilepsy result from such insults (Barker-Haliski et al., 2015). Seizures

themselves can then further cause morphological and functional changes contributing to progression in some epilepsy syndromes (Walker et al., 2002).

The latent period between insult and development of epilepsy can vary from days to over 10 years; such a long latent period could be explained by a second hit hypothesis in which the initial insult leads to a lowering of seizure threshold and a second, later insult is necessary for the development of epilepsy (Walker et al., 2002).This time interval offers a potential opportunity for the prevention of epileptogenesis and subsequent unprovoked seizures (Löscher, 2012).

Pathways of epileptogenesis are not well understood, however, there is growing evidence for the involvement of certain mechanisms. Structural and cellular changes that have been implicated in epileptogenesis include axonal regeneration within hippocampal dentate gyrus with sprouting of excitatory fibres, dendritic remodelling, neurogenesis, gliosis, and neuronal cell death. Moreover, synaptic modifications, and alterations in neuronal excitability secondary to acquired channelopathies have been described. Synaptic alterations include downregulation of GABAergic signalling, and upregulation of N-methyl-D-aspartate (NMDA) receptors (Pitkänen and Lukasiuk, 2009). All these changes lead to increased excitability of neurons and neuronal networks.

Hippocampal sclerosis is the commonest pathology in TLE, which is the most common type of drug-resistant epilepsy in adults (Manford et al., 1992). This thesis is solely concerned with a TLE model of epilepsy and status epilepticus induced hippocampal damage, and so I will first review here hippocampal structure and pathology. Examples will be related primarily to TLE animal model, in particular the perforant path stimulation (PPS) model.

2.3 Hippocampal formation

2.3.1 Overview

The hippocampus, located in the medial temporal lobe, forms a part of the limbic system (**Figure 1.1**). It is a phylogenically preserved structure that captivated by its physical appearance anatomist from the time of ancient Egypt and the current name derived from the Latin for seahorse: hippocampus. The hippocampus (*hippocampus proper*), and nearby structures - *entorhinal cortex, subiculum, presubiculum, parasubiculum* and the *dentate gyrus* (DG) constitute the *hippocampal formation*. (Spiers, 2012). The hippocampal formation plays a central role in short term memory and spatial navigation. It is the most vulnerable structure to seizures, as well as the most common site of drug-resistant seizures.

2.3.2 Cellular anatomy of the hippocampus

The primary excitatory cells of the hippocampus are pyramidal cells - multipolar neurons: their dendrites extend in both directions from the cell body, forming apical and basal dendrites (**Figure 1.3**) (Shepherd, 2004). The pyramidal cell layer of the hippocampus proper has three main 'Cornu Ammonis' (CA) subfields: CA1, CA2 and CA3. CA translates as 'Amun's horns', named after the ancient Egyptian god whose symbol was a ram's horn. Unlike the neocortex where pyramidal cells form multiple layers, in CA regions pyramidal cells are aligned in a densely packed single cell layer (Spiers, 2012). These regions receive different inputs: CA3 receives projections from the axons of dentate granule cells - mossy fibers. CA2 is a small area between CA1 and CA3: the cell bodies resemble CA3 cells however do not receive mossy fiber input. CA2 region is also distinct in that it is more resistant to epileptic cell death (Shepherd, 2004).

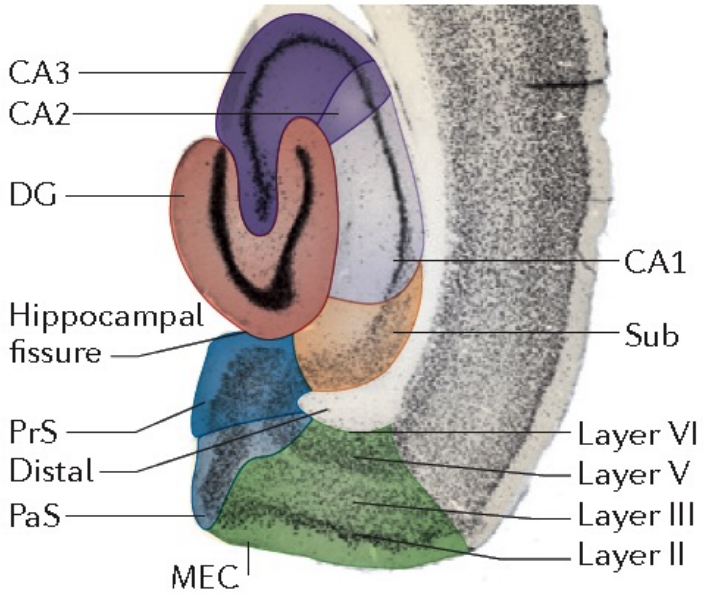

Figure 1.1. Hippocampal formation and parahippocampal region.

The image is the illustration of right hemisphere horizontal section of a rat brain. Principal hippocampal and parahippocampal areas are shown with colour code for the individual subregion: the dentate gyrus (DG), CA1–CA3, the subiculum (Sub), the medial entorhinal cortex (MEC), presubiculum (PrS) and parasubiculum (PaS). The figure was taken from (Moser et al., 2014).

Dentate gyrus does not have pyramidal cells, but consists of densely packed small granule cells (Spiers, 2012). The dentate gyrus has three layers: the *molecular layer (outer and inner)*, the main *granule cell layer* (principal cell bodies), and diffuse *polymorphic cell layer* – hilus. The *Molecular layer* is relatively acellular, contains mainly the dendrites of the granule cells and the perforant path fibers projecting from the entorhinal cortex. Also, a small number of interneurons are present in the molecular layer as well as variety of extrinsic input fibers. The *granule cell layer* is the principal cell layer, densely packed with granule cells (excitatory cells). Basket cells, the most studied inhibitory interneurons in dentate gyrus, are located typically just within the granule cell layer at the border with the polymorphic layer. *In the polymorphic cell layer*, the principal cell type is the *mossy cells* (excitatory cells). In addition, this layer contains two main interneurons types (**Figure 1.2**): 1) A long-spined multipolar *hilar perforant path-associated cell* (HIPP cells), their axons extend into outer molecular layer i.e., the perforant path zone (Amaral et al., 2007). They receive input from granule cells, contributing to feedback inhibition (Savanthrapadian et al., 2014). HIPP cells are atypical interneurons. 2) Multipolar cells with thin, aspiny dendrites, hilar commissural-associational pathway related cells (HICAP cells) (Amaral et al., 2007). HICAP and basket cells receive input from commissural associational path, the perforant path in molecular layer and the granule cells; they mediate feedback and feedforward inhibition (Savanthrapadian et al., 2014). Axons of HICAP cells extend through the granule cell layer and branch profusely in the inner molecular layer (Amaral et al., 2007).

Mossy fibers originating from dentate granule cells form abundant synaptic connections collaterals with hilar interneurons that project back to the granule cells (Moser et al., 2014). Granule cells do not make direct excitatory connections between each other.

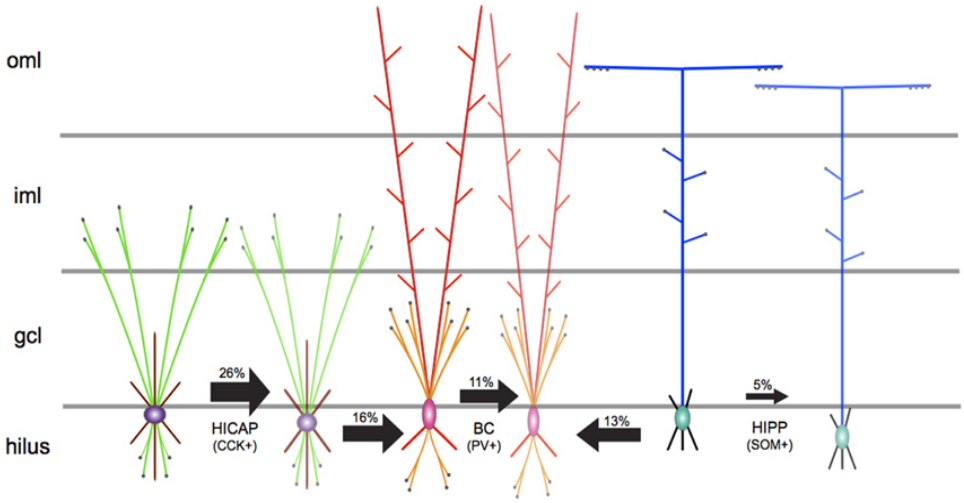

Figure 1.2 Schematic illustration of principal GABAergic interneuron microcircuit in dentate gyrus

(Ramaswamy, 2015). Grey lines indicate layer borders: oml, outer molecular layer; iml, inner molecular layer; gcl, granule cell layer. Axons, soma and dendrites of the cells indicated by distinct colour: axons) green –HICAP cell, orange – basket cells (BC), blue- HIPP cells; soma) purple –HICAP, pink –BC, green - HIPP interneurons; dendrites) maroon –HICAP, red –BC, black –HIPP cells. Arrows depict unidirectional inhibitory synaptic connections between interneurons; the connection probability shown in %. The figure was taken from (Ramaswamy, 2015).

2.3.3 Intra and Extra Hippocampal connections

The unidirectional excitatory hippocampal pathway connecting its part to each other was termed trisynaptic circuit (**Figure 1.3**). Glutamate is the main neurotransmitters in these pathways. The entorhinal cortex (EC) is the starting point of the circuit, as it is where the majority of the sensory input enters the hippocampus: it has a central role in connecting other brain regions with the hippocampus (Shepherd, 2004).

The entorhinal cortex forms two pathways to connect with the hippocampus (Spiers, 2012). The *perforant pathway* starts from layer II (stellate cells) of the entorhinal cortex, passes through subiculum (perforates) and projects to the molecular layer of the DG and stratum lacunosum-moleculare of the CA3 and CA2 areas (Shepherd, 2004; Moser et al., 2014). Neurons from layer III of the entorhinal cortex project to CA1 via subiculum bypassing dentate gyrus and CA3 forming the *temporoammonic pathway* (Spiers, 2012). Dentate gyrus granule cells send input to CA3 proximal dendrites via mossy fibers; projections from CA3 to CA1 are called *Schaffer collaterals*. *Commissural fibers* from the contralateral hippocampus form connections from one hippocampus to the other.

The hippocampus sends output to the entorhinal cortex via subiculum. Pathways from the CA1 and the subiculum end in the layer V of the entorhinal cortex from where the output passes to the neocortex and other brain regions (Moser et al., 2014).

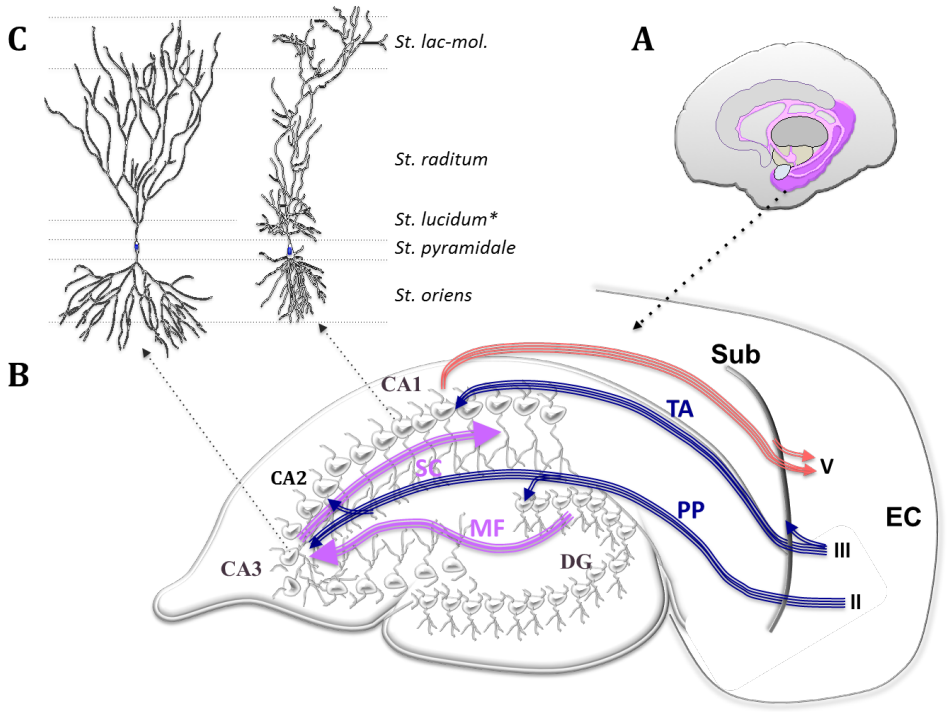

Figure 1.3 Intra and Extra Hippocampal connections.

A – Illustrates the position of the hippocampus in the brain. B – Hippocampal formation and four main intra and extra hippocampal connections. Enthorhinal cortex (EC) sends projections via two pathways, perforant path (PP) from layer II to DG and CA2/CA3 and temporoammonic (TA) pathway from layer III to the subiculum and CA1. Mossy fibers (MF) project from DG selectively to CA3. Projections from CA3 to CA1 form Schaffer collaterals (SC). Pathways from CA1 and subiculum project to layers V of EC. C – pyramidal CA1 and CA3 cells, * -st. lucidum identified in CA3, but not in CA1. Information adopted the following sources (Spiers, 2012; Ojo et al., 2013; Moser et al., 2014)

2.3.4 Lamellar structure

According to the original hypothesis of the laminar hippocampal organisation excitatory activity travels from the entorhinal cortex and through the hippocampus via a trisynaptic circuit lying within a series of parallel hippocampal slices or lamellae (Andersen et al., 1971). In this way, it was envisaged that temporal lobe interactions between the entorhinal cortex and the hippocampus were organized topographically, and that lamellae might operate independently, permitting a relatively simple structure to mediate complex behaviours. Each specific layer of the entorhinal cortex projects fibers to a restricted segment of the hippocampus (Sloviter and Lømo, 2012).

3. Cell death in status epilepticus

3.1 Status Epilepticus

Status epilepticus (SE) is an extreme manifestation of epilepsy or an expression of an acute life-threatening brain disorder such as anoxic brain damage, encephalitis, or trauma. SE is conventionally defined as a single clinical seizure lasting > 30 minute or repetitive seizures lasting < 30 minutes without full recovery of consciousness between seizures (International League Against Epilepsy, 1993). However, due to the high risk of brain damage from prolonged seizures and risk to life, a practical definition was suggested: SE is defined as continuous clinical and/or electrographic seizure activity or recurrent seizure activity without recovery between seizures lasting over 5 minute (Brophy et al., 2012) and requires immediate treatment. The majority of generalized tonic-clonic seizure (GTCS) typically last less than 2-3 minutes (Trinka et al., 2012). SE is one of the most common emergencies in neurology;

the annual incidence of SE is 10-41 per 100,000. Mortality rates associated with SE can reach 20%. Over 50% of patients presenting with SE have no history of previous seizures or epilepsy (Trinka et al., 2012). SE is broadly divided into two types, convulsive and non-convulsive SE. SE can lead to irreversible damage to neurons and alterations in synaptic network.

Underlying mechanisms that lead to prolonged seizures or SE are not well understood. It has been suggested that SE could be a result of misbalance in excitation and inhibition i.e. increase in excitatory and exhaustion of inhibitory processes. Modulation of γ-aminobutyric acid (GABA) receptor function through various mechanisms that decreases GABA function has been suggested in a number of studies. Alterations in other inhibitory pathways have also been proposed (Walker, 2009). The trisynaptic excitatory circuit in the hippocampus that creates a closed loop could be responsible for the development and persistence of self-sustained SE (Andersen et al., 1966).

Prolonged seizures can damage neuronal cells, leading to cell loss. Cell death following status epilepticus (SE) is observed in human epilepsies as well as animal models. One of the challenging questions however is whether cell death contributes to epileptogenesis or is an antiepileptogenetic process (Walker, 2007). Nevertheless, it has been shown that cell damage is involved in other pathological processes associated with epilepsy such as cognitive impairment and neurological deficit (Walker et al., 2002) affecting patients' quality of life. Below I will review patterns and mechanisms of cell death in TLE model.

3.2 Patterns of cell death

3.2.1 Cell loss areas

In 'classical' hippocampal sclerosis selective loss of pyramidal neurons in CA1 and dentate hilus region was reported, however, cell loss sometimes can only be confined to hilar region (Matthew et al., 2006). The hilus is the most vulnerable area

to cell death in TLE; cell death initially occurs in this area and the damage is more extensive. Loss of both excitatory mossy cells and inhibitory interneurons in this area was observed in TLE in humans and animal models (Schwarcz and Witter, 2002). In perforant path stimulation (PPS) model, hilar cells, CA1 and CA3 were the most damaged areas whereas CA2 and dentate granule cells were relatively spared (Sloviter, 1983). However, other studies also suggested that CA1 and CA4 (or CA3c) were the most vulnerable to cell death, whereas CA3 and dentate gyrus cells were less affected and a big variation was seen in CA2 (Pauli et al., 2006). Damage to the same areas was seen during autopsy of humans with TLE and from surgical specimens obtained from patients with TLE (Thom, 2014). With 2 hour continuous perforant path stimulation lesions (clear, round spaces) were also observed in extrahippocampal areas: the subiculum, lateral septum, dorso-lateral thalamus and amygdala**.** However, with intermittent 24 h stimulation damage was confined to hippocampus only (Sloviter, 1983). High vulnerability of hilar cells to damage was proposed to be due to highly convergent input from granule cells and release of high concentrations of excitatory neurotransmitters from large mossy fiber terminals (Sloviter and Damiano, 1981).

Both loss of principal neurons and interneurons can be observed in hippocampal sclerosis. The pattern of loss and cell types that are most vulnerable may differ among epilepsy models, species and brain areas (Houser, 2014). Loss of GABAergic interneurons expressing neuropeptide Y and somatostatin that are abundant in the hilar region were observed in hippocampal sclerosis. However, it was speculated that these neurons are not specifically targeted and are lost in the proportion to the overall cell loss (Matthew et al., 2006). Nevertheless, loss of somatatin-containing neurons in hilar region is the most consistent and very well established finding in epileptic brains; this was observed in almost all animal epilepsy models as well as in human TLE. Similarly, in stratum oriens of CA1 region somatastatin cells are also commonly affected cells. Loss of pavalbumin expressing neurons in hilar dentate has also been described in several animal epilepsy models, both basket cells and axo-axonic cells were affected. However, in the same animals the loss of parvalbumin-expressing neurons in the dentate gyrus was generally less severe than that of somatostatin interneurons (Houser, 2014).

Granule cells are resistant to cell damage relative to other excitatory cell types (Matthew et al., 2006).

3.2.2 Laterality of cell loss in relation to the damage site

Some studies have shown similar damage ipsi- and contralateral to the insult (Gorter et al., 2003), others have shown more severe damage on the ipsilateral side (Sloviter, 1983) and some others suggested complete sparing of the contralateral side (Kienzler et al., 2006). Sloviter et al. suggested that PPS on a side of the brain evoking unilateral seizures caused only ipsilateral damage (with low-frequency stimulation 2-2.5 Hz), whereas higher frequency stimulation (20 Hz) that caused bilateral discharges led to damage in both hippocampi (Sloviter, 1983). In contrast, a study in mice showed no damage in contralateral hippocampus with 20 Hz stimulation (Kienzler et al., 2006). Gorter et al. reported that in PPS laterality of the damage was linked to the severity of the disease; progressive epilepsy was associated with similar damage bilaterally whereas in non-progressive disease cell reduction on the side contralateral to the damage was less pronounced (Gorter et al., 2003). Evidence from human magnetic resonance imaging (MRI) studies has also shown that on the side of the seizure focus hippocampal as well as temporal lobe shrinkage was significant compared to the contralateral side (Lencz et al., 1992). The ipsilateral hippocampal damage caused by PPS was also explained by limited anatomical connection between the two hippocampi and temporal lobes (Sloviter et al. 1983).

3.3 Duration of SE and cell death

The degree of cell damage also depends on the duration of status epilepticus. Longer initial stimulation in animal models as well as longer self-sustaining status epilepticus (SSSE), i.e. periodic epileptiform discharges (1-2 Hz) after stimulation, correlated positively with more severe hilar cell loss (Gorter et al., 2003; Norwood et al., 2011). A study published by Norwood et al. showed that

35 min stimulation did not lead to hippocampal cell damage, whereas 40 min stimulation led to hilar cell loss but preserved CA3 area. Longer duration of stimulation, 60 min and more resulted in an additional cell loss in CA3 area. This challenges the hypothesis that an individual brief seizure can cause neuronal damage, as up to 40 min stimulation did not lead to neuronal loss in the hippocampus (Norwood 2011). Cell death is also determined by the severity of the initial stimulation in animal models.

The highest degree of cell death was observed in the first 1-2 days following SE and continued until one week but no further cell death was seen after that. TUNEL staining of the hippocampus that identifies apoptotic and necrotic neurons, showed significant increase in necrotic neurons at day 1 after induced SE and with a peak at 1 week followed by a sharp decrease necrotic cell death afterwards. This highlights the need to stop SE early in the disease course. Therefore, neuroprotective drugs can be useful in the first week following SE and might not be effective in the chronic phase (Gorter et al., 2003).

3.4 Mechanisms of cell death

Neuronal death in epilepsy is related to excessive neuronal firing such as occurs in status epilepticus (Pitkänen et al., 2002). Seizure related brain damage was associated with pre-synaptic release of excitatory neurotransmitters; this leads to the post-synaptic changes causing dendritic swelling and cell death. These changes were also seen in epileptic brain tissue removed during surgery from patients with pharmacoresistant epilepsy (Sloviter, 1983).

Excessive neuronal firing requires increased energy substrates to maintain ionic balance (Kovac et al., 2012). Energy depletion leads to excess glutamate release which in turn causes Ca^{2+} influx into cells, as well as release of Ca^{2+} from intracellular stores. This triggers a Ca^{2+}-dependent cascade of intracellular processes that results in the production of free radicals (Walker et al., 2002).

Free radical species generating oxidative stress contribute to mitochondrial dysfunction and cell death (Menon et al., 2012).

3.5 Consequences of cell death and development of chronic epilepsy

Prolonged seizures or SE that cause cell death in animal models promote epileptogenesis, leading to the conception that cell death is an epileptogenetic process. Although some studies have suggested that neuronal loss is not necessary for the development of chronic epilepsy lack of neuronal loss is not easy to prove. Conventionally, the link between cell loss and epileptogenesis was explained by recapitulation of the development hypothesis - when input from dying cells is lost this induces axonal sprouting and synaptic reorganisation in the hippocampus, termed mossy fiber sprouting (Dingledine et al., 2014).

Mossy fiber sprouting is one of the most prominent changes observed in the hippocampus during epileptogenesis in mesial TLE and involves axonal regeneration in the dentate gyrus (Pun et al., 2012). The entorhinal cortex and perforant path as the main source of excitatory input to the hippocampus, have been implicated in mesial TLE. Dentate granule cells play a role of a gatekeeper in this pathway, modifying input to the hippocampus (Scimemi et al., 2006). Due to sprouting of granule cell mossy fibre axons into the dentate molecular layer, this function of the DG is impaired during epileptogenesis, leading to recurrent excitatory circuits. Moreover, neurogenesis also occurs in the hippocampus during epileptogenesis and newly born granule cells form anomalous basal dendrites and are ectopically placed in the dentate gyrus (Pun et al., 2012). Increased release probability of glutamate by N-methyl-D-aspartate (NMDA) receptors leading to increased neurotransmission at the perforant path to dentate granule cell is a common mechanism that enhances the epileptogenic process. Increased cross talk between medial and lateral

perforant path was found in epileptic tissue, which also increases excitability and reduces the specificity of perforant path which in turn impairs hippocampal function. These processes may contribute to lowering of the seizure threshold (Scimemi et al., 2006).

A new hypothesis of cell death related epileptogenesis, a neuronal death pathway, has been suggested. According to this hypothesis epileptogenesis after cell death occurs due to activation of the biochemical pathways leading to programmed neurodegeneration, rather than due to neuronal loss itself. Various cell death pathways have been described. Therefore, even cell death per se is not the factor that is leading to epileptogenesis; the cell death pathway activates molecular mechanisms that may be leading to it. Interestingly, preventing cell death does not necessarily prevent seizure occurrence or their severity (Dingledine et al., 2014).

Brain inflammation is one such pathways that can be triggered by brain injury and excitotoxicity and can contribute to epileptogenesis. A plethora of evidence suggests the key role of brain inflammation in the pathology of various types of drug resistant epilepsies, and that inflammation can change seizure threshold significantly in susceptible brain regions. Activation of the interleukin-1 Receptor/Toll-like receptor, the Transforming Growth Factor (TGF)-β signalling and the Cyclooxygenase-2 (COX-2) pathway are the main inflammatory pathways described in epileptic brain. These molecules are involved in processes associated with epileptogenesis such as neurodegeneration, neurogenesis, synaptic plasticity and regulation of blood brain barrier permeability. Immune responses in the brain to injury or excitotoxicity are mediated mainly via microglia and astrocytes. However, neurons are also involved in immune responses, for instance, via release of prostaglandins. Chronic inflammatory processes that present in the brain during epileptogenesis mediated by cytokines and chemokines; astrogliosis and microglia activation, leukocytosis from blood are involved in particular in brain injury models. Inflammatory processes were observed in chronic epilepsy as

well as during the period before development of spontaneous seizures suggesting contribution of inflammation to seizure generation and the development of epilepsy. However, their direct role in the development of epilepsy is yet unclear (Vezzani et al., 2013).

3.6 Chronic seizures and cell death

Another unanswered question in epilepsy research is whether chronic epilepsy i.e. recurrent spontaneous seizures induce cell death or not. Some studies have suggested occurrence of neuronal loss in chronic epilepsy. However, these studies were done in the kindling model where seizure stage five with secondary generalisation occur, therefore it was suggested that cell death may be due to secondary hypoxic cell death (Gorter et al., 2003). There is some evidence to suggest that cell death depends on the type of seizures. For example, it was suggested that short seizures such as absence seizures lasting 5-10 second do not cause cell loss (Dingledine et al., 2014). However, case reports have described the development of hippocampal sclerosis after several GTCS or partial seizures (Briellmann et al., 2001; Worrell et al., 2002). However, in one of these cases the patient sustained a minor head injury prior to the onset of GTSC seizures, in the other case acute thrombosis of an ipsilateral parietal venous angioma preceded new-onset partial seizures. Undoubtedly, prolonged and repetitive seizures that define SE cause extensive cell death. Cell death in a model of SE has been described to relate to initial SE and not to seizure frequency in chronic phase if seizures are short (<2 min) (Gorter et al., 2003). Neuropathological analysis of hippocampal specimen from patients who underwent temporal lobe resection showed no correlation between the degree of cell loss and the disease duration (Pauli et al., 2006) suggesting that chronic seizure do not cause significant cell damage.

4. Antiepileptic drugs (AEDs)

To prevent or stop seizures, AEDs act on targets involved in seizure generation and propagation. The most common targets are:

- Modulation of voltage-gated ion channels. By targeting these channels inhibition of neuronal firing, synchronization and seizure spread can be achieved.
- Enhancement of synaptic inhibition
- Inhibition of synaptic excitation
- Modulation of neurotransmitter release via presynaptic mechanisms (Porter et al., 2012).

However, the mechanism of action of each AED is unique and drugs acting on the same target can vary in their clinical efficacy. Multiple targets for certain drugs also recognised. Moreover, for some AEDs mechanism of action is not completely understood (Porter et al., 2012). The main target of current AEDs are described below (see **Table 1.1** and **Table 1.2**):

Voltage-gated sodium channels. Agents acting on sodium channels comprise the majority of AEDs. Drugs modulating voltage-gated sodium channel inhibit high frequency repetitive spike firing without altering physiological activity. They do not directly affect synaptic inhibition or excitation. Interictal discharges are short and therefore sodium channel blocking agents do not change their frequency. These agents are particularly effective against generalised tonic-clonic and partial seizures.

Voltage-gated calcium channels. Some AEDs inhibit high voltage activated (HVA) calcium channels (P/Q type). HVA calcium channels open with strong membrane depolarisation and are responsible for calcium entry and hence neurotransmitter release. Drugs targeting these types of calcium channels are effective in some epilepsy syndromes however do not have effect in absence

seizures. Whereas a drug (*Ethosuximide*) that acts on low voltage activated type calcium channels (T-type) in thalamic neurons is effective in absence epilepsy. T-type calcium channels are involved in the pathology of absences (Rogawski and Löscher, 2004).

Potassium. Opening of potassium channels hyperpolarise membrane potential and reduce cell excitability. An AED that acts on potassium channels, *Retigabine,* positively modulates K_v7 potassium channels ($K_v7.2$ to $K_v7.5$) in the nervous system. $K_{V.}7$ brain potassium channels mediate M-current, that increases when the membrane potential in neurons close to action potential threshold. K_v7 limits further neuronal firing after an action potential and therefore serve as *a "*brake" on epileptic firing (Rogawski and Löscher, 2004).

GABA. $GABA_A$ receptors localized at the postsynaptic membrane of inhibitory synapses transmit fast neuronal inhibition, whereas $GABA_A$ located extrasynaptically mediate tonic (long-term) inhibition. Benzodiazepines enhance synaptic inhibition via modulating synaptic $GABA_A$ receptors containing the $\gamma 2$ subunit that leads to increase of the GABA-induced chloride channel opening frequency. However, Barbiturates (phenobarbital) do not increase the channel opening frequency but increase the channel open time. Inhibition of GABA transporter GAT-1 is the main mechanism of action of *Tiagabine;* this suppresses the translocation of extracellular GABA into the intracellular medium, therefore increases extracellular GABA levels that may activate extrasynaptic GABA receptors. This leads to enhancement of tonic GABA inhibition (Wyllie, 2015).

Table 1.1. Main targets of AEDs.

Targets	Drugs	Approved indications in epilepsy
Modulation of ion channels		
N^+ channel blockers	*Phenytoin* *Carbamazepine*	PGCS
	Oxcarbazepine *Eslicarbazepine* *Lacosamide* *Zonisamide* *Retigabine*	Partial seizures
	Lamotrigine	PGCS, Lennox–Gastaut synd
	Ethosuximade	Absence seizurse
Ca^{2+} channel blockers	*Lacosamide* *Zonisamide* *Ethosuximade*	
K^+ channel potentiation	*Retigabine*	
HCN channels	*Lamotrigine*	
Increase GABA-ergic inhibition		
GABA potentiation	*Benzodiazepines*	Convulsive disorders, status epilepticus
	Vigabatrin	Infantile spasms, complex partial seizures
	Tiagabin	Partial seizures
Decrease in glutamergic inhibition		
AMPA inhibitor	*Perampanel*	Partial seizures
Modulation of neurotransmitter release via presynaptic mechanisms		
α2δ subunit (accessory subunit of Ca channel	*Gabapentine/Pregabalin*	PGCS
SV2A modulation	*Levetiracetam*	PGCS, partial seizures, GTCS, JME

Table 1.2. AEDs with multiple mechanism of action

Targets	Drugs with Multiple mechanisms of action			
	Valproate	***Felbamate***	***Topiramate***	***Phenobarbital***
N^+ channel blockers	+	+	+	
Ca^{2+} channel blockers	T-type	HVA	HVA	HVA
K^+ channel enhancing	+		+	
GABA potentiation	+	+	+	+
Glutamate inhibitor	NMDA	NMDA	AMPA/KA	AMPA/KA
Approved indication in epilepsy	PGCS, absence seizures	PGCS, Lennox–Gastaut syndrome	PGCS, Lennox–Gastaut syndrome	PGCS

The following sources were used (Rogawski and Löscher, 2004; Löscher et al., 2013; Wyllie, 2015).

Glutamate. Although glutamate is the main excitatory neurotransmitter in the brain drugs blocking glutamate receptors have not been very effective in seizure reduction (Rogawski and Löscher, 2004). Although NMDA receptors involved in seizure activity, inhibition of these receptors does not stop epileptiform activity in seizure models. However, inhibition of AMPA receptors had antiseizure effect in animal seizure models. *Perampanel* is the only potent selective antagonist of AMPA receptors; it does not affect NMDA receptors or other ion channels (Wyllie, 2015).

About 30% of patient with new onset epilepsy are resistant to treatment with current AEDs and approximately 50% of patients will have at least one adverse effect with the first line agents. According to long-term studies 14% of patients with new onset childhood epilepsy will go on to develop drug-resistance while remaining on treatment after several years (Schmidt and Schachter, 2014).

However, the majority of currently used antiepileptic drugs (AEDs) have similar mechanisms and targets (Loscher 2011). Moreover, current anticonvulsant drugs are symptomatic that is they reduce the occurrence of seizures but do not modify disease (e.g. cure the epilepsy) or prevent epileptogenesis (Walker et al., 2002). Patients who are seizure free on antiepileptic medication are at high risk of recurrent seizures after discontinuation of the treatment (Wyllie et al., 2012).

Identifying new drug targets for the prevention of disease development i.e. disease modifying treatment is therefore an important step in the treatment of epilepsy. Novel anti-epileptogenic approaches could also target early stage of neuronal network reorganisation and thus prevent development of intractable post-insult epilepsy. Drug development in epilepsy should also aim to prevent neuronal damage and death. This could reduce cognitive decline and other co-morbidities caused by neuronal loss (Walker et al., 2002).

5. TRP channels

Transient receptor potential (TRP) ion channels are a superfamily of cation channels with polymodal (activated by various types of stimulus, whether thermal, mechanical or chemical) activation properties (Ramsey et al., 2006). TRP channel subunits consist of six transmembrane domains that assemble to form non-selective cationic channels. These channels are permeable to Ca^{2+} and monovalent cations. Calcium enters the cell at hyperpolarized membrane

potentials (Clapham et al., 2001).TRP channels facilitate the influx of cations through the membrane into cells against their electrochemical gradients. This raises intracellular concentrations of Ca^{2+} and Na^{+} leading to depolarisation of the cell (Ramsey et al., 2006).The channel subfamily shares a common property of activation or modulation by phosphatidylinositol signal transduction pathways (Clapham et al., 2001).

TRP channels are widely expressed in the body and have various functions. Some TRP channels have been identified in the CNS, however, they are abundantly expressed in variety of sensory receptors cells such as those mediating vision, pheromone sensation, thermal sensation, taste, touch and cell volume regulation. TRP channels have critical roles in sensing and transmission of a broad variety of external or internal stimuli, including mechanical stress, painful stimuli, etc. (Yin and Kuebler, 2010). They are also involved in repletion of intracellular calcium stores, receptor-mediated excitation and modulation of the cell cycle (Clapham et al., 2001). Involvement of these channels in cellular guidance mediation and chemotaxis has also been suggested (Ramsey et al., 2006). There are seven main subfamilies in the TRP channel family: the TRPC (Canonical), the TRPV (Vanilloid), the TRPM (Melastatin), the TRPP (Polycystin), the TRPML (Mucolipin), the TRPA (Ankyrin) and the TRPN (NOMP) family (Nilius and Voets, 2005). TRPN subfamily has only been found in Drosophila and zebrafish to date. Eight channels (TRPM1-8) have been identified in the TRPM group. The name of the subfamily has derived from the founding member of the subfamily - melastanin (TRPM1) (Fleig and Penner, 2004).

5.1 TRPM7 channel

TRPM7 (previously known as LTRPC7 - long TRP channel 7) is a ubiquitously expressed ligand-gated cation channel. The TRPM7 channel gene is located on chromosome 15 and consists of 39 exons (Paravicini et al., 2012). It is a unique channel which possesses both channel and kinase properties. Due to

the presence of a protein kinase domain at C-termini the channel is referred to as a chanzyme. This domain also exists as an independent enzyme (Montell, 2005). TRPM7 channel kinase is classified as an atypical alpha protein kinase (Harteneck 2005). The specific function of the channel and whether the kinase domain is important for channel activity is unclear. TRPM6 is a chanzyme with biophysical properties similar to those of TRPM7, however, TRPM6 has a limited expression profile: epiltelial cells of the renal convoluted tubule and the intestine (Chubanov et al., 2005).

TRPM7 is a constitutively active channel, suppressed by physiological concentrations of intracellular Mg^{2+} (McNulty and Fonfria, 2005). TRMP7 is a non-selective divalent permeable channel, however, it has a high affinity for Ca^{2+} and Mg^{2+}. In physiological conditions (-40 to -80 mV) inward currents are only conducted by divalent cations, however, in the absence of extracellular divalents (both Mg^{2+} and Ca^{2+}), the channel conducts monovalent cations, such as Na^{+}. The TRPM7 channel is permeable to many essential as well as toxic divalent metals with the following permeability sequence: $Zn^{2+} \approx Ni^{2+} >> Ba^{2+} > Co^{2+} > Mg^{2+} \geq Mn^{2+} \geq Sr^{2+} \geq Cd^{2+} \geq Ca^{2+}$, while trivalent ions such as La^{3+} and Gd^{3+} are not measurably permeable (Monteilh-Zoller et al., 2003). Entry of toxic metal ions like Zn^{2+} and Ni^{2+} through TRPM7 during severe metabolic stress conditions such as hypoxia or hypoglycaemia may contribute to the accumulation and toxicity of these metals (Montell, 2005; Nadler et al., 2001).

5.1.1 Structure of TRPM7 and Physiological role

TRPM7 channels consist of six transmembrane segments flanked by cytoplasmic N-terminal and C-terminal tails (**Figure 1.4**). The N-termini contain four stretches of amino acids having similar sequence. The C-terminal sequences of the TRPM family vary in length and structure. The C-terminal regions of TRPM6 and TRPM7 contain a kinase domain with similar

biochemical properties (Fleig and Penner, 2004). Although in physiological ionic conditions TRPM7 has a small inward current at voltages ranging from -100 to -40 mV, decreased extracellular pH dramatically increases the inward current. The effect of protons on TRPM7 currents is concentration-dependent (Jiang et al., 2005).

The exact function of TRMP7 channel and its regulatory role are not yet completely understood. However, it is one of the essential channels in cell viability. A global deletion mutation was lethal in mice (Sun et al., 2009). Moreover, TRPM7 has a central role in Mg^{2+} homeostasis. It is one of a few identified Mg^{2+} transporters in vertebrates (Schmitz et al., 2007).

The channel has also been implicated in many cellular processes such as synaptic transmission, cell cycle, normal growth and development, regulation of vascular smooth muscle cells and proliferation of retinoblastoma cells (Cook et al., 2009).

Various mutations have different effects on the function of TRPM7 channel. A deletion mutation in DT-40 cell line affected cell viability (Nadler et al., 2001). Some mutations only led to growth arrest without disrupting Mg^{2+} homeostasis (Jin et al., 2008) whereas others impaired cell Mg^{2+} homeostasis too (Schmitz et al., 2003). Extracellular Mg^{2+} supplementation in some mutations affecting Mg^{2+} homeostasis and cell growth have rescued cell viability and proliferation (Jin et al., 2008). Moreover, TRPM7 channel deficiency resulted in severe abnormalities of skeletal development in mutant zebrafish (Elizondo et al., 2005).

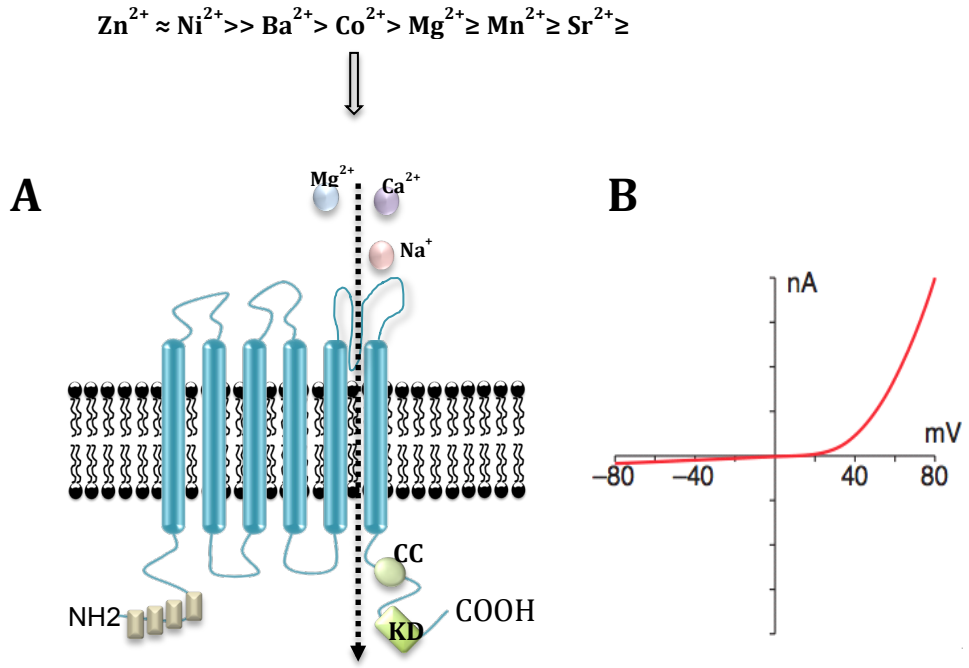

Figure 1.4. Structure of TRPM7 channel.

(A) The diagram illustrates putative membrane topology of a TRPM7 channel. TRPM7 channel contains six transmembrane segments and a pore-forming loop between S5 and S. KD-kinase domain, MHR- the N-terminal region that contain four major homology regions (MHR) (stretches of amino acids that share some sequence similarity), CC- coiled coli region. TRPM7 channel conducts both monovalent ions, such as, Na^{+} and divalent ions, such as, Ca^{2+} and Mg^{2+} and other trace metal ions; permeability sequence for divalent shown. (B) Representative current-voltage (I-V) curve shows that at negative membrane potential TRPM7 conducts small inward current, the potential reverses at 0mV and at positive membrane potential it conducts strong outward current in the presence of normal external concentrations of Ca^{2+} and Mg^{2+}. The information adopted from (Monteilh-Zoller et al., 2003; Fleig and Penner, 2004; Park et al 2014). Figure (B) taken from (Fleig and Penner, 2004).

5.1.2 The kinase domain

Annexin 1, which is a member of Ca^{2+} and lipid binding proteins, is a physiological substrate for the TRPM7 kinase domain. Phosphorylation of annexin 1 by TRPM7 might be involved in physiological functions of the channel (Chubanov et al., 2005). The kinase domain possesses autophosphorylation property and it can phosphorylate prototypic kinase substrates, such as myelic basic protein and histone H3, and annexin 1. This activity of the kinase depends on adenosine triphosphate (ATP) and requires magnesium (Harteneck, 2005).

The role of the kinase domain in activation of TRPM7 channel is somewhat controversial. It was initially suggested that the kinase is important for the channel's function (Runnels et al., 2001). Kinases in general have been known for having a role in ion channel regulation. TRPM7 is unique in that it has its own kinase domain. Additionally, the kinase presents at the sixth transmembrane segment that appears to be involved in the gating of ion channels (Runnels et al., 2001). A single point mutation in the kinase domain has been shown to impair Mg-nucleotide dependent inhibition of the channel (Demeuse et al., 2006). However, this mutation did not abolish Mg^{2+} dependent inhibition although slightly reduced the efficacy. Surprisingly, a mutation leading to complete deletion of the kinase domain restored nucleotide dependent inhibition of the channel (Demeuse et al. 2006). The authors suggested that this could be due to exposure of a previously blocked binding site of Mg^{2+} nucleotides. However, Schimtz and collegues suggested that although the channels kinase domain by itself is not essential for the activation of TRPM7, it acts by an unknown coupling mechanism to regulate channel gating and Mg^{2+} uptake (Schmitz et al., 2003). A recent study in kinase-inactive mutant mice has also suggested that kinase domain is not important for channel activity (Kaitsuka et al., 2014).

5.1.3 Activation and inhibition mechanisms

TRPM7 channels are activated by oxidative stress, low extracellular Mg^{2+} concentration and reduction of intracellular pH (Chokshi et al., 2012). ATP, a functional kinase domain and autophosphorylation of the channel are all necessary for the activation of the channel (McNulty and Fonfria, 2005). The data available in the literature to date regarding various aspects of the channel's modulation is controversial. Nevertheless, there is strong evidence to suggest that the channel is inhibited by free intracellular Mg^{2+}; physiological concentrations (4-6mM) inhibit the channel activity whereas low Mg^{2+} concentrations (0-2mM) activate the channel. Some data suggest that Mg*ATP more potently inhibits the channel than free Mg^{2+} although it has been proposed that intracellular Mg^{2+} but not ATP is important for the suppression of the channel by Mg*ATP (Kozak and Cahalan, 2003).

Magnesium nucleotides. Physiological concentrations of Mg*ATP suppress the channel and strongly increase the inhibitory effect of free Mg^{2+}. Likewise, Mg*ADP had a similar but smaller effect. Almost all magnesium nucleotides were shown to inhibit TRPM7 current and have stronger effect than free Mg^{2+} alone. The following rank in potency of nucleotides has been suggested: TP > TTP > CTP ≥ GTP ≥ UTP > ITP ≈ free Mg^{2+} alone (Demeuse et al., 2006). The presence of two binding sites on the channel that in combination modulate TRPM7 channel activity has been suggested; they provide synergic inhibition by both Mg^{2+} and Mg-nucleotides. The Mg^{2+} binding site is extrinsic and the nucleotide binding site is intrinsic to the TRPM7 kinase domain (Demeuse et al., 2006). However, it has shown that inhibition of the TRPM7 channel by Mg*ATP is lost when using a strong Mg^{2+} chelator, HEDTA, suggesting that the Mg^{2+} nucleotide effect can be explained by free Mg^{2+} alone (Kozak and Cahalan, 2003).Due to sensitivity to physiological Mg*ATP levels, TRPM7 is implicated in regulation of divalent exchange across the plasma membrane to adjust to the metabolic state of the cell (Nadler et al., 2001).

Adenosine triphosphate. The role of ATP on TRPM7 channel's activity is not conclusive based on current research data. The activation of the channel by ATP via the kinase domain was described by Runnels and colleagues (Runnels et al., 2001). However, another study has suggested the opposite effect: the channel was inhibited by addition of ATP to the internal solution (Nadler et al., 2001).Nevertheless, the role of ATP is apparent in TRPM7 inhibition: Mg^{2+} *ATP has stronger blocking effect on the channel than Mg^{2+} alone. 3 mM of free Mg^{2+} is required to completely block the channel, whereas 6 mM of Mg*ATP that contains 670 μM to 800 μM free Mg^{2+} is sufficient to inhibit the channel. This indicates the importance of ATP in inhibiting the channel at lower Mg^{2+} concentrations.

Phosphatidylinositol 4,5-bisphosphate (PIP2), Cyclic adenosine monophosphate (cAMP). TRPM7 can be positively regulated by G-protein coupled receptors, through adenosine 3,5 -monophosphate (cAMP) and protein kinase A (PKA) pathway (Harteneck, 2005). The protein kinase domain mediates the effects of cAMP on the channel activity. Elevation of cAMP concentrations promoted TRPM7-dependent currents, and this effect was inhibited by loss of function mutations of TRPM7 kinase (Montell, 2005). TRPM7 upregulation via the PKA pathway also requires a functional TRPM7 kinase domain (Demeuse et al. 2006).

Numerous studies demonstrated that phosphatidylinositol 4,5-bisphosphate (PIP2), which is a component of cell membrane and the substrate of PLC, is a key regulator of TRPM7. PIP2 has inhibitory effect on TRPM7 channel. Activation of PLC results in the hydrolysis of localized PIP2, leading to inactivation of the TRPM7 channel (Runnel et al. 2002). Therefore, the channels activity depends on the activity of PLC and subsequently upon the concentration of PIP2. TRPM7 channel is activated when PIP2 concentrations are depleted, whereas activity of phophoinositide kinases inhibits the channels by restoring PIP2 concentrations (Harteneck, 2005). Tyrosine kinase receptors also block the channel via activation of PLC (Runnels et al., 2002). Mg^{2+}

mediated activation of PLC associated with the chanzyme was assumed to reduce PIP2 concentration. Indeed, Mg^{2+} - activated PLCs have been described in certain cell types (Montell, 2005).

Activation by stretch, swelling and Oxidative stress. A study showed that TRPM7 channels are activated by stretch and swelling and thus they can be involved in volume regulation in human epithelial cells. A further study has demonstrated that shear stress induced activation is directly mediated by mechano-stress receptors (Numata et al., 2007). A study in hippocampal slices has reported that TRPM7 channels are activated under oxidative stress conditions (Lipski et al., 2006).

β-adrenergic stimulation induced TRPM7 activation, whereas muscarinic stimulation suppressed the activity (Harteneck, 2005).

5.1.1 TRPM7 in the brain pathology

TRPM7 channels are widely expressed in the nervous system (Jiang et al., 2003; Tian et al., 2007) however their function in the brain is unknown. Jiang et al. demonstrated that the channel was inhibited by increased intracellular Mg^{2+} but not affected by cell swelling or a different range of intracellular Ca^{2+} concentrations. Tyrosine kinase inhibitors had inhibitory effect on TRPM7 channels in microglia (Jiang et al., 2003). Several studies have demonstrated an essential role of TRPM7 in anoxia induced death of cortical neurons (Aarts et al., 2003; Nicotera and Bano, 2003; Sun et al., 2009). Cardiac arrest led to neuronal death of CA1 hippocampal area, followed by memory and cognition dysfunction. Suppression of TRPM7 in CA1 by viral shRNA against TRPM7 into the rodent hippocampus prevented this cell death in rats. This silencing resulted in neuronal resistance to ischemic death, preserved neuronal function and prevented ischemia-induced deficits in LTP and preserved performance in memory tasks. TRPM7 suppression did not affect neuronal excitability,

plasticity and had no adverse effect on animal survival, neuronal and dendritic morphology. TRPM7 suppression following brain injury inhibited Ca^{2+} influx and neuronal recovery was enhanced (Sun et al., 2009).These effects can also be explained by a decrease in TRPM7-mediated Ca^{2+} or Zn^{2+} influx (Zierler et al., 2011).

Hypoxia-ischemia induced delayed cell death in the brain is a feature of stoke and neurodegenerative disorders (Sun et al. 2009). Therefore, TRPM7 has been linked to neurological pathology such as brain ischemia, trauma, and neurodegeneration due to oxidative stress induced cell death. Moreover, TRPM7 could play a role in traumatic brain injury due to facilitation of cation influx and involvement in Mg^{2+} homeostasis. In addition, the channel kinase may have role in posttraumatic inflammatory processes (Cook et al., 2009).

5.1.2 TRPM7 channels and epilepsy

As described above opening of TRPM7 channels is induced by a decrease in intracellular Mg^{2+} and extracellular Ca^{2+} concentrations, oxidative stress and decreased extracellular pH (Kozak and Cahalan, 2003; Monteilh-Zoller et al., 2003; Jiang et al. 2005; Lipski et al. 2006). These changes occur during seizure activity. Thus, TRPM7 activation, and Ca^{2+} and Na^{+} influx into cell may play a role in neuronal depolarisation contributing to seizure activity. Moreover, Ca^{2+} influx as well as entry of trace metals through the channel may induce seizure-dependent neuronal death. Elevated intracellular Ca^{2+} is one of the main factors leading to neuronal cell death in neurological disorders.

TRPM7 may also play a role in epilepsy and other neurological disorders linked to Zn^{2+} induced neurotoxicity. It has been shown that neurotoxicity of Zn^{2+} is mediated via it is entry to cells through TRPM7 channel (Inoue et al., 2010).

5.1.3 TRPM7 channel antagonists

The inhibitory effect of the following agents on TRPM7 channels have been described: 2-aminoethyl-diphenylborinate (2-APB), lanthanum (La^{3+}), gadolinium (Gd^{3+}), SKF-96365, spermine, carvacrol, and 5-lipoxygenase inhibitors. None of these agents is specific for TRPM7 channel and they affect other ion channels, e.g. calcium release activated channels (CRAC) or other TRP channel family members, and/or lack sufficient efficacy (Zierler et al., 2011).

La^{3+}, Gd^{3+}, and SKF-96365 block TRPM7 channel but also inhibit other Ca^{2+} permeable channels, including CRAC. **SKF-96365** also blocks other TRP channels, such as TRPC.

The polyamine **spermine** distinguishes between CRAC and TRPM7 channels, blocking only monovalent TRPM7 currents at micromolar concentrations. However, spermine also inhibits conductance of monovalents such as Na^+, K^+, $NMDG^+$ (Kucherenko and Lang, 2010).

The 5-lipoxygenase inhibitors: ***nordihydroguaiaretic acid, AA861, and MK886*** have also been shown to affect TRPM7 channels in the micromolar range independently of lipoxygenase activity; however, they also affect K^+ and Cl^- channels (Zierler 2011).

Nafamostat mesilate (NM) is a synthetic serine protease inhibitor. NM blocks TRPM7 currents in inverse relationship to the concentration of extracellular divalent cations: in the absence of extracellular divalent cations (Ca^{2+} and Mg^{2+}) it blocks TRPM7 current, however, in physiological concentrations of extracellular divalents NM activates the channel (Chen et al., 2010). NM reversibly blocks acid-sensing ion channels (Ugawa et al., 2007).

Carvacrol inhibited mammalian TRPM7 channels in HEK cells and in CA3/CA1 cells in hippocampal cultures. However, carvacrol activated thermo TRP

channels, TRPV3 and TRPA1 (Parnas et al., 2009). Carvacrol also inhibited drosophila TRPL channels which is considered mammalian TRPC channel analogue. TRPC are non-selective Ca^{2+} permeable cation channels although the selectivity ratio PCa/PNa varies significantly between different members of the family (Pedersen et al., 2005). Chen et al. has also shown the inhibition of TRPM7 current in HEK cells by carvacrol (Chen et al., 2015).

2-Aminoethoxydiphenyl borate (2-APB) produces dual effect on TRPM7 activity but not on TRPM6 or TRPM6/7. Concentrations <1 mM of 2-APB inhibited TRPM7 currents, however higher concentrations increased TRPM7 channel activation. Overall, micromolar concentrations of 2-APB enhanced TRPM6 however inhibited TRPM7 activity, whereas at millimolar concentrations, 2-APB increased both TRPM7 and TRPM6/7 currents (Li et al., 2006). 2-APB also affects variety of other TRP channels. It activates TRPV1, TRPV2, and TRPV3 channels (Hu et al., 2004) and also affects CRAC channels (Peinelt et al., 2008).

A recent study identified a potentially specific inhibitor of the TRPM7 channel – **Waixencin A** which is a marine-derived natural product. Waixencin A is xenicane diterpenoid produced from the Hawaiian soft coral Sarcothelia edmondsonia. It demonstrated high potency and selective inhibition for the TRPM7 channel (Zierler et al. 2011). The compound did not have inhibitory effect on close homologue, TRPM6 channel and had insignificant effect on TRPM2 and TRPM4 channels. Waixencin A did not affect CRAC.

For the purpose of the current research to study the effect of TRPM7 channels in epilepsy carvacrol was selected as a blocking agent. We were unable to obtain Waxiencin A initially. Due to difficulties and delays in obtaining Waxiencin A I started my initial experiments with carvacrol. Moreover, because this study aims to test the effect of TRPM7 blocking both *in vitro* and *in vivo*, I aimed to use a compound that is also safe to apply *in vivo*. Although Waxiencin A is the only potentially selective blocker of TRPM7 channel, it is a new

compound that has not been tested *in vivo* yet and is available only in small quantities for research. Whereas carvacrol is a naturally occurring compound with a simple structure that is unlikely to have many adverse effects on animals. Moreover, carvacrol has already been used in *in vivo* studies and was well tolerated without known toxic effects. In addition, to our knowledge to date it does not affect pathways that can modulate cell excitability. Nafamostat mesilate was not chosen because it has opposite effects on TRPM7 channels depending on extracellular divalent concentrations.

Table 1.3. TRPM7 channel antagonists

Additional targets	TRPM7 channel antagonists						
	Carvacrol	***SKF-96365***	***La^{3+} Gd^{3+}***	***NM***	***2-APB***	***Spermine***	***5-lipo xygenase inhibitors***
CRAC		+	+		+		
Ca2+		+	+			+	
K+				+		+	+
Cl-							+
Na+	Peripherally					+	
IP3					+		
TRP channels	TRPC	TRPC			TRPV1, TRPV2, and TRPV3		

CRAC - calcium release activated channels, **+** indicates that the compound has inhibitory effect on the target.

6. *In vitro seizure models*

Studying various of epileptic processes to understand their mechanisms on animal brain slices is a valuable tool. The effects of various drugs can be studied easily without confounders such as liver metabolism and the blood brain barrier. Moreover, brain cells in slices behave similarly to brain cells *in vivo* and different brain regions can be studied in isolation (Mosfeldt Laursen, 1984). A number of *in vitro* models have been used to induce epileptiform activity. Widely used *in vitro* models are low Mg^{2+}, 4-Aminopyridine (4-AP), and Pentylenetetrazol (PTZ) models. Low Ca^{2+} and high K^+ models have also been used to induce epileptiform activity *in vitro*; both these conditions present during seizure activity in humans (Pitkänen et al., 2005). Elevated K^+ levels could be responsible for propagation of epileptic activity (Mosfeldt Laursen, 1984). High K^+ levels successfully generated epileptiform activity *in vitro* (Pitkänen et al., 2005). Moreover, to elicit epileptform events in other seizure models higher K^+ concentration used 4-AP is a potassium channel blocker, which induces epileptiform activity by reducing K^+ efflux from cells (Yamaguchi and Rogawski, 1992). For the current study two *in vitro* models were selected, low Mg^{2+} and PTZ. These are distinct in that one relies on enhancement of excitatory pathways (low Mg^{2+}) and the other inhibition of inhibitory pathways (PTZ) to generate seizure-like activity.

Low Mg^{2+} model is a well-established and widely used *in vitro* model of epilepsy. Artificial cerebrospinal fluid ACSF containing low Mg^{2+} is used to unblock NMDA receptors. The low Mg^{2+} *in vitro* model is a powerful tool to study prolonged seizure activity in brain tissue; acute or cultured brain slices (Pitkänen et al., 2005). Seizure-like event can be induced in brain slices from all epilepsy-sensitive regions and in particular hippocampus (Dreier and Heinemann, 1991). Furthermore, epileptogenesis induced in this model is resistant to most current AEDs and therefore serves as a good model of drug resistant epilepsy (Dreier et al., 1998). In low Mg^{2+} conditions NMDA block will

be released and $GABA_A$ will be supressed. Moreover, release of glutamate from presynaptic neurons inhibited in normal Mg^{2+} concentrations, therefore reduced extracellular Mg^{2+} will trigger glutamate release (Baaij et al., 2015). Pentylenetetrazol (PTZ) is a convulsant agent that is frequently used to study seizure activity. PTZ blocks inhibitory neurotransmitters, in particular GABA which results in depolarisation of neurones. PTZ acts via binding to picrotoxin-binding site of the post-synaptic $GABA_A$ receptor (Rozsa et al., 2008). PTZ model have been widely used *in vivo* and to a less extend *in vitro* to study epilepsy. Intraperitoneal injections of PTZ in animals leads to tonic-clonic seizures (Brito et al., 2006). Addition of PTZ to normal ACSF generates prolonged interictal –like activity *in vitro.*

7. In vivo epilepsy models

Animal models have a fundamental role in identifying new and testing existing AEDs. One of the problems in improvement of drug discovery for epilepsy is possibly the use of the same seizure models for decades such as maximal electroshock seizures (MES) or PTZ administration. These models are effective only in identifying drugs with similar characteristics to existing AEDs and have failed to identify compounds that work through different mechanisms. The majority of animal models used in epilepsy research represent seizure models rather than epilepsy models. Hence models such as MES, whereby acute seizure are induced in non-epileptic animals, are not representative of an epilepsy model which should have spontaneous recurrent seizures. True models of epilepsy that are more closely related to human epilepsy are those animal mutants or transgenic animals with spontaneously recurrent seizures, and chemically or electrically induced epileptogenesis resulting in spontaneous recurrent seizures (Löscher, 2011).

Table 1.4*. In vivo* epilepsy and seizure models

Model	Type of epilepsy or seizure modeled
Acquired electrically induced models	
MES	Acute (induced) generalize tonic-clonic seizures
6 Hz psychomotor	Acute (induced) partial seizures
Electrical kindling	Chronic (induced) limbic seizures or chronic TLE
PPS	TLE, SE
Amygdala stimulation	TLE, SE
Acquired chemiconvulsant induced models	
Chemical kindling	Chronic (induced) limbic seizures or chronic TLE
Kainic acid	*TLE, SE*
Pilocarpine	*TLE, SE*
PTZ	*generalized tonic-clonic seizures and absence seizures*
Tetanus toxin	*Partial epilepsies*
Genetic models	
GAERS	*Absence epilepsy*
DBA/2 mice	*reflex generalized tonic–clonic seizures*
GEPRs	*reflex generalized tonic–clonic seizures*
tottering	*Absence epilepsy, partial epilepsy*

MES – maximal electroshock model, GAERS - genetic absence epilepsy in rats from Strasbourg, DBA - dilute brown agouti coat color, GEPRs - Genetically epilepsy-prone rats. Information in the table adopted from several sources (Seyfried and Glaser, 1985; Pitkänen et al., 2005) Löscher, 2011; De Sarro et al., 2015).

Epilepsy models are divided into generalised and partial epilepsy models as well as into genetic models and induction of epilepsy in normal animals. The table compares some epilepsy *in vivo* models (see Table 1.4).

Generalised epilepsy syndromes primarily studied in transgenic animals whereas partial epilepsies are induced in normal animals by chemical compounds or by electrical stimulation of certain brain areas (Löscher, 2011). An ideal model to study epilepsy and disease modification should have high incidence of seizure development after an insult, and similarities with human epilepsy such as cell death as well as cognitive comorbidities. Also, epilepsy must develop after similar insult as in humans, for example SE, stroke, tumour, and trauma (Barker Halski 2015). For the purpose of this study I was interested in chronic TLE and status epilepticus model. Some of the most commonly used models of epilepsy, in particular TLE models will be briefly reviewed below.

7.1 Chemoconvulsant models

Kainic acid model is one of the widely used and studied models of epilepsy. Kainic acid is an analog of L-glutamate and a potent agonist of kainate glutamate receptors (Lévesque and Avoli, 2013). It has a strong convulsive effect. Kainic acid model has been used in particular to model TLE and has many electrographic and neuropathological similarities with human TLE. Kainic acid can be administered intracerebrally or intraperitoneally to induce SE, either a single dose or in multiple small doses. This causes damage to CA1, CA3, dentate hilus and the damage is typically bilateral. It is a robust model, however, animals of different strain, sex, weight and age exhibit variable sensitivity to kainic acid (Reddy and Kuruba, 2013). The latent period from administration of Kainic acid in the hippocampus and subsequent SE to the development of spontaneous seizures can vary between 5 days to one month (Lévesque and Avoli, 2013).

Pilocapine model is another well established TLE model. Pilocarpine hydrochloride is an agonist of muscarinic acetylcholine receptors expressed widely in the hippocampus (Rubio et al., 2010). Activation of M1 muscarinic receptors initiates seizures (Kow et al., 2014). Seizures originate in the hippocampus initially, and then propagate to the amygdala with later spread to neocortex. Although SE in this model is initiated by hyperactivation of cholinergic receptors, but glutamine receptor activation proposed to play role to maintain the activity. Therefore, neuronal cell death and spontaneous seizures also linked to glutamate release (Reddy and Kuruba, 2013). Pilocarpine also can be administered both inracerebrally and systemically (Kow et al., 2014). Pilocaprine leads to similar neuronal damage as kainic acid however wider spread to neocortex is seen (Reddy and Kuruba, 2013). Animals develop spontaneous seizures a few weeks following induction of SE. (Kow et al., 2014).

The major limitation of these models is the direct neurotoxic effect, hence chemoconvulsant induced damage is difficult to distinguish from seizure induced damage (Reddy and Kuruba, 2013). Pilocarpine leads to severe seizures, with extensive brain damage and mortality is high compared to kainic acid model. Furthermore, systemic acetylcholine activation following pilocarpine administration leads to side effects such as hypersalivation, lacrimation which causes distress to animals.

7.2 Electrically induced seizurure models

Electroshock model produces tonic-clonic seizures and severity of seizures depend on the intensity of the stimulation. 2 ms duration high electric currents (25 -150 mA) and frequency of 50 Hz has been used to induce seizures. Such electroshock stimulation activates extensive brain area and leads to generalized neuronal firing. Repetitive low intensity daily stimulation however induces limbic kindling which leads to predominantly granule hippocampal cells, as well as neocortex and piriform cortex discharges (Rubio et al., 2010).

Electrical kindling model has been extensively used to study TLE. Spontaneous seizures develop with prolonged kindling. It involves induction of focal seizures by electrical stimulation with progressive change in response to subsequent daily stimulation. Stimulation is delivered through implanted electrode with high frequency stimulation (~60 Hz) with intensity of ~400 μA. Eventually, over a long period of time animals develop spontaneous seizures. The main disadvantage of this model is it is very labour intensive. In addition, it does not share similarities with human TLE as compared to the models described above. Although some studies report damage to the hippocampus with high number of repetitions these results were inconsistent (Pitkänen et al., 2005). Moreover, epilepsy in kindling model is no induced by initial damage as in human TLE.

For the purpose of this study the perforant path stimulation model was chosen as it does not rely upon an exogenous convulsant that may lead to drug specific actions.

7.2.1 Perforant path stimulation

The perforant path stimulation (PPS) model is a well-established and reliable model of acquired chronic epilepsy (in particular MTLE) and status epilepticus. This model is very close to human epilepsy and very robust (Vicedomini and Nadler, 1987). PPS has been used with some variations. 24 hour or 2 hour repetitive stimulation in either anaesthetised or unanaesthetised rats was used initially (Sloviter, 1983; Olney et al., 1983; Walker et al., 1999; Norwood et al., 2011). A more widely used protocol involves continued stimulation of hippocampal afferent pathways for two hour in the unanaesthetised rat. Repetitive stimulation is delivered through electrodes implanted in the angular bundle or fimbria of the brain. Following stimulation animals develop SE (Vicedomini and Nadler, 1987). PPS induces granule cell population firing and ictal-like activity. Population spikes represent activation of axons that terminate on hilar neurons and the pyramidal CA3 cells (Walker et al., 1999). Post

stimulation recurrent inhibitory activity in the granule cell layer was inhibited (Sloviter, 1983).

The PPS model enables an analysis of the biochemical and physiological properties of seizures, status epilepticus, and neuronal cell death. PPS causes excitatory hippocampal damage similar to kainic acid induced epilepsy. One major advantage, however, is that the PPS model avoids direct neurotoxic effects of chemoconvulsants. The model also enables easy monitoring of EEG and behaviour. Furthermore, PPS reproduces the behavioural, electrographic and neuropathologic changes typical for human SE (Vicedomini & Nadler 1987). Structural changes in the PPS model resemble hippocampal damage in humans caused by SE. Most prominent neuronal damage is seen in the dentate hilus, CA1 and CA3 hippocampal regions with relative preservation of CA2 and the dentate granule cells (Walker et al. 1999). Damage to other parahippocampal structures was also seen (Sloviter, 1983). PPS is an ideal model to study epilepsy and disease modification. One of the main drawbacks of PPS is however the necessity of electrode implantation which makes the model complicated and time-consuming compared to chemiconvulsant models (Reddy and Kuruba, 2013).

8. Aim

The current research aimed to investigate the role of TRPM7 channels in epilepsy. In particular, I aimed to test the effects of inhibiting the channel on seizure activity, and also neuronal death, epileptigenesis and cognitive deficits following status epilepticus. There is no study so far that investigated the role TRPM7 in epilepsy.

9. Hypotheses

1. TRPM7 channels contribute to seizure generation and blocking the channel stops seizure activity

2. TRPM7 channels contribute to seizure related neuronal death in epilepsy and blocking TRPM7 channels would have a neuroprotective effect following status epilepticus and will prevent cognitive decline and the development of epilepsy (epileptognesis).

Chapter 2. General methods

1. Animals

Animals were housed in the Institute of Neurology, UCL animal facility under controlled conditions; at a temperature of 22 ^{0}C, maintained on a 12/12 hour dark/light cycle with free access to food and water. All animal care and procedures were carried out with local ethical approval and adhered to the UK Home Office Animal (Scientific Procedures) Act, 1986.

2. In vitro electrophysiology experiments

Male Sprague-Dawley rats aged 3-3.5 weeks were used to prepare acute brain slices for the in vitro electrophysiological recordings.

2.1 Preparing brain slices

All compounds for preparing solutions were purchased from Sigma Aldrich, UK. To obtain acute brain slices, the rats were culled with isoflurane overdose and then decapitated. Following decapitation, the brain was rapidly removed and placed in

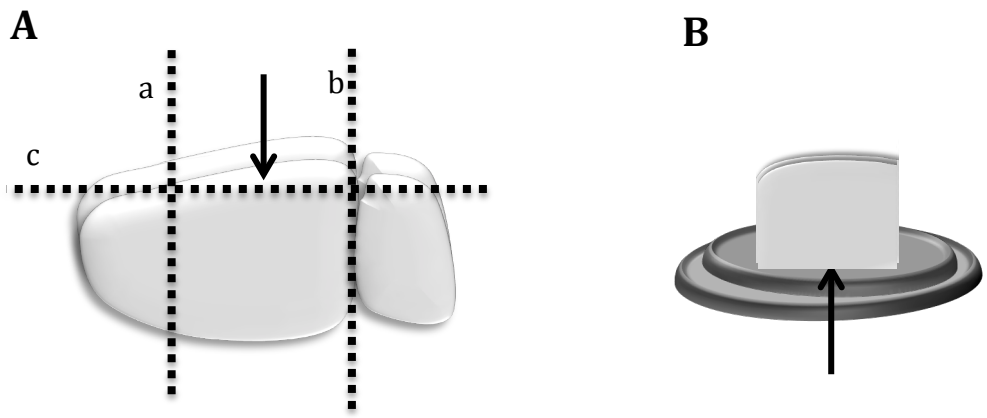

Figure 2.1. Preparation of horizontal brain slices.

A - the areas of brain that were removed a) distal third of the frontal brain , b) cerebellum c) and a part of apical fronto-parietal cortex**. B –** Both hemispheres were glued on the specimen holder facing down with fronto-parietal cortex part. Arrows show the part that was glued to the surface

ice-cold (2-4°C) slicing solution (75 mM sucrose, 2.5 mM KCl, 87 mM NaCl, 1.25 mM NaH_2PO_4, 7 mM $MgCl_2*H_2O$, 5.5 mM D-glucose, 2.6 mM $NaHCO_3$, 0.5 mM $CaCl_2$, osmolality 315 mOsm/kg) to minimise metabolic activity. All procedures for slice preparation were then performed in ice-cold slicing solution.

The cerebellum and distal third of the frontal brain were removed and the hemispheres were separated with a scalpel (see **Figure 2.1**). Then both hemispheres were glued onto the centre of the specimen holder with cyano-acrylic glue. Horizontal brain slices comprising the hippocampal formation, dentate gyrus and entorhinal cortex were prepared on the vibratome (Leica VT1200S, Leica mycrosystems, Nussloch, Germany). A slice thickness of 350μm, speed of slicing 0.09 mm/s and amplitude 0.75mV were selected.

Then, about 3-4 slices from the same area of each hemisphere were selected and transferred into storage solution (119 mM NaCl, 2.5 mM KCl, 1.3 mM $MgSO_4$*7H2O, 0.9 mM NaH_2PO_4, 14 mM D-glucose, 1 mM $CaCl_2$, 1.7 mM $MgCl_2$ 2.6 mM $NaHCO_3$, osmolality 296 mOsm/kg). Slices were incubated in a bath at the temperature of 33°C for 30 min to allow recovery from the damage that resulted from the dissection procedure and to adjust to the new artificial environment. Following the recovery time, slices were kept at room temperature for about 45 min before starting experiments. All solutions were bubbled with 95% O2/5%CO2 gas to maintain pH 7.4-7.35 and to oxygenate the tissue.

2.2 Micropipette preparation

Recording electrodes were prepared from Borosilicate standard wall capillaries with filament and flame polished ends by pulling on a horizontal puller (DMZ universal puller, Zeitz Instruments, Germany). The puller settings were adjusted to achieve a pipette resistance of 1-2MΩ in artificial cerebrospinal fluid (ACSF).

2.3 Low Mg^{2+} and PTZ seizure models

The effect of TRPM7 antagonists on *in vitro* epileptiform activity was tested in two seizure models. I first used low Mg^{2+} model to test the effect of TRPM7 channel blocker on seizure-like activity. As low magnesium condition is ideal for opening TRPM7 channels this was chosen as the first step to test the involvement of TRPM7 channels in seizure generation via blocking the channel. I then used PTZ seizure model to see if the results obtained could be extrapolated to another model that was not dependent on magnesium concentrations, i.e. whether TRPM7 channels are activated during seizure activity regardless of magnesium concentrations. Acute combined hippocampal-enthorhinal cortex slices were used.

Acute brain slices from a total of 28 rats were used for low magnesium experiments. To induce epileptiform activity ACSF solution was prepared (126 mM NaCl, 5 mM KCl, 0.9 mM NaH_2PO_4, 14 mM D-glucose, 2.5 mM $CaCl_2$, 2.6 mM $NaHCO_3$, osmolality 296 mOsm/kg) without adding Mg^{2+} and potassium concentration was increased to 5 mM. An individual slice was transferred to this solution and kept for ~30 min to initiate epileptiform activity.

In total 38 rats were used to prepare acute brain slices for the PTZ induced seizure experiments. To a normal ACSF solution 2 mM of PTZ was added and potassium was increased to 5-6 mM to induce epileptiform activity. An individual slice was kept in the solution for about 30 min to initiate epileptiform activity.

2.3.1 Electrophysiology

For the electrophysiology experiments, acute brain slices must be provided with adequate oxygen, appropriate pH, osmolality and temperature. Moreover, good visual control and mechanical access to slices is also important. For this reason a submersion superfusion chamber was used, in which a slice rests on

a submerged net to permit slice perfusion from below and above. The submersion recording chamber was continuously perfused with ACSF/95%O_2/5%CO_2 at the rate of ~4 ml/min and temperature was controlled to be maintained at ~33°C.

An individual combined hippocampal - entorhinal cortex slice was placed in the recording chamber. Low Mg^{2+} or PTZ induced epileptiform discharges were recorded from CA1 region of the hippocampus (see **Figure 2.2**). The recording electrode was filled with the perfusion solution (low Mg^{2+} or PTZ added ACSF).

Recordings were initiated if regular stable epileptiform discharges were present for about 10 min. Recordings were obtained using a Multi-Clamp 700B or Axopatch 200B amplifier (Molecular Devices), and were low-pass filtered at 4 kHz. WinEDR (Strathclyde Electrophysiology Software) was used for data acquisition. Sampling rate was 0.1 ms (i.e. 10 kHz).

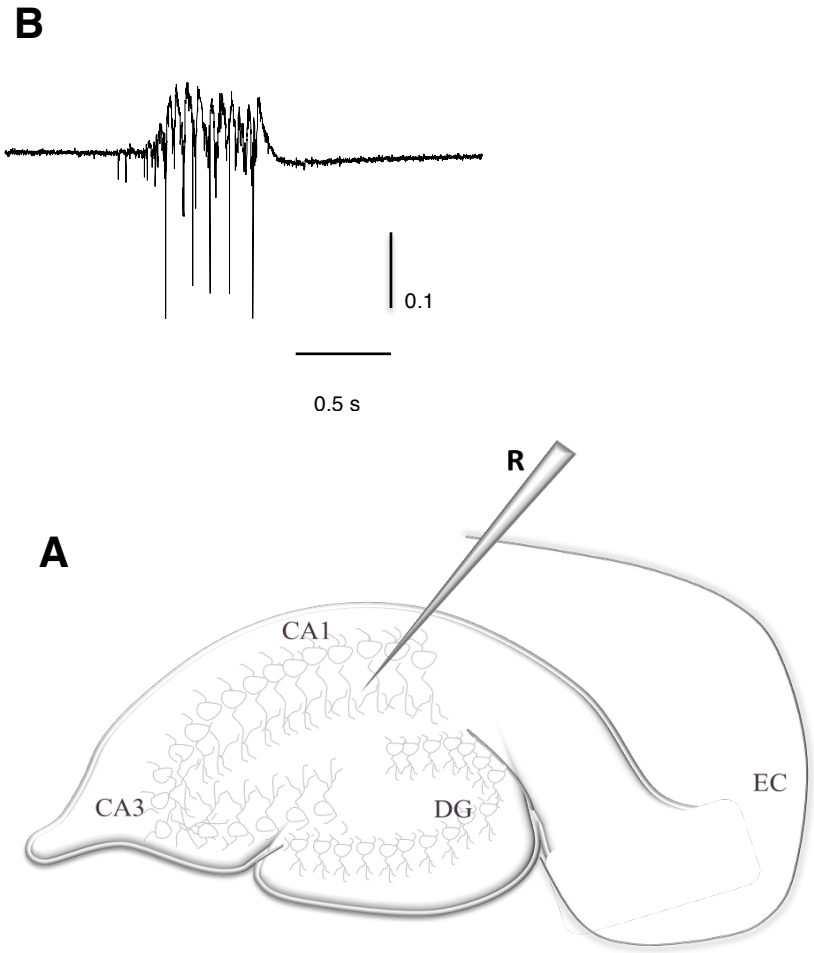

Figure 2.2. Seizure-like activity recording.

A) Schematic illustrations of a combined hippocampal-entorhinal cortex slice and electrode positioning for seizure-like activity recording: R - recording electrode filled with appropriate aCSF solution (Low Mg^{2+} or PTZ containing) and positioned in CA1 area. EC – entorhinal cortex **B**) An example of PTZ induced seizure-like burst recorded from CA1

2.4 Evoked field EPSP experiments

Evoked extracellular field excitatory postsynaptic potentials (fEPSPs) were recorded from CA1 region of the hippocampus. Ex vivo combined hippocampal-enthorinal cortex slices were used. The recording electrode, a borosilicate glass microelectrode of 1–2mΩ resistance filled with ACSF was placed in stratum radiatum of CA1 region (**Figure 2.3**).

A bipolar stimulating electrode was placed in the Schaffer collaterals/commissural fibre region (see **Figure 2.3**). Stimulation intensity of 0.3-0.27 mA was used and single pulses [100μs width] with a 20 s intervals were delivered. After 20 min of recording, drug or vehicle was added to the perfusion solution and recorded for another 20 min. Recordings were filtered at 4 kHz, obtained using a MultiClamp 700B amplifier (Molecular Devices) and digitized at 10 kHz. The LabView (National Instruments) software was used for data acquisition and off-line analysis.

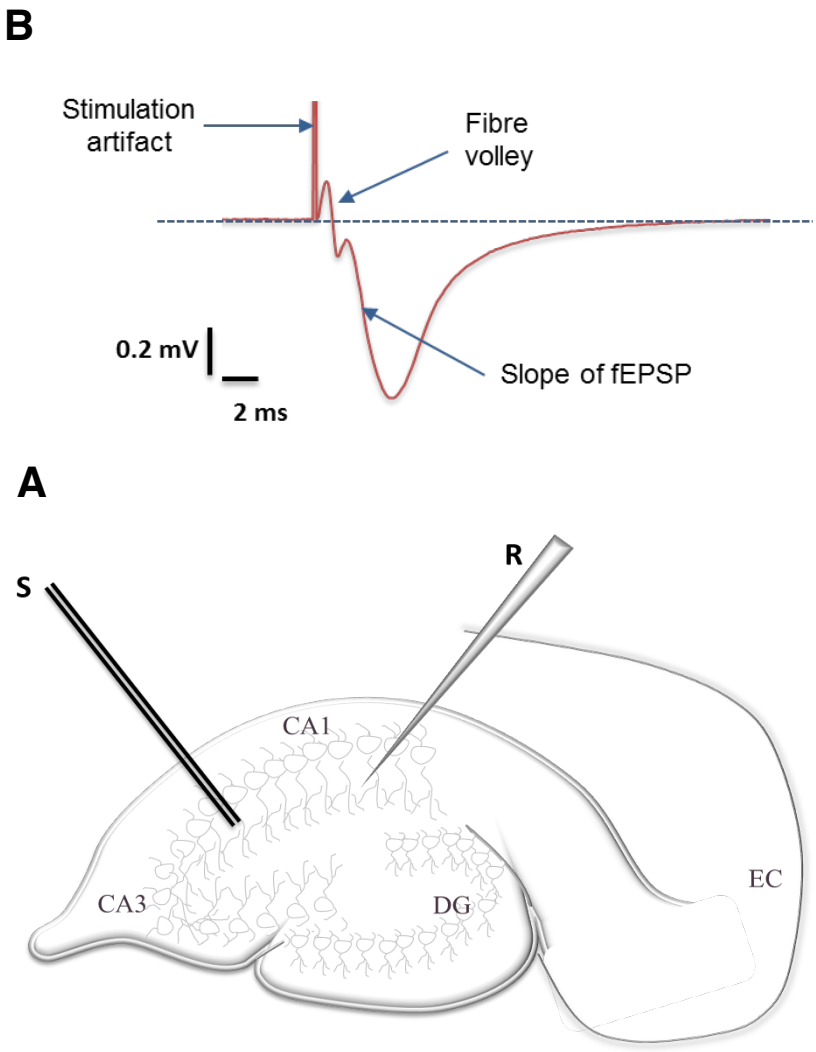

Figure 2.3. Evoked extracellular field potential recording.

B) Electrode positioning: **R -** Recording electrode filled with normal aCSF solution and positioned in CA1 area **S-** bipolar stimulating electrode on Schaffer collaterals region**.** EC – entorhinal cortex **A)** An example trace of fEPSP in CA1 after stimulation of Schaffer collateral (single pulse stimulus of 100µs duration) during baseline recording.

2.5 Data analyses and statistics

For in vitro seizure recordings with unstable baseline - amplitude gradually decreasing or increasing by 10% - were excluded from analyses both in control and drug-treated groups. To check for Gaussian distribution Shapiro-Wilk and Anderson Darling tests were carried out.

2.5.1 In vitro seizure experiments

All in vitro recordings obtained from WinEDR 3.1.9. (Strathclyde Electrophysiology Software) and were analysed using pCLAMP 10.3 software (see **Figure 2.4**). Each event was selected manually after applying a threshold detection tool. The data were transferred into an excel datasheet to perform further analysis. OriginPro 9.0 (OriginLab) software was used for creating figures. Recordings with both ictal-like and interictal-like activity were included in the analyses in the low Mg^{2+} in vitro model to test the effect of the TRPM7 blocker. Ictal-like activities occurred every 3-4 minute lasting 0.5-1.5 minutes. Therefore, overall activity was assessed in 5 minute intervals. All data with both Low Mg^{2+} and PTZ induced seizure models are illustrated in mean 5 minute intervals; mean frequency and amplitude for each 5 minute activity were calculated and then the values were normalised to baseline mean values. Epileptiform bursts were defined as field potential activity with an amplitude more than three times that of baseline, containing more than 2 subsequent spikes that do not return to baseline, and with overall duration ≥ 40 ms. Single spikes and polyspikes not meeting this criteria were not included in analyses.

Normalised frequency and normalised amplitude were compared in drug-treated and control samples. Descriptive data expressed in mean±SEM. Statistical

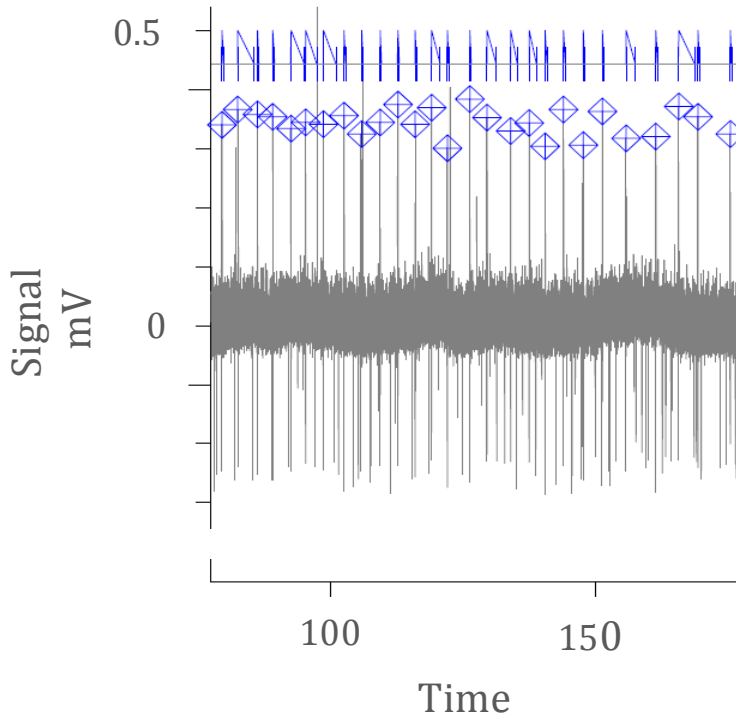

Figure 2.4. PClamp Seizure like activity analysis window.

Each blue rhomb-like shape represents counted seizure-like activity.

analyses were carried out using STATA V.11. Mean discharge frequency and mean discharge amplitude in drug-treated experiments was compared versus control recordings using Student t-test, P-values of ≤ 0.05 were considered as significant.

2.5.2 Evoked fEPSP experiments

Data was analysed using Lab view (National Instruments) software. Average traces of last 10 min of baseline time and last 10 min after addition of carvacrol were used. fEPSP and fibre volley slopes were normalised to baseline; mean slope of last 10 min during baseline and drug-treated time were compared using paired t-test.

3. In vivo experiments

3.1 Perforant path stimulation/chronic epilepsy model

Male Sprague-Dawley rats (280-310g) were used for all in vivo experiments. Animals were allowed to acclimatise to the animal house for at least 1 week after arrival.

3.1.1 Electrode implantation

All electrodes were purchased from Plastics One Inc, Bilaney Consultants UK Ltd. To prepare a bipolar stimulating electrode two steel teflon-coated electrodes (diameter 0.15 mm) were twisted manually (to prevent coating being removed from the remainder of the wire) and conductive tips were exposed and left ~0.8mm apart. The tip of the recording electrode, a steel teflon- coated electrode (diameter 0.28mm) was also exposed for about 1 mm. The reference electrode was prepared by soldering about 4 cm silver wire (diameter 0.125 mm) to a steel gold plated socket contact.

The procedure was undertaken in a stereotaxic frame (David Kopf Instruments, USA) with the animal under isoflurane anaesthesia (2-3 % in 2 L/min O_2). A small area on the head of the animal was shaved and cleaned with iodine (Videne, MidMeds Ltd., UK). Then Buprenorphine 0.2 mg/kg was administered subcutaneously (40 min onset, 12 hour analgesia). Once sufficient anaesthesia was confirmed with absence of response to ear and toe pinch, about 1cm^2 area of skin on the top of the head was cut and subcutaneous tissue was cleared for better surface for glue/dental cement and to reduce infection.

Table 2.1. Electrode coordinates: distance from bregma

Electrodes	A-P (cm)	M-L (cm)
Stimulating electrode	-0.81	-0.44
Recording electrode	-0.4	-0.25

A-P –Anterio-posterior, M-L -medio-lateral

A drill attached to the stereotaxic frame was used to drill holes through the skull; one for a stimulating, one for a recording electrode and additional three holes for screws to secure the head piece (see **Figure 2.5**). The positions for electrodes were calculated as follows (see **Table 2.1**): 1) for the stimulation electrode -8.1mm antero-posterior and -4.4mm medio-lateral from the bregma, 2) for the recording electrode -4mm anteriolateral and -2.5mm medio-lateral from the bregma. The reference electrode was wound around the screws to secure it and the free end was placed subcutaneously (see **Figure 2.5**). The stimulation electrode was inserted into the angular bundle and recording were made from the dentate granule cells.

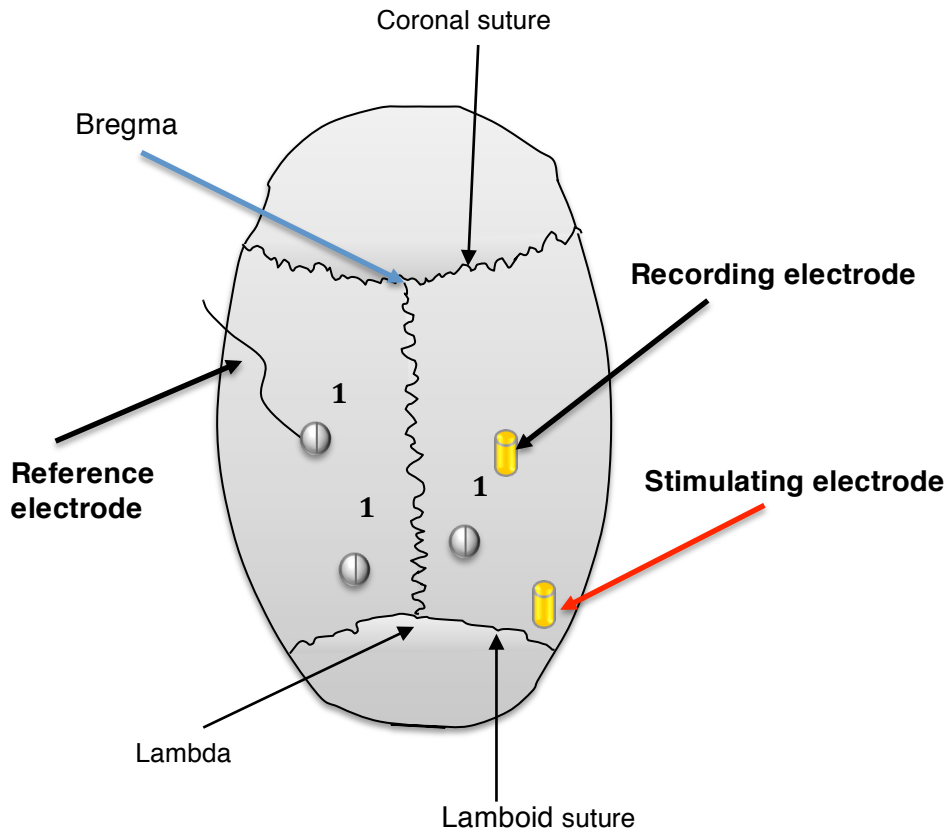

Figure 2.5. Electrode implantation sites in the rat skull in PPS.

After taking coordinates for bregma *stimulation* and *recording electrode* positions were calculated. **1** - 3 screws were inserted to stabilise head peace. *Reference electrode* is a silver wire bounded to screw in one end and the other end placed subcutaneously near the skull area

The optimal position for electrodes was identified by lowering slowly the recording and the stimulating electrodes into the brain until maximal population field excitatory postsynaptic potential (fEPSP) was achieved. A single pulse stimulus of 3.5 mA and 150μs width was delivered from a Neurolog system (Digitimer Ltd, Welwyn Garden City, UK) and a stimulus isolator (Digitimer, UK). Recordings were bandpass-filtered at 0.1-50 Hz. The presence of positive going field potentials with >2 mV population spike indicated that the electrodes were correctly positioned. At this point, isoflurane level was reduced to 1-1.5 %. Then the other end of electrodes was inserted into six-channel pedestal (Plastics One, UK) and this was fixed with dental cement. The anaesthesia was disconnected and 5 ml 0.9% w/v saline was administered subcutaneously and rats were monitored until recovery.

Single pulse stimulus generated population spike after insertion of electrodes into the perforant path. This was done during electrode implantation to ensure the electrode in the right position. Population spikes recorded from the implanted electrodes represent activation of a system of axons that terminate on hilar neurons and the pyramidal cells of CA3 (Walker et al., 1999).

3.1.2 Induction of Status Epilepticus

The perforant path was stimulated through implanted bipolar electrodes 7-10 days postoperatively. Animals were randomly divided into 3 groups: naive controls (had surgery but not stimulated), epileptic stimulated (stimulated, not given the drug) and epileptic treated group (stimulated and given the drug).

The 6-channel pedestral on the head of the animal was connected to a counterbalanced six-channel commutator via a cable. Stimulation was delivered from a Neurolog system with intensity selected at 50-75 % of the maximum population spike amplitude. 50 μs alternating monopolar pulses at 20 Hz were continuously delivered for 2 hours after initial 10 min baseline recording.

Impulses were bandpass-filtered (0.1-50 Hz), digitized at 100 Hz (CED micro 1401; CED, Cambridge, UK) and recorded using Spike 2 software (CED, Cambridge, UK).

During stimulation and subsequent self-sustaining status epilepticus (SSSE) period behaviour, seizure type and severity were monitored and recorded for every 15 min. Behavioural seizures were graded according to the Racine scale (Racine, 1972). After 2 hours the stimulation was stopped. The recording was continued and monitored for 10-20 min to ensure animal had developed SSSE. Then diazepam (10 mg/kg IP) was given and recording continued for 20-30 min to ensure SE was stopped.

3.1.3 Racine scale

During induction of the SE seizure severity was assessed for each animal every 15 min based on the Racine scale (see **Table 2.2**) (Racine, 1972).

Table 2.2 Seizure severity scale (Racine)

Stages	Seizure characteristics
Stage 1	mouth and facial movements
Stage 2	Head nodding
Stage 3	forelimb clonus
Stage 4	seizures characterized by rearing
Stage 5	full motor seizure with loss of postural controlling

3.2 Histology

3.2.1 Perfusion/fixation

Three to four weeks following induction of status epilepticus/epilepsy animals were culled using transcardial perfusion method. For this purpose, transcardial infusion of 0.01M phosphate-buffer saline (PBS) - regular PBS solution, to remove blood from the body was followed by the infusion of 4% paraformaldehyde (PFA) solution in 0.01M PBS [pH was adjusted to 7.2-7.4] to fixate the brain. Not stimlated control animals were also culled after the same time following surgery, 3-4 weeks.

After sedating animal with isofurane, a sublethal dose of pentobarbital (140mg/kg) was administrated intraperitoneally (i.p.). Once unresponsive to toe pinch, the animal was fixed on a surgical table for the perfusion. The chest of the animal was opened to expose the thoracic cavity and a needle filled with heparinised PBS was inserted approximately 5mm into the left ventricle. Heparin was used to prevent the blood from coagulating and to enable complete removal of the blood from the brain as it can auto-fluoresce or contribute to non-specific antibody staining. The needle was attached to the tubing and the solution was pumped transcardially through the inserted needle. A cut was made at the top of the right atrium to allow free blood flow. When the liver and lungs lightened in colour and the solution run clear the perfusion solution was switched to 4% PFA/PBS to fixate the brain. Around 150 ml of 4% PFA/PBS was perfused. During perfusion with PFA muscles twitching was observed in the animal due to skeletal muscle fixation indicating efficient fixation. The brain was removed and placed in a tube containing 4%PFA/PBS solution and kept overnight at 4^{o}C.The following day the fixed brain tissue was removed from 4 % PFA solution and washed several times with regular PBS solution.

3.2.2 Dissection and selecting slices for immunostaining

Slicing was performed in PBS solution. For immunohistochemistry 45 μm slice thickness were selected for optimal penetration of the antibody. Coronal brain sections were made using Leica vibratome (Leica mycrosystems, Nussloch, Germany). First, frontal part of the brain as well as cerebellum was cut and the hemispheres were separated with a scalpel. Then a hemisphere was glued onto the surface of the specimen holder with cyano-acrylic glue.

To ensure that the same area of the hippocampus is analysed in all animals, slicing was performed in a systematic randomised fashion as follows: for each animal brain when slicing was initiated and once the dentate gyrus was seen in the coronal section the first 5 slices were discarded. Then, all slices from the dorsal hippocampus (this part of the hippocampus appears first in coronal view) were collected until the junction between ventral and dorsal hippocampus appears. The slices were placed in wells in the same order as they appeared in the hippocampus and they were numbered as 1, 2, 3 etc. Thereafter, 6 non-adjacent slices were taken from each right medial dorsal hippocampus in the following order: every third slice starting from 12th slice in the order (this is where the whole hippocampus was visible). Then slices were placed in wells of a plate containing PBS. The right hemisphere was used in all animals for immunohistochemistry because this was the part of the brain that was stimulated for seizure induction and therefore was assumed to be the primary side of cell damage. *Anti-NeuN* (1:400) was used as a primary antibody due to specificity to neurons; it does not stain glia or other cells. However, anti-NeuN does not differentiate between different types of neurons. To stain TRPM7 channels *anit-TRPM7* (1:300) was used after initial testing for optimal concentrations.

Initially to test the antibody the staining was done only with anti-NeuN. Then for the main staining *DAPI* (4',6-diamidino-2-phenylindole) was also added. DAPI is a fluorescent stain that specifically stains regions of DNA; this was used to

confirm the presence of nucleus and whether it was damaged or not. DAPI is not specific to neurons, stains any nucleus, however can clearly define edges of a nucleus.

3.3 Immunostaining

3.3.1 Immunostaining protocol optimisation

Firstly, to test the primary antibody and to optimise subsequent staining protocol the following combination of compounds were tested (see **Table 2.3**): 1) with and without adding Triton X-100, a detergent that used to permeabilise cell membrane 2) with and without primary antibody added 3) different combination of blocking agents such as 5% *Normal Goat Serum* (NGS) alone, 3% *Bovine Serum Albumin* (BSA) alone and combination of both - NGS (3%) / BSA(1%). Although the concentration of Anti-NeuN 1:400 was well established in the lab, other parameters still needed to be tested as well as optimal concentrations for anti-TRPM7 antibody had to be established before main staining. The most optimal protocol then was used for subsequent immunostaining.

3.3.2 Main staining protocol

The hippocampal slices were washed 3-4 times for 15 min with PBS on a rocker to remove all free PFA as this can affect immunostaining (see **Table 2.4**). Then slices were blocked for an hour with 5-10% normal goat serum/PBS on a rocker at room temperature after which they were incubated overnight at 4^{o}C on a rocker in mouse anti NeuN antibody (1:400) and goat anti TRPM7 (1:300).

The next day slices were washed with PBS at room temperature and then incubated with the secondary antibody. For secondary antibody a *Goat Anti-*

mouse (Alexa Fluor) secondary was used (e.g. goat-anti-mouse Alexa 546). *Normal Goat Serum* was used as a blocking agent.

Table 2.3. Immunostaining protocol developmentTable 2.3

Wells	Triton X-100 (0.2%)	Blocking agent	Primary antibody		Secondary antibody	
			Anti-NeuN (1:400)	Anti-TRPM7	Alexa 546 (1:500)	Alexa 488 (1:500)
1	+	BSA	+	1:600	+	+
2	+	BSA/NGS	+	1:300	+	+
3	+	NGS	+	1:600	+	+
4	+	NGS	-	-	+	+
5	-	BSA	+	1:300	+	+
6	-	BSA/NGS	+	1:600	+	+
7	-	NGS	+	1:300	+	+
8	-	BSA	-	-	+	+
9	+	BSA	+	1:300	+	+
10	+	BSA/NGS	+	1:600	+	+
11	+	NGS	+	1:50	+	+
12	+	BSA/NGS	-	-	+	+
13	-	BSA	+	1:50	+	+
14	-	BSA/NGS	+	1:50	+	+
15	-	NGS	+	1:50	+	+
16	-	BSA/NGS	-	-	+	+

BSA -bovine serum albumin, NGS –normal goat serum, Alexa - goat anti mouse, **+** substance added, **-** not added

Table 2.4. Immunostaining main protocol

Steps	Procedure
Step 1	Wash slices (10-15 min 3x) with regular PBS
Step 2	Block for 60 minutes with 5-10% normal goat serum/PBS on a rocker at room temperature
Step 3	Wash slices with PBS (10-15 min 3x)
Step 4	Incubate overnight at 4^{o}C on a rocker in the **primary antibody**- mouse **anti-NeuN** (1:400), **anti-TRPM7** (1:300)/ 0.5% normal goat serum /PBS
Step 5	Wash with PBS at room temperature (10-15 min 3x)
Step 6	Incubate with the **secondary antibody** (i.e. goat-anti-mouse Alexa 546 1:500, Alexa 488 1:500) 2 h at room temperature on a rocker
Step 7	Wash slices (10-15 min 3x) with PBS
Step 8	Wash slices (10-15 min 3x) with deionised water
Step 9	Add DAPI (1:1000)
Step 10	Wash slices (10-15 min 3x) with deionised water
Step 11	Mount the slices onto a coverslip

Slices were also stained with *DAPI*. Then slices were mounted onto a coverslip with Vectashield mounting medium. About 30 min after mounting edges of cover slips were sealed with nail varnish to prevent drying.

3.4 Confocal imaging and cell counting

Zeiss LSM 710 Confocal Microscope was used for imaging. The following confocal settings were used: x20 optical magnification, range indicator, Pinhole of 8 µm, laser intensity was adjusted for each image to maximise visibility of cells. The tile scan configuration was used that enables a large area of interest whilst taking continuous multiple images. Imaging and subsequent cell counting was done in a blinded fashion for all three groups: epileptic, epileptic-treated and controls.

First, the whole hippocampus was scanned using tiles (mazoik method) with optical magnification of x10 (see **Figure 2.6**) to capture the whole hippocampus. Then regions of interest were selected in three zones of hippocampus (CA1, CA3, hilus). Following this, magnification of x20 was used to scan images in three selected regions of the hippocampus. Single plane images were obtained; this avoided the possible confounder of counting neurons multiple times.

The number of cells in the following three areas of the hippocampus was calculated - CA3, CA1 and hilus- in all three groups of animals. In the software Image J the plugin Cell Counter was used to count the number of neurons. Only bright, clearly visible anti-NeuN stained cells that were also confirmed with DAPI staining were counted. Brightness and contrast were adjusted to reveal the maximum number of cells. 75% zoom in imageJ was selected for all images during counting.

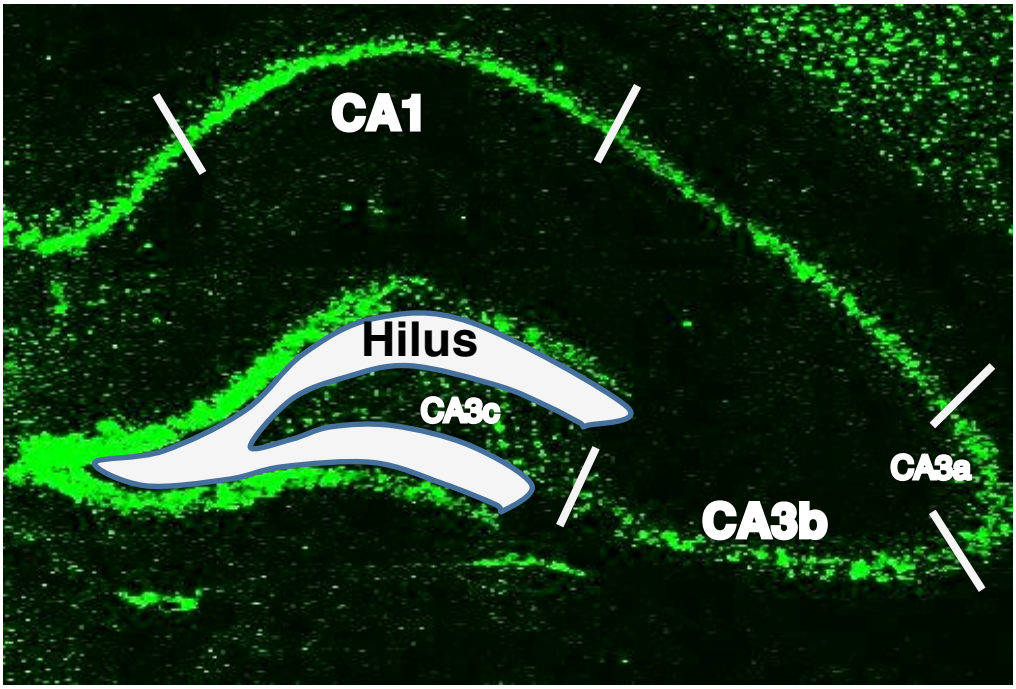

Figure 2.6. A Confocal image (x10 magnification) of the hippocampus showing cell counting areas three hippocampal regions.

Cells were counted in the marked areas of the CA1 and hilus and in CA3b area of CA3. 3 areas of 300 µm in CA1, 3 areas of 300 µm in CA3 were selected for cell counting, that represented the whole CA1/CA3 regions. In the hilus cells between DG and CA3c were counted.

Hilus cell counting: CA3 area has three parts: CA3a, CA3b and CA3c (see **Figure 2.6**). CA3c (sometimes referred as CA4) is between two dentage gyrus blades. The hilar cells are between dentate gyrus and CA3c area. In order to differentiate hilus from CA3c area, cells within a distance of 20 μm or less from CA3c were not included. The rest of the region between DG and CA3c were selected and the area was measured. Cells in this area were counted followed by cell density calculation. The region highlighted 'hilus' in the figure 2.6. was selected and its area was measured. Thereafter number of cells was counted in this selected region, followed by calculation of density (Cell count/area=density). Shrinkage of the tissue due to fixation can occur, which will affect the density calculation, however, the same procedure was applied to tissues from all three groups of animals and the shrinkage level would be expected to be the same. Moreover, no significant difference in area was seen between epileptic and control groups.

CA1 cell counting: Cells in this region were counted as number of cells per length of CA1. For this purpose three areas of 300 μm length each were selected. First, a 300 μm-long area was selected in the centre of the CA1, and then other two areas of the same length on either side with about 50-100 μm distance between them depending on the size of CA1 area. Cells that were apart from main CA1 cell cluster were included if they were within 45 μm of cell area.

CA3 cell counting: Cells were counted in the middle part of CA3 area i.e. CA3b. As in CA1 area the number of cells per length of CA3 was counted in three areas of 300 μm length each, and about 20-50 μm apart from each other depending on the length of the CA3 area. Cells that were apart from the main CA3 area were only counted if they were within 45 μm of this area.

3.4.1 Data analysis and statistics

In hilar region cell density was measured for each slice i.e. number of cells per area in a slice. Mean hilar cell density per animal was calculated by averaging cell density from six slices for each animal. Number of cells per length of the CA3 and CA1 was measured in three areas then this was summed for each slice followed by calculation of the average (six slices from each animal) cell number in each animal. To check for Gaussian distribution Shapiro-Wilk and Anderson Darling tests were carried out. One way ANOVA test was used to compare cell number between the groups. This was carried out using OriginPro 9.0 (OriginLab) software.

3.5 PPS model with implanted wireless subcutaneous EEG transmitters

The stimulation electrode used for these surgeries consisted of a two-channel threaded plastic pedestal with two stainless twisted leads attached to it [Plastics One Inc], each with a diameter of 0.125 mm; the tips of the electrode were exposed about 1-2 mm (see 0).

3.5.1 Wireless Subcutaneous EEG Transmitter implantation

A Wireless Subcutaneous Transmitter (A3019D, Open Source Instruments) is a small, battery-powered sensor with an antenna, which is a loop of stainless steel wire, and two electrode leads (stainless steel springs), all enclosed in silicone (see **Figure 2.7**).

A transmitter was implanted subcutaneously in the dorsal part of the rat body. The reference and the recording electrodes were inserted down into the scalp through the drilled holes (see **Figure 2.8**). The recording electrode was positioned 2 mm further down intracranially to enable recordings from the cortex, with the coordinates as described above. The reference electrode with a screw attached to its end was implanted in the contralateral side of the brain. 7-10 days following surgery the same protocol as described above was used for inducing status epilepticus and subsequent drug administration. Animals were then transferred to the telemetry unit with Subcutaneous Transmitter System (Open Source Instruments) for continuous 24 hour electroencephalogram (EEG) recording.

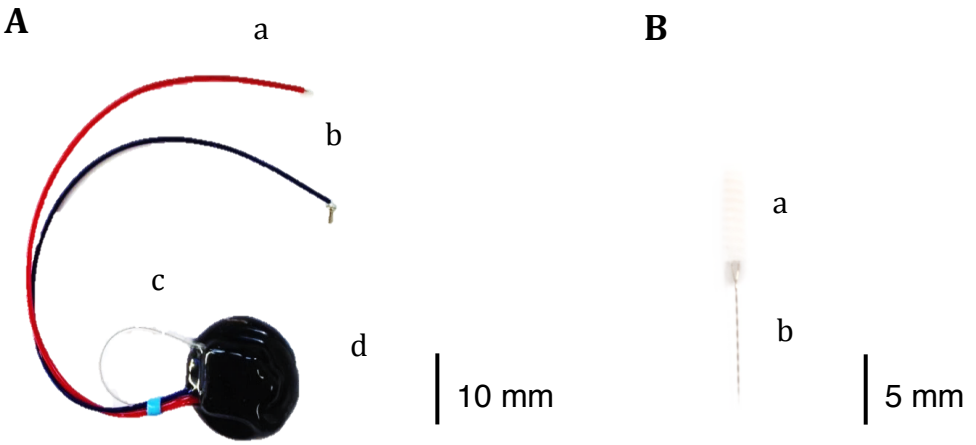

Figure 2.7. A - Subcutaneous transmitter.

A) Recording electrode b) Reference electrode c) antenna d) battery-powered sensor. **B -** Stimulating electrode a) plastic pedestal b) stainless twisted leads

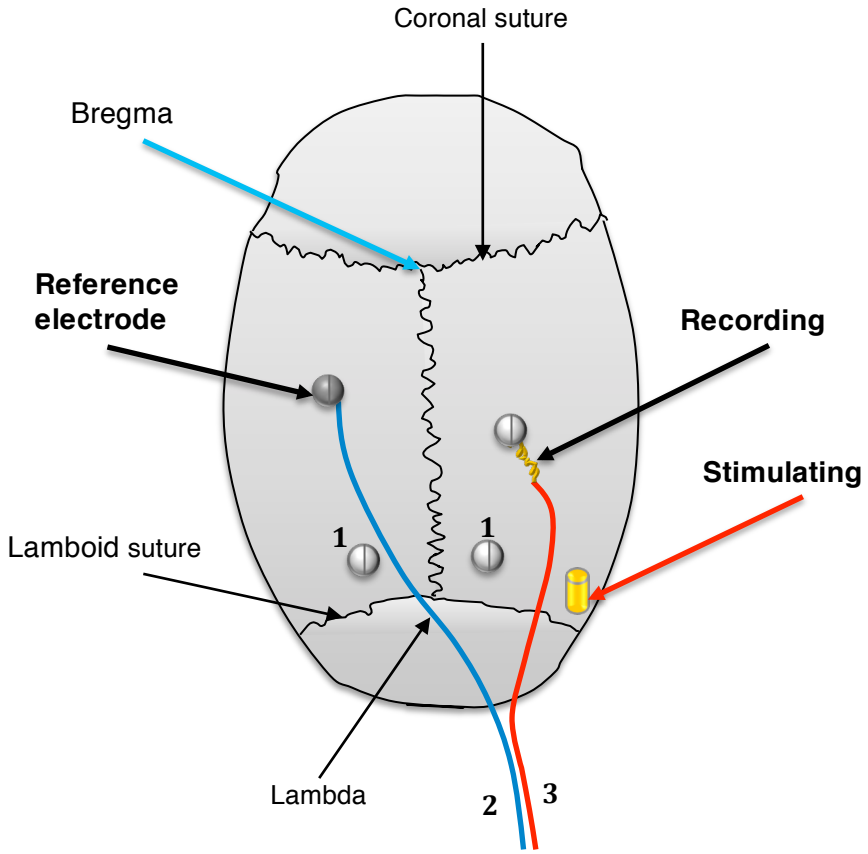

Figure 2.8. Electrode implantation sites in the rat skull in PPS.

After taking coordinates for bregma *stimulation* and *recording electrode* position was calculated. **1** - 2 screws were inserted to stabilise head peace. *Reference electrode* with screw attached to t was inserted in the contralateral side to stimulation side. *Recording electrode* was inserted intracranially and then secured with a screw. **2, 3** – wires were tunnelled under the skin

3.5.2 Wireless Subcutaneous Transmitter System

The system (circuit) includes a subcutaneous transmitter with a loop antenna, external antenna, antenna combiner, data receiver and Long-wire-data acquisition (LWDAQ) driver (see **Figure 2.9**).

The transmitter conveys signals to the external antenna that acts as a signal receiver, via radio transmission over a distance of between 50-300cm. External interference was isolated by use of Faraday cages; up to two animal cages in each. Each Faraday cage had an independent antenna, outside the animal cage. Antenna conducts signal to the Data Receiver via the antenna combiner (Chang et al., 2011).

The Data Receiver connects to the LWDAQ driver with Ethernet interface, which provides an interface between the Internet and the Data Receiver. The LWDAQ driver transmits the signal to the computer that records and stores the signal. In the software a Recorder instrument enables to download data from the Data Receiver and a *Neuroarchiver Tool* used to record and analyse transmitter signals (Chang et al., 2011). Sampling rate was 512 Hz for all recordings.

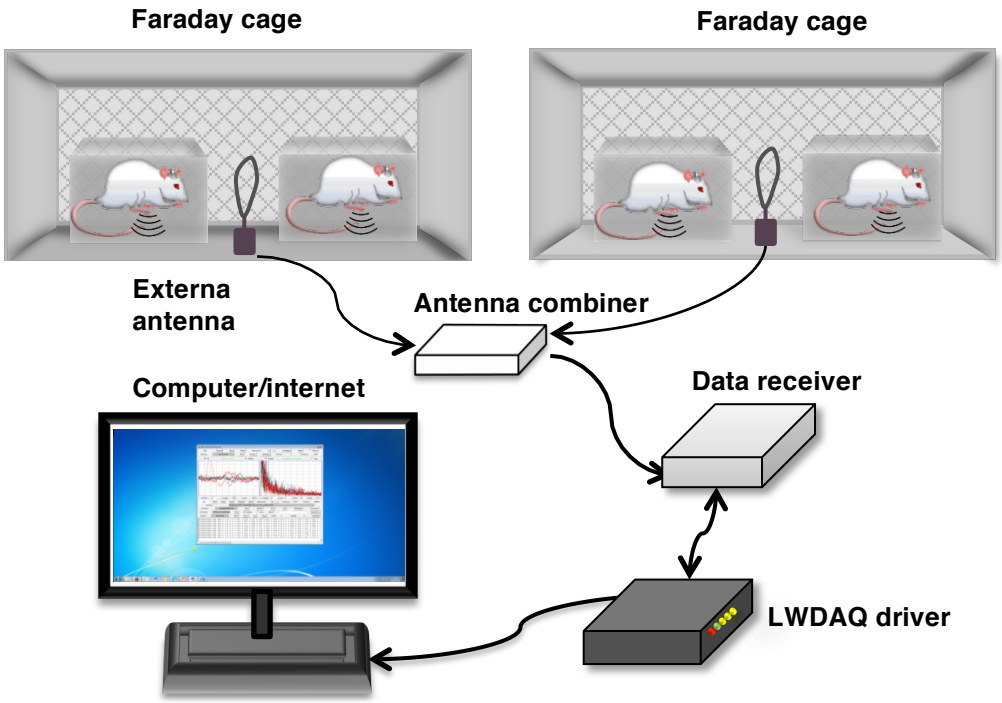

Figure 2.9. Schematic illustration of the of the wireless transmitter circuit.

Each *Faraday cages* contains two rat cages. Two faraday cages are connected via *Antenna Combiner* and then transmit signals to the *Data Receiver*. The latter connected to the computer via *LWDAQ driver* and internet.

3.5.3 Automatic Seizure detection tool

The *Event Classifier* program in Neuroarchiver was used to detect seizures. It detects events automatically based on comparison of pre-selected events in an *Event library* (**Figure 2.10**). The Classifier operates based on the baseline power and the interval metrics (Open source instruments).

1.1 Event detection library

In order to create an Event detection library different types of events were selected and added to the library from each animal's EEG. 1 s epochs of events were included in the library; this time period was validated for better detection of seizures. EEG Recordings of a week or more from each animal that were selected at random times from stimulation date were visually processed to identify seizures and detected seizures were recoded. Various seizure types from each animal were included in the library; fragments from different parts of seizures as well as afterdischarges were included. Then other seizure-related activities such as high frequency, interictal events, short spikes etc. were also included. Thereafter, various EEG events due to noise, muscle artefacts from eating or moving were added to the library. Events were classified in the library as seizure, eating artefact, high frequency etc. and all non-specific artefacts were categorised as non-event.

Then the Event library was tested and modified multiple times with addition or exclusion of some events until desirable balance of seizures and non-seizure events are present in the library i.e. it has high sensitivity and detects all various types of seizures. To confirm this all previously identified seizures had to be correctly detected. However, a perfect library was not possible to create. Moreover, because the library identifies only 1 s long events interictal activity was also detected as a seizure. Therefore, this automatic analysis was followed by visual detection of to further classify detected activity (i.e. this was a semi-automated approach).

A

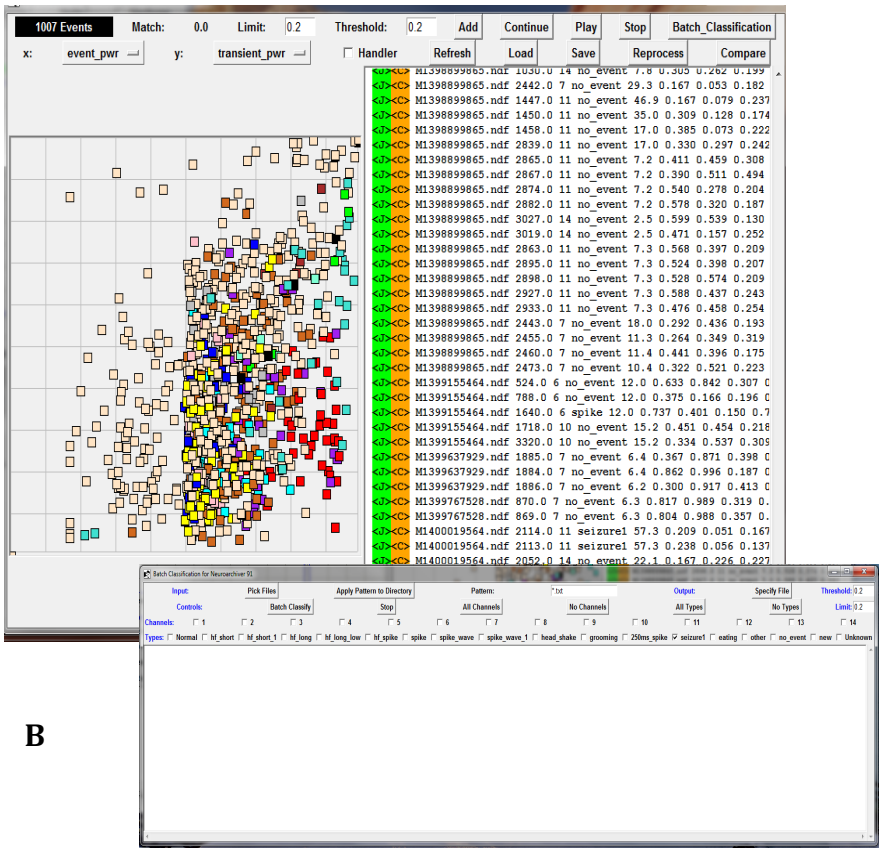

B

Figure 2.10. Event Classifier.

A - Event Classifier opens in a new window. Different type of seizures from all animals (n=13) were included in the library, 1007 events in total. Left-hand side of the window shows event map and the right side event list. **B –** Batch classification window. The text files uploaded and channel and event of interest is selected (i.e. seizure) for batch analysis.

Seizure counting: Seizure counting was done on blinded fashion, for treatment and epileptic groups. Only events of 20 s duration or more were included, with spiking frequency more than 3 Hz and evolution of spiking activity. These are conservative criteria but were selected in order to identify definite seizures rather than runs of spikes or polyspike activity.

Seizure duration measuring: Duration of seizure was counted from the start of seizure till the end when the frequency of spiking was less than 3 Hz. The start of the seizure was defined when there was an abrupt change in baseline power and continuous activity with a frequency of 3Hz occurred. Afterdischarges following a seizure were not included.

3.5.4 Coastline analyses

A coastline length of the EEG is the sum of absolute difference in voltage between consecutive data points. Neuroarchiver tool determined EEG power for different frequency bands; 6-8 hour EEG periods were processed in Neuroarchiver. Then exported text files were uploaded into Labview (National Instruments) for coastline analysis. "*Glitches were excluded if they exceeded 5 × root mean square, and the signal was high pass–filtered at 10 Hz before calculating the coastline*" (Wykes et al., 2012).

3.6 Behavioural study: alternating T maze

Perforant path stimulated rats were tested 3-4 month following SE induction.

The alternating T maze is widely used to assess cognitive function in rodents, in particular memory and spatial learning. Rats and mice have natural tendency to alternate between branches: this reflects the animal's desire to explore the surrounding environment and locate the presence of resources such as food. Alternation test (Both spontaneous and rewarded) is very reliable in detecting hippocampal dysfunction and is superior to other behavioural tests. Rewarded t-maze is more reliable and precise (Deacon and Rawlins, 2006). Although radial maze and water maze are also used to test spatial memory function, the alternating t-maze was chosen in the current study for the following reasons. Radial maze has certain disadvantages: animals may solve the maze without relying on spatial memory function, such as chaining or a serial strategy. Animals may enter each arm successively in a systematic order, either always turning to the right or left and entering adjacent arm and this may not measure working memory efficiently. Although experimenter observes animal for such chaining behaviour irregular chaining patterns can be difficult to distinguish from working memory (Vorhees and Williams, 2014). Although the water-maze is a very robust test, the task is dependent on recognising visual cues; since SD rats that I used in this study have poor vision this test would not be the best option.

3.6.1 Apparatus

The t-maze apparatus [Med Associates, Inc. , USA; UK distributor: Sandown Scientific, UK; Standard T-Maze Package for Rat] consisted of Rat T-Maze Hub, 2 Rat Modular Maze Runways, Rat Modular Maze Runway, Start/Goal Box and 3 Manual Guillotine Doors. The walls made of transparent plastic material (see **Figure 2.11**).

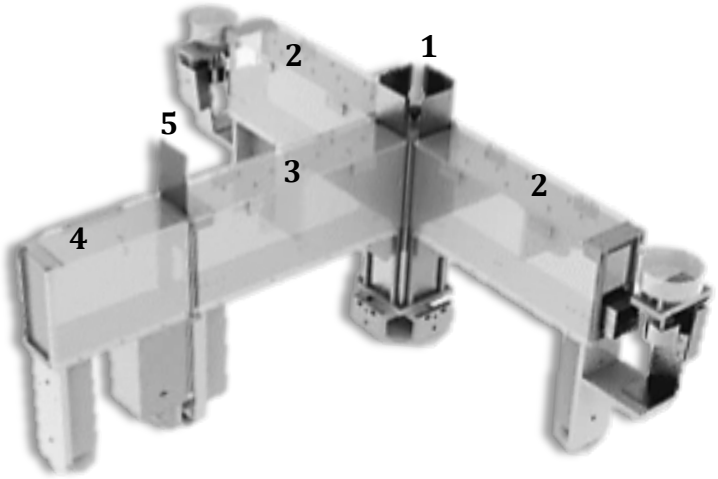

Figure 2.11. T maze apparatus.

1) Rat T-Maze Hub, 2) Rat Modular Maze Runways (46 cm), 3) Rat Modular Maze Runway (31 cm), 4) Start/Goal Box (25.4 cm) and 5) Manual Guillotine Door.

3.6.2 Procedure

The protocol described by Deacon and Rawlins (Deacon and Rawlins, 2006) was used with little variations. Reward t-maze test consisted of the following parts: habituation, training, main experiments. Animal were weighed 2 subsequent days before starting restricted diet to obtain baseline weight.

Then on daily basis to ensure that animals maintain 90-95% of their free-feeding body weight. Animals were brought in to study room 5-10 min before starting trial: if left longer they may fall asleep and not perform well whereas starting trial immediately may result in the rats being over-excited with poor concentration.

3.6.3 Habituation

Animals were handled for couple of days several times a day until they are thoroughly tamed. Only if well habituated and relaxed an animal will learn well (Deacon and Rawlins, 2006). Animals were familiarised with reward pellets (45mg dustless precision pellets) in their home cages for a couple of days. Then the night before starting habituation all regular diet was removed from the cages and animal were given only restricted amount (4-5g/100 g rat) of reward pellets. The following day animals were weighed. An individual animal was placed in the t-maze with all arms open to freely explore the maze. Both arms were full of reward pellets. Animals were allowed no more than 3 min to freely explore the maze: this is adequate time to explore the maze and eat pellets however longer exposure may induce aversion to unknown environment and following exposure can cause anxiety. Then animals immediately returned to the home cages. This procedure was repeated 3-4 times per rat every day until they each eat several pellets on both sides of the maze. Once animal fully habituated then following the training started.

2.1 Initial training

Initial training procedure aimed to allow animal to explore the maze and to reduce anxiety to the novel environment. Moreover, to train animals to eat reward pellets in the goal arms. This training had six steps (see **Table 2.5**).

3.1 Main training

Access to the correct choice arm was restricted. Animal were placed in the start arm. The sample arm was baited with one pellet and the choice arm with 2 pellets. Once animal reaches the end of sample arm and consumed the pellet it was placed back to the start arm not facing T junction. Then the door to choice arm was open animal was allowed to make a choice. If the correct arm was chosen, the rat was given time to eat both pellets and then returned back to the cage. If an incorrect arm was chosen then rat still remained in the arm for the duration of time necessary to consume the pellet and thereafter was removed from the maze. Left/Right (R/L) arm sequence during training and main experiments were randomised so that all rats receive the same number of both left and right arm; the sequence to one side was no more than three times, for example, RRRLLL, LRRL, but not RRRRL.

Table 2.5. T maze initial training steps

Training steps	Procedure
Step 1	Access to start arm was closed and goal arms were filled with reward pellets. Animals were placed from one arm to the maze. Once each rat eats several pellets they were returned back to the cage.
Step 2	Rats are placed on a goal arm and access to the rest of the maze was restricted. The aim is to ensure each rats eats about 6 pellets.
Step 3	Access to the start arm was blocked; both goal arms were available and full of food
Step 4	Starts as step 3 then the block was removed
Step 5	Similar to step 3 without block.
Step 6	Animal was placed on the distal end of the start arm with no block

During the main test animal was given 5 second retention interval (the time period between expose to sample and choice phase) before making choice of arm, and then 60 seconds. Increasing retention interval can help to reveal dysfunction better. Time from when animal started going towards T junction to make a choice until it entered a goal arm with 4 feet was noted as delay time.

3.6.4 Data analysis: T-maze

The average correct choice (%) for all trails was calculated per animal group. Shapiro-Wilk and Anderson Darling tests were carried out to check for Gaussian distribution. One way ANOVA test, followed by Tukey's post hoc test was carried out to compare correct arm choice between the groups.

Chapter 3. Blocking TRPM7 channels inhibits *in vitro* epileptiform activity

1. Introduction

The association between low Mg^{2+} and epilepsy is well known. Seizures commonly occur in genetic Mg^{2+} deficiency syndromes and in acquired hypomagnesaemia, due to malabsorption, alcoholism and certain medications (Baaij et al., 2015). In addition, magnesium sulphate is the first line treatment in eclampsia - pregnancy induced seizures. The exact mechanism of this is not well known, and it has been suggested that the magnesium may be having effects by vasodilation and lowering the blood pressure. There have also been reports of the successful treatment of SE with intravenous magnesium, but other studies have not found such an effect, possibly because increasing peripheral magnesium levels has a minimal effect on central nervous system (CNS) levels (Baaij et al., 2015). Furthermore, lowering extracellular Mg^{2+} is a very well established method to induce *in vitro* seizure-like activity. Initially, it was thought that low Mg^{2+} model induced epileptiform activity through releasing the magnesium block of NMDA receptors. Although blocking NMDA receptors in the early stages can prevent the induction of epileptiform activity, NMDA antagonists fail to block epileptiform activity in the later stages. This raises the possibility that other mechanisms contribute to late sustained seizure-like activity in this model. Opening of TRPM7 channels is one possibility, as TRPM7 channels are also activated by low intracellular Mg^{2+}. Once open, TRPM7 channels can depolarise neurons, as the channels are also permeable to sodium and calcium, and such depolarisation could exacerbate epileptic activity.

What about the possible role of TRPM7 channels in seizure activity that is not the result of lowering magnesium concentrations? Since low extracellular Ca^{2+} concentrations, oxidative stress and decreased pH also open TRPM7 channels and these processes occur during seizure activity, then TRPM7 channels could play a role in seizure-like activity generated in conditions when magnesium concentrations are not reduced.

Therefore the current study, for the first time, aimed to test the involvement of TRPM7 channels in seizure generation in low magnesium and normal magnesium conditions.

I used two different blockers of TRPM7 channels to test my hypotheses. The drugs used were carvacrol and a novel, possibly more specific antagonist, Waxienicin A. As explained previously carvacrol was the most appropriate of other antagonists to extend to *in vivo* studies (see chapter 1). It is a naturally occurring compound with a simple structure that is unlikely to have many adverse effects on animals. Moreover, carvacrol has already been used in *in vivo* studies and was well tolerated without known toxic effects. However, carvacrol later has been reported to have an effect on sodium channels (Joca et al., 2012), then I wished also to investigate further the specificity of carvacrol.

1.1 Aims and hypotheses

Hypothesis 1. TRPM7 current will increase during low Mg^{2+} induced seizure activity. We hypothesized that blocking TRPM7 channel by antagonists added to the extracellular medium would decrease or abolish *in vitro* epileptiform activity by reducing influx of cations, such as Na^{+} and Ca^{2+} to cells and thus decrease cell depolarisation.

Hypothesis 2. TRPM7 channels will also be activated during seizure activity induced in physiological Mg^{2+} concentrations, under the influence of other mechanism that open the channel and take place during seizure activity, such as decreased low extracellular Ca^{2+}, low pH and reactive oxygen species (ROS) formation.

Aim 1: To investigate the effect of TRPM7 channel inhibition on *in vitro* epileptiform activity in two different models – one with reduced extracellular magnesium and the other with physiological magnesium.

Aim 2: To determine whether carvacrol has relevant effects on sodium channels that would reduce it's potential to be used as a specific inhibitor of TRPM7 channels.

2. Methods

To test the above hypotheses two different TRPM7 channel blockers were used. *Carvacrol*, a non-specific blockers. *Waxiencin A* is a newly identified specific blocker of the channel, which was obtained recently from Hawaii Pacific University.

2.1 Carvacrol experiments

For the drug-treated experiment after initial 20 minute baseline recording 1 mM carvacrol (Sigma Aldrich, UK) was added to the perfusion solution and the effects were recorded for 20 minute (see **Figure 3.1**). Then the drug was washed out from the slice for an hour. In 7 out of 14 experiments carvacrol was dissolved in DMSO (0.26%) prior to adding to the perfusion solution and in other seven experiments carvacrol was added without DMSO.

For the control recordings the same procedure was applied and recorded for the same total amount of time (100 minute). In 6 out of total 13 control experiments DMSO was added as a vehicle to the perfusion solution (0.26%) after 20 minute of the baseline recording. This was recorded for next 20 minute. Then, DMSO was washed out during one hour. In 7 control recordings vehicle was not added. This was done in order to have 2 types of control recordings that matched drug treated experiments.

Half of experiments with carvacrol in drug and control groups were conducted with DMSO and half without. There was no significant difference between these two sets of experiments, therefore they were combined for analyses.

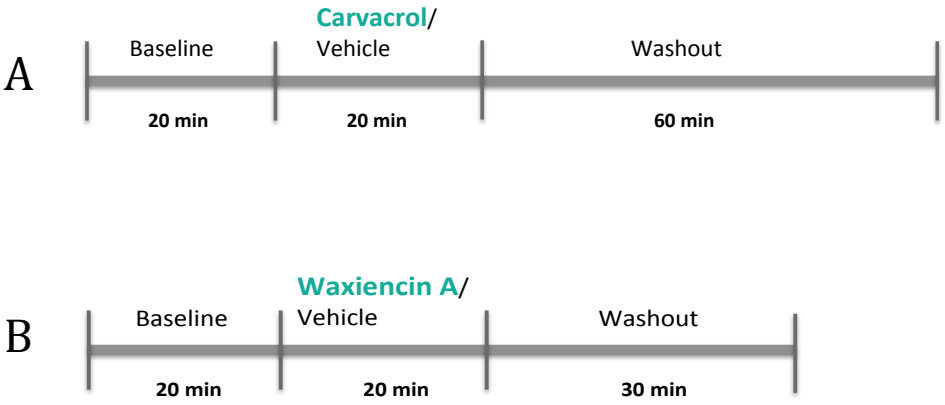

Figure 3.1. Timeline of *in vitro* experiment protocols treated with:

A –Carvacrol, **B** and **C** - Waxiencin A

2.2 Waxienicin A experiments

Waxiencin A is a potentially selective TRPM7 channel blocker (Zierler et al., 2011). It was isolated from Hawaiian soft coral in Hawaii Pacific University. I used the minimal effective dose (10 μM) for PTZ and 10-20 μM for low Mg^{2+} experiments.

Dissolving Waxiencin A: The specific protocol provided by DH from Hawaii Pacific University was used to dissolve Waxiencin A. In brief, 50 µl of 99% methanol was added to the vial containing 50 µg Waxiencin A, then once half of methanol volume evaporated 1035 µl of a buffer (PTZ or low Mg^{2+} containing ACSF) was added to dissolve the compound completely. Then this solution was added to the perfusion solution to make required concentration. Final concentration of methanol in the perfusion solution was 0.23% in PTZ and 0.46% in Low Mg^{2+} experiments.

Low Mg^{2+} induced activity. After 20 minute of baseline activity, 10-20 µM of Waxiencin A dissolved in methanol was added to the perfusion solution. After 20 minute Waxiencin A was washed out from the slice by low Mg^{2+} containing ACSF and recorded for another 30 minute (see **Figure 3.1).** Similar to carvacrol Waxiencin A also inhibited both ictal and interictal like activity induced by low Mg^{2+}.

PTZ induced activity After 20 minute of baseline activity, 10 µM of Waxiencin A dissolved in methanol was added to the perfusion solution. After 20 minute Waxiencin A was washed out from the slice by PTZ containing ACSF and recorded for another 30 minute.

Control recordings. In control recordings 0.23 % methanol was added to the perfusion solution in PTZ experiments and 0.46 % methanol in low Mg^{2+} experiments after 20 minute of baseline recording and after 20 minute was washed out from the slice for 30 minute.

The frequency and amplitude of epileptiform activity in all *in vitro* experiments were averaged per 5 minute. The data (frequency and amplitude of epileptiform activity in each group) was normally distributed ($p > .05$, Shapiro Wilk test – cannot reject normality) in all set of *in vitro* experiments. Therefore, appropriate parametric tests were employed: *unpaired t-test* to compare unmatched groups and *paired t-test* for comparing matched data. To compare the effect of

the compounds mean last 10 minute of drug versus vehicle administration interval were compared.

3. Results

3.1 Carvacrol inhibited *in vitro* seizure-like activity

3.1.1 Low Mg^{2+} experiments

Types of activity: In low Mg^{2+} seizure model both ictal-like and interictal-like epileptiform activities are generated in combined hippocampo-cortical slices (see **Figure 3.2** and **Figure 3.3**). Ictal-like activity occurred every 3-4 minutes and lasted about 0.5-1.5 minute. Ictal-like activity is purportedly generated in entorhinal cortex and spreads to CA3 and CA1 areas, whereas interictal activity is generated in CA3 and then spreads to CA1 area (Jefferys et al., 2012). Spikes and polyspike events occurred throughout some recordings, more frequently in PTZ induced activities. These were not included in the analysis. An epileptiform burst was defined as field potential activity with an amplitude more than three times that of baseline, containing more than 2 subsequent spikes that do not return to baseline, and with overall duration ≥ 40 ms. Single spikes and polyspikes not meeting this criteria were not included in analyses. Epileptiform discharges initiated in combined hippocampal-entorhinal cortex slices 20-30 minutes after transferring the slices into low Mg^{2+} containing ACSF solution. Both ictal and interictal-like activity were used to assess the effect of the TRPM7 channel blocker.

Carvacrol significantly inhibited the frequency and amplitude of low Mg^{2+} induced epileptiform activity (p <0.001, two sample t-test, for both frequency and amplitude) (see **Figure 3.4**). In carvacrol treated slices after 5 minute of

the drug administration epileptiform activity started to decrease. The activity was completely abolished after about 10 minute following carvacrol administration. Carvacrol had the same inhibitory effect on both ictal and interictal-like activity. During washout of the drug with low Mg^{2+} ACSF only very little restoration of the activity was observed towards the end of washout period. Random short single spikes or polyspikes were observed in all experiments that were distinct from baseline epileptiform activity, and were not included in the count of burst activity (see **Figure 3.3 C**). Frequency and amplitude of epileptiform activity in control recordings were constant over the first 80 minute with a small decrease in some recordings thereafter.

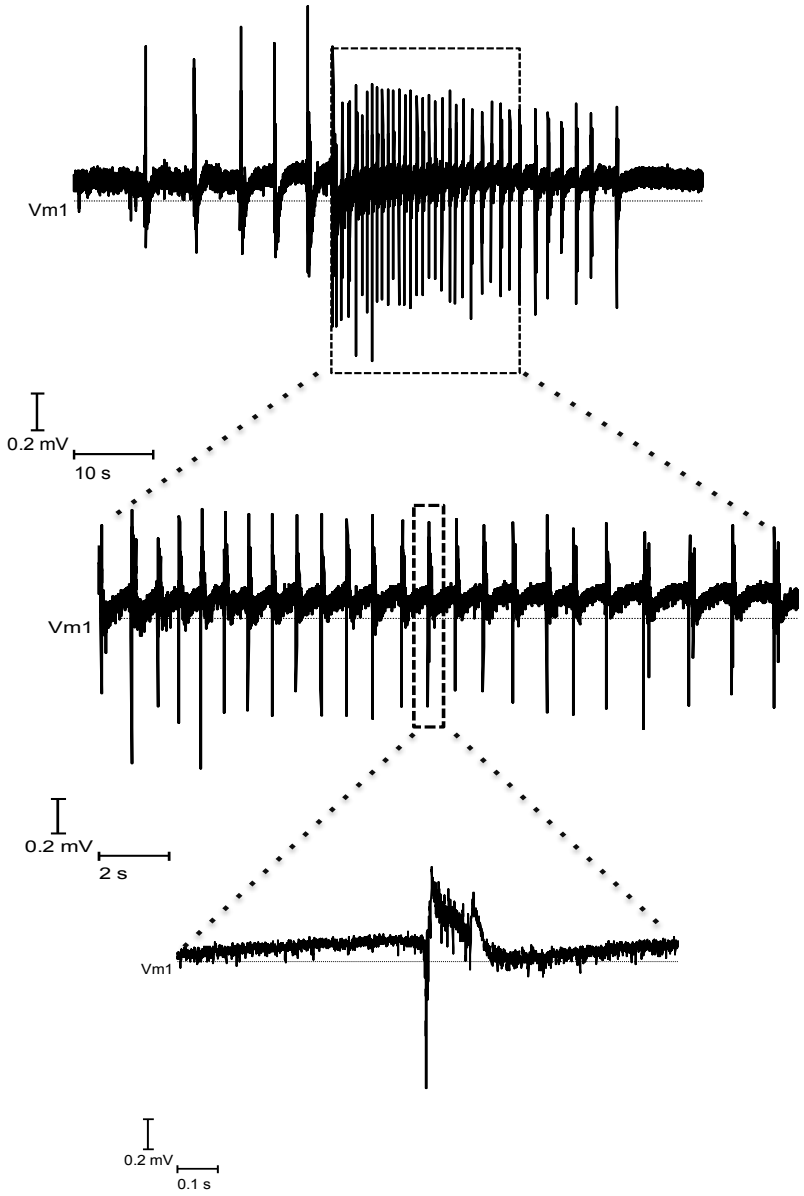

Figure 3.2. An example trace of ictal like activity induced by low Mg^{2+}

Ictal like activity occurred every 3-4 minutes and lasted about 0.5-1.5 minute. Frequency of epileptoform discharges initially is high, then this gradually decreases

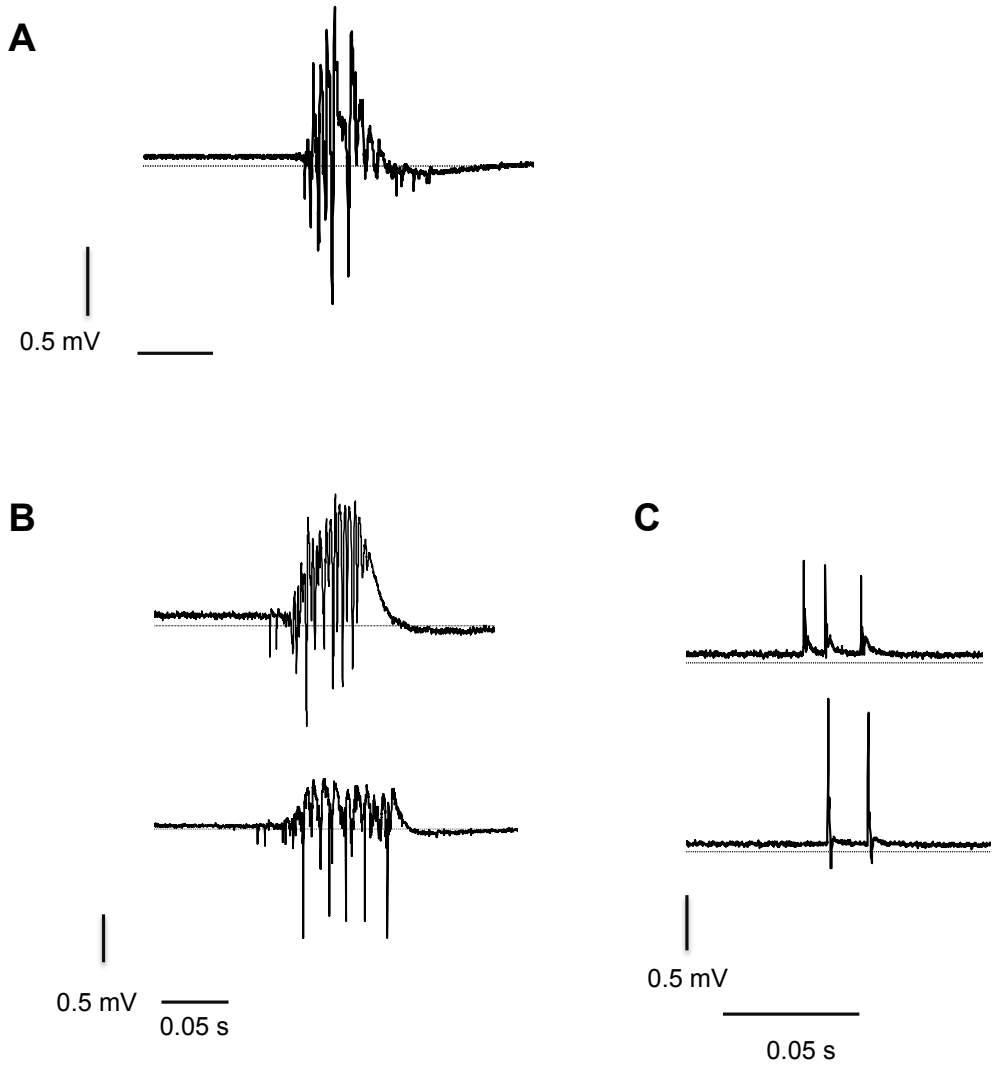

Figure 3.3. Example traces of inter-ictal like activity induced by:

Low Mg^{2+} (A) and PTZ (B); and spike-like activities (C)

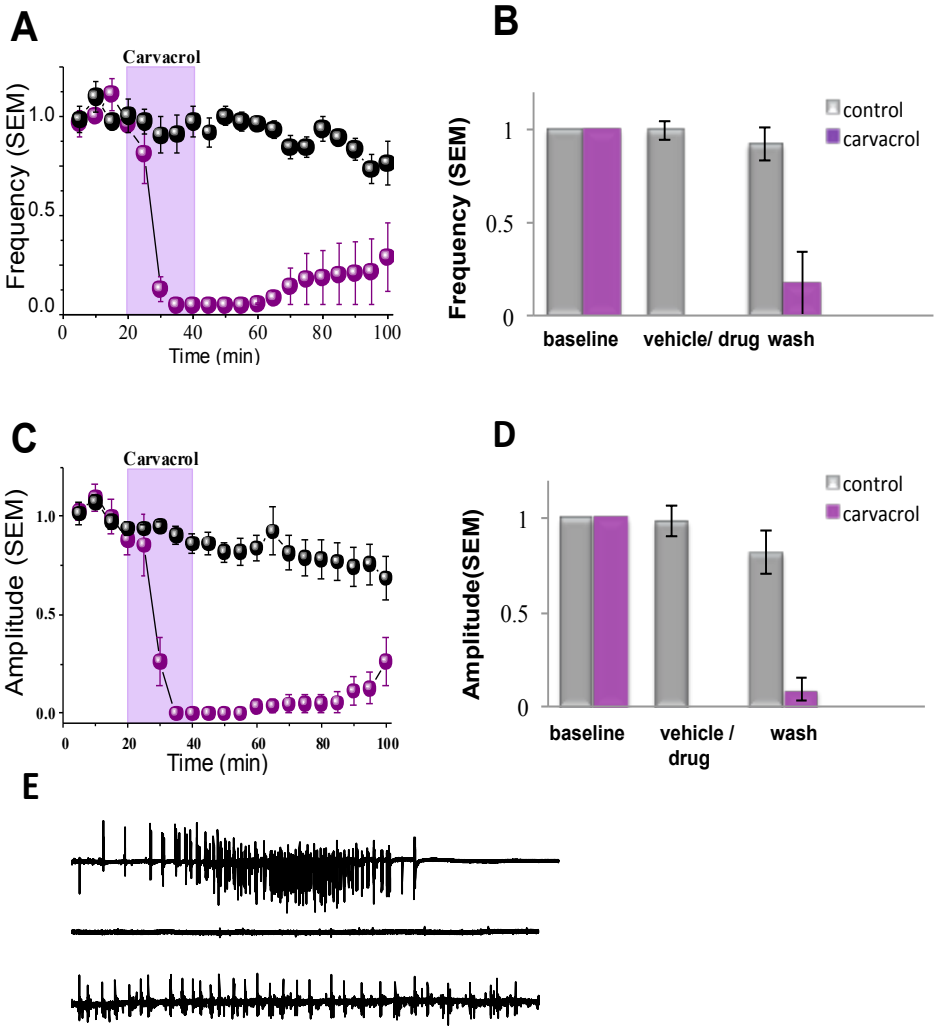

Figure 3.4. Carvacrol inhibited low Mg^{2+} induced seizure-like activity in hippocampal-entorhinal cortex slices:

A - scatter plot shows frequency of epileptiform discharges (mean±SEM) (normalised to baseline) of carvacrol–treated (1 mM) (n=7) and control experiments (n=6), averaged to 5 minute. **B** - bar charts represent mean±SEM frequency of baseline, vehicle/carvacrol-treated and washout periods, ***P .001 (two sample t-test). **C** - scatter plot shows amplitude of epileptiform discharges (mean±SEM) (normalised to baseline) of carvacrol –treated and control experiments, averaged to 5 minute. **D** - bar charts represent mean±SEM amplitude of baseline, vehicle/carvacrol-treated and washout periods, ***P .001(two sample t-test). **E** – Low Mg^{2+} induced ictal-like epileptiform activity recorded from CA1 region of the hippocampus during; 1) baseline activity 2)-carvacrol-treated and 3)- washout periods

3.1.2 PTZ experiments

One possible confounder in the above experiments could be that low Mg^{2+}may preferentially open TRPM7 channels. I, therefore, used an alternative *in vitro* seizure model where epileptiform activity is induced in normal extracellular magnesium concentrations, using the $GABA_A$ receptor antagonist PTZ. PTZ (2 mM) induced epileptiform events in combined hippocampo-entorhinal cortex slices after ~30-40 minute of exposure. PTZ generates almost exclusively interictal-like epileptiform activity. However, this activity tends to cluster sometimes.

In carvacrol treated slices epileptiform activity started to diminish about 5 minute after drug administration and completely stopped within 10 minute. Carvacrol significantly reduced the frequency and amplitude of PTZ induced epileptiform discharges [two sample t- test P <0.001 for both] (see **Figure 3.5**). During washout period there is a partial restoration of the activity towards the end of the washout period. However, in some recordings inhibition of epileptiform activity was not reversible. Control recordings had stable frequency and amplitude over

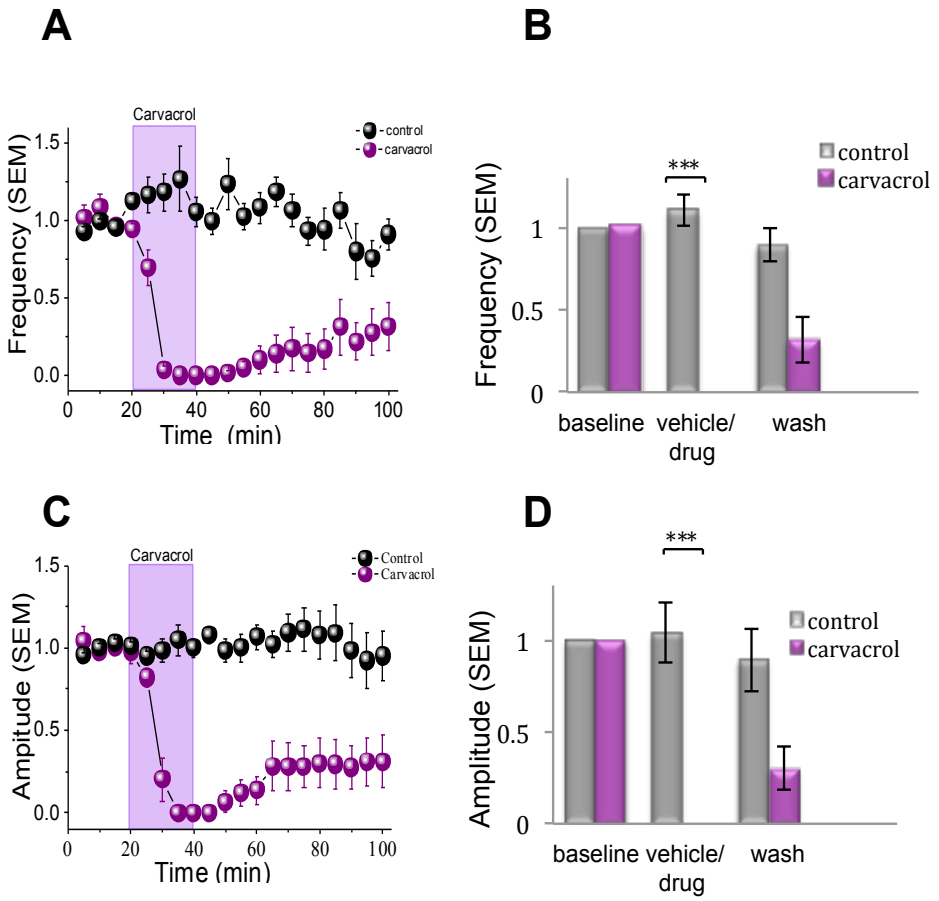

Figure 3.5. Carvacrol inhibits low PTZ induced epileptiform discharges in hippocampal-entorhinal cortex slices:

A - scatter plot shows frequency of epileptiform discharges (mean± SEM) (normalised to baseline) of carvacrol–treated (1 mM) (n=7) and control experiments (n=7), averaged to 5 minute. **B** - bar charts represent mean± SEM frequency of baseline, vehicle/carvacrol-treated and washout periods, ***p<.001 (two sample t-test). **C** - scatter plot shows amplitude of epileptiform discharges (mean± SEM) (normalised to baseline) of carvacrol –treated and control experiments, averaged to 5 minute. **D** - bar charts represent mean± SEM amplitude of baseline, vehicle/carvacrol-treated and washout periods, ***p <.001(two sample t-test).

the recording time. As with Low Mg^{2+} induced activity, the PTZ induced activity also decreased in both frequency and amplitude after about 80 minute of recording in some control recordings.

3.2 Effect of Carvacrol on fEPSP

Since carvacrol is the most convenient of the two inhibitors to be used for *in vivo* experiments, (more easily obtainable than waxiencin A), but has been reported to have effects on peripheral sodium channels, I wished to test its action on central neurotransmission. After 20 minute of baseline recording of fEPSP, carvacrol (1mM) was added to the perfusion solution for 20 minutes. Carvacrol increased the amplitude and slope of fEPSPs; the slope and amplitude started to increase 3-4 minute after adding carvacrol to the perfusion solution (see **Figure 3.6**). The normalised mean slope during carvacrol treatment period was significantly greater than the baseline ($p< .05$ paired t-test*).* There was no significant change in fibre volley slope after carvacrol addition suggesting that carvacrol does not affect sodium channels in acute brain slices.

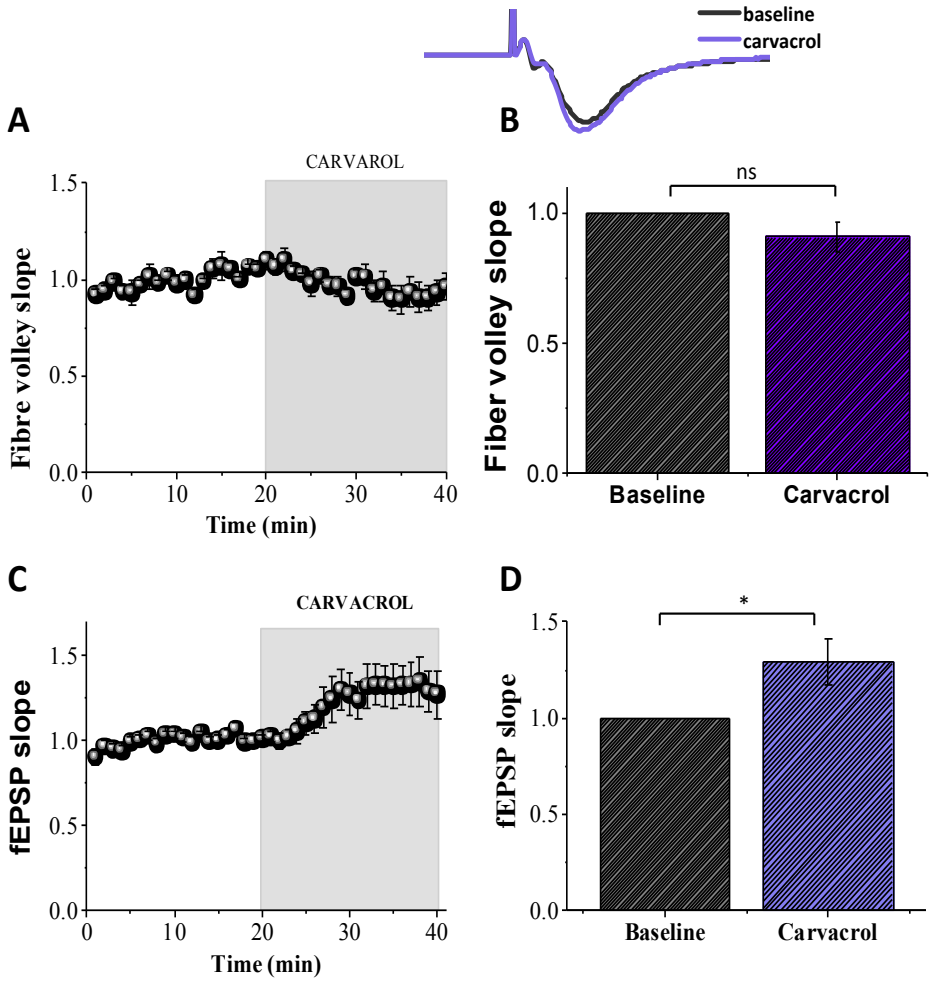

Figure 3.6. Effect of carvacrol (1mM) on single pulse induced fEPSP.

A - Scatter plot of normalised (mean ± SEM) fibre volley slope over 40 min, averaged for 1 min (n=7). Carvacrol was added after 20 minute of baseline recording. **B** – Average trace of fEPSP and bar charts represents mean ± SEM fibre volley slope of baseline period and carvacrol-treated time, ns P>0.05 (paired t-test). **C** - Scatter plot of normalised fEPSP slope (mean ± SEM) over 40 min, averaged for 1 min (n=7). **D** – bar chart represents mean (SEM) slope of fEPSP, Carvacrol significantly increased the slope of fEPSP, * P<0.05 (paired t-test).

3.3 Waxiencin A inhibited in vitro epileptiform activity

3.3.1 Low Mg^{2+} experiments

In Waxiencin A added slices low Mg^{2+} induced epileptiform activity started to diminish immediately after the drug administration: the activity substantially decreased within 5 minute and completely stopped by 20 minute from the drug addition time. Blocking TRPM7 channel by Waxiencin A significantly reduced frequency of epileptiform discharges [p <.001, two sample t- test] (see **Figure 3.7**). During washout of the drug the epileptiform activity was partially restored. Control recordings had stable frequency and amplitude over the recording time.

3.3.2 PTZ experiments

In Waxiencin A treated slices epileptiform activity induced by PTZ started to decline immediately after the drug administration and completely stopped by 15 minute. Waxiencin A significantly reduced frequency of PTZ induced epileptiform discharges [two sample t- test p<.001] (see **Figure 3.8**). During washout period the activity although partially restored but did not reach baseline level. Control recordings had stable frequency and amplitude over the recording time.

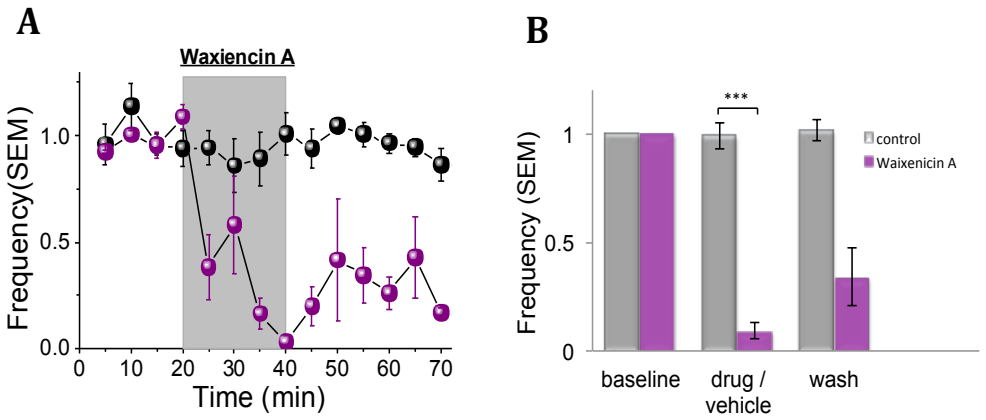

Figure 3.7. Waxiencin A inhibits low Mg^{2+} induced epileptiform discharges in hippocampal-entorhinal cortex slices:

A - scatter plot shows frequency of epileptiform discharges (mean± SEM) (normalised to baseline) of Waixenicin A –treated (10-20 μM) (n=5) and control experiments (n=5), averaged to 5 minute. **B** - bar charts represent mean± SEM frequency of baseline, vehicle/carvacrol-treated and washout periods, ***P< .001 (two sample t-test).

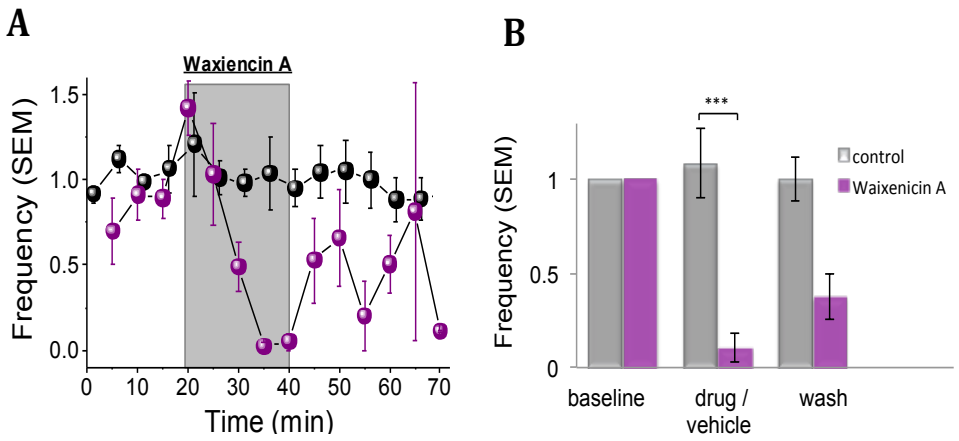

Figure 3.8. Waxiencin A inhibits PTZ induced epileptiform discharges in hippocampal-entorhinal cortex slices:

A - scatter plot shows frequency of epileptiform discharges (mean± SEM) (normalised to baseline) of Waixenicin A –treated (10 μM) (n=5) and control experiments (n=5), averaged to 5 minute. **B** - bar charts represent mean± SEM frequency of baseline, vehicle/carvacrol-treated and washout periods, ***P< .001 (two sample t-test).

4. Discussion

The present study for the first time assessed the effect of TRPM7 channel antagonists on *in vitro* seizure-like activity; here we provide evidence of TRPM7 channel involvement in seizure generation in two *in vitro* seizure models. The inhibitory effect of TRPM7 channel blocking on seizure-like activity is shown with two different TRPM7 channel antagonists.

Carvacrol, a non-selective TRPM7 channel antagonist completely abolished epileptiform activity in both low Mg^{2+} and PTZ *in vitro* seizure models. This study used carvacrol for the first time to assess its effect on epileptiform activity *in vitro* through blocking TRPM7 channel currents.

Carvacrol completely blocks epileptiform discharges within 10 minute of addition to the perfusion solution. During washout period in both low Mg^{2+} and PTZ experiments only a small reversible activity was seen. Insufficient washout may be caused by high affinity of carvacrol to the binding sites of TRPM7 channel. This can also be due to slow restoration of the TRPM7 channel currents. An alternative, and perhaps more likely, explanation is that there is significant non-specific binding of carvacrol in the slice preparation.. Control recordings had constant frequency and amplitude over about 80 minute with only a slight decrease of both amplitude and frequency thereafter.

However, it is not clear if such remarkable effect of carvacrol is exclusively due to TRPM7 channel inhibition or alternative pathways are also involved. Carvacrol has numerous therapeutic effects: antimicrobial, antifungal, antitumor and antidepressant-like effects. Of the TRP family carvacrol has stimulatory effect on thermo TRP channels, TRPV3 and TRPA1 and inhibits drosophila TRPL channel which is a mammalian TPRC analogue (Parnas et al., 2009). Nevertheless, none of these channels have known effects on neuronal excitation. Only one study suggested inhibition of sodium channels by carvacrol. The study showed a block of the compound action potentials (CAP)

with carvacrol. In our experiments carvacrol not only did not inhibit but potentiated fEPSPs in hippocampal-entorhinal cortex slices and also had no effect on the fibre volley, suggesting that a significant inhibitory effect on sodium channels did not occur in this preparation. This could possibly be explained by different variants of sodium channels in peripheral nerves and CNS, and different duration of application. In the above mentioned study inhibition of CAP was observed after 180 minute of carvacrol administration, which is much longer than the administration used in the current study.

Waxiencin A, a potentially specific antagonist of TRPM7 channel, had significant inhibitory effect on epileptiform activity in small concentrations in both low Mg^{2+} and PTZ induced activity. Waxiencin A initiates an effect almost immediately as it reaches the slice. The minimal effective concentration of Waxiencin A (10µm) was sufficient to inhibit epileptiform activity induced in the presence of normal Mg^{2+} concentrations and in low Mg^{2+} conditions. Zierler et al. reported that that higher dose of Waxienicin A needed to block TRPM7 current in low Mg^{2+} concentrations (Zierler et al., 2011). 10 μM Waxiencin A blocks the channel current completely in physiological intracellular Mg^{2+} (700 μM) concentrations but the same concentration blocks the current by 50% in zero Mg^{2+} conditions. However, when in addition extracellular Mg^{2+} was also removed Waxiencin A supressed the channel's activity only by 30% (Zierler et al., 2011). Waixenicin A was initially tested in low magnesium model with 20µm because of concerns that in low magnesium conditions channels activate and large dose maybe needed to block it. However, when later I tried smaller doses (10 µm) this concentration also decreased the epileptiform activity. When I analysed the results I saw no difference between i.e. in both concentrations (10 µm and 20 µm) Waxiencin A significantly inhibited epileptiform activity. This suggests that TRPM7 channel play a role in seizure activity whether under low Mg^{2+} or physiological Mg^{2+} concentrations.

Both non-specific and a potentially specific TRPM7 channels antagonists block *in vitro* epileptiform activity generated by both PTZ and low Mg^{2+}. This two

seizure models induce epileptiform activity via different mechanisms; increasing excitability (low Mg^2) and decreasing inhibition (PTZ) in the network. The low Mg^{2+} ASCF solution would activate TRPM7 channels due to decreased extracellular Mg^{2+} concentrations whereas PTZ induces seizure through a mechanism that does not change Mg^{2+} levels. This shows that activation of TRPM7 channels in epilepsy may occur not only due to reduced low magnesium concentrations but also through other mechanisms such as oxidative stress and low pH.

In vitro seizure models can be used to study as defined electrographic excessive neuronal discharge in an isolated brain tissue. This is a useful tool for initial investigation of the effect of certain compounds on isolated abnormal activity to identify a possible targets involved in seizure generation. Benefit of such *in vitro* experiments is that they can be employed to detect subtle changes in isolated tissue, and the blood brain barrier and other pharmacokinetic issues are avoided. However, the *in vitro* seizure-like activity may differ mechanistically from *in vivo* seizure activity, and together with the pharmacokinetic considerations, *in vitro* data should be used cautiously to extrapolate to the *in vivo* situation.

5. Summary of the chapter

The effect of blocking TRPM7 channel on epileptiform activity was assessed in two *in vitro* seizure models: low Mg^{2+} and PTZ with two different TRPM7 channel antagonists. Carvacrol, a non-selective blocker of the TRPM7 channel, completely abolished epileptiform activity induced by both low Mg^{2+} and PTZ after 10 minute of administration. Waxiencin A, a potentially selective blocker of TRPM7 channel substantially decreased epileptiform activity induced by both low Mg^{2+} and PTZ after 5 minute of administration, completely abolishing the activity after ~15 minute.

Chapter 4. Carvacrol prevents cell death following status epilepticus

1. Introduction

Status epilepticus causes cell damage in the hippocampus and related structures. In perforant path stimulation animal model of status epilepticus, cell loss is most prevalent the first day following induced SE, reaching the peak during first 24 hours and some damage continues to occur during the first week. Cell loss in TLE is more prominent in the hilus followed by CA1 and to a lesser extend in CA3 area. In animal models (PPS) with shorter duration of stimulation, less than 60 minute, damage is confined to the hilus, whereas longer stimulation period causes damage to other parts of hippocampus and related structures (Norwood et al., 2011). Post SE cell damage was related to excessive neuronal firing and Ca^{2+} influx to the cell triggering excitotoxicity related cell death pathways. One of the goals in disease modification in epilepsy is to prevent neurodegeneration/cell death and thus, related functional deficits and possibly prevent epileptogenesis.

Although NMDA receptors are thought to play an essential role in excitotoxic cell death in conditions such as stroke, anoxia, brain trauma and epilepsy the role of TRPM7 channels in this process is now becoming widely recognised. Blocking NMDA and L-type channels alone did not prevent anoxia induced cell damage in clinical trials (Nicotera and Bano, 2003). Therefore, involvement of other pathways in excitotoxicity was suggested, such as TRPM7 channels. Oxidative stress and ROS production induced by excessive NMDA activation leads to TRPM7 channel activation, allowing further CA^{2+} influx, and this in turn triggers further ROS production, which contributes to positive feedback loop, opening more TRPM7 channels. Moreover, the TRPM7 channel was suggested to predominate in this pathway and play essential role even in the absence of NMDA receptor block (Nicotera and Bano, 2003). Therefore, even though NMDA receptors play a role initially in excitotoxicity later TRPM7 channel activation in such stress conditions leads to continuous cell firing and damage.

Blocking TRPM7 channels had neuroprotective effect in an *in vivo* stroke model (Sun et al., 2009) in CA1 region of the hippocampus. Moreover, other studies have also shown neuroprotective effects following ischemia –hypoxia induced cell damage by blocking TRPM7 channel with carvacrol (Yu et al., 2012; Chen et al., 2015). However, the involvement of TRPM7 channels in epilepsy related cell death has not been investigated yet.

Given that TRPM7 antagonists also have antiseizure effects *in vitro*, I also wished to test whether carvacrol could stop status epilepticus, unfortunately due to toxicity this experiment was not possible (see below).

Aim: To test the effect of TRPM7 channel inhibition on cell survival after SE induced hippocampal damage

Hypothesis: TRPM7 channel activation during excessive neuronal firing will contribute to cell depolarisation, and Ca^{2+} entry via the channel can trigger a cascade of processes contributing to cell toxicity and death. Moreover, Zn^{2+} as well as other trace metals entering the cells in stress conditions via TRPM7 channel can play a role in cell death. Therefore, blocking TRPM7 channel would prevent or reduce cell damage in vulnerable areas of the hippocampus.

2. Methods

In order to assess neuronal cell loss in the hippocampus cells were counted in six non-adjacent slices per hippocampus representing dorsal part of the hippocampus. Cell counting described in details previously (see chapter 2). Cell death was quantified in CA1, CA3 and hilar regions of the hippocampus in epileptic, epileptic treated and control animals three to four weeks following induction of SE. Because maximum cell death in PPS model is observed in the first week following induced SE, this time window would be sufficient to detect hippocampal damage. Initially, carvacrol was given to animals in doses of 200 mg/kg to test if carvacrol could stop SE. However, this dose of carvacrol was

poorly tolerated by the animals. Therefore, these experiments were discontinued. Lower doses of carvacrol (75 mg/kg) instead were used to test its effect on preventing cell death following SE.

Although some authors reported that similar damage occur ipsi- and contralateral to the stimulation side in PPS model, other studies have shown that contralateral sparing does occur. Therefore, I assessed cell death ipsilateral to the stimulation, i.e. right hemisphere.

2.1 Carvacrol protocol development

In order to choose the appropriate dose of the carvacrol for the in vivo use i.e. that could be tolerated well by animals several different protocols were tried.

Protocol I. After stopping stimulation and ensuring the SSSE had developed 200 mg/kg of carvacrol in DMSO was administered i.p. to animals in the treatment group. Then recording of SSSE was continued for 3 hours. To terminate SE after 3 hour 10 mg/kg diazepam was given i.p. and 5 ml saline was administrated s.c. to hydrate the animal. Carvacrol did not stop SE, and the animals died after diazepam administration. This could possibly be due to combined inhibitory effect of carvacrol and diazepam on respiration. Two drug treated animals died after injecting diazepam. Although minor respiratory depression was observed in control-stimulated animals after diazepam administration this improved later. In one of two drug treated PPS experiments inhibition of both motor and electrographic seizures for 30-40 minutes was observed with later reverse of seizure discharges on EEG but not behavioural seizures.

Protocol II. The same procedure as above was applied with reduced dose of carvacrol - 100 mg/kg. The following day a small proportion of animals displayed features of distress and following vet advice were culled and therefore not included in this study.

Final protocol. After stopping stimulation and ensuring the SSSE had developed, diazepam (10 mg/kg IP) was given and EEG was observed for 20-30 minutes to ensure SE had stopped. 5 ml saline was administrated S.C. to hydrate the animal. Following this, drug treatment group (n=6) received 75mg/kg i.p. of carvacrol without DMSO (see **Figure 4.1**). Stimulated control group (n=6) received the same amount of IP saline injection. Then next two doses of carvacrol and saline were administrated (i.p.) about every 8 hour so that animals received 3 doses of carvacrol during the first 24 hour after SE induction. Control animals (n=6) that were not stimulated did not receive any treatment. All animals that developed SSSE after perforant path stimulation were included in study. Animals that were unwell after stimulation and those that lost headpiece were culled early and excluded from the analysis (two in epileptic, two in drug treated group).

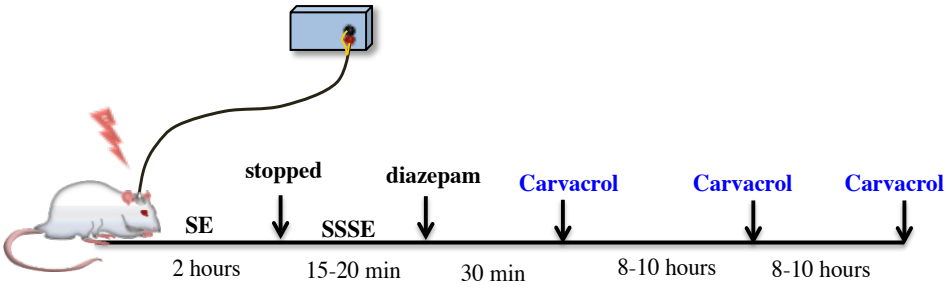

Figure 4.1. Time line of carvacrol treatment protocol.

Carvacrol was given 3 times during first 24 hour after induction of status epilepticus (SE): first dose after 30 min of diazepam injection then next 2 doses with about 8-10 hour intervals between injections.

Perfusion/fixation and immunostaining protocol as well as cell counting is reported in the general methods chapter (see chapter 2.). Due to difficulty in differentiating between cells in hilar and CA3c area I used the criteria described in the general methods section (see chapter 2.). When counting NeuN stained cells if uncertain i.e. staining is not very bright, checking DAPI on the same cell by switching between channels enabled to confirm presence of a neuron.

3. Results

3.1 PPS reliably induced SE

Perforant pathway stimulation following a week of electrode implantation reliably induces self-sustaining status epilepticus after 2 hours of stimulation (see **Figure 4.2**) in about 95% of animals. Seizure severity during stimulation varied between stage 3 (forelimb clonus) and stage 5 (full motor seizure with loss of postural controlling) based on Racine scale. Most animal develop stage 1 and stage 2 seizures initially, immediately or within the first 10-15 minutes. Afterwards seizure severity was between stage 3 to stage 5 for the rest of the stimilation duration. After stopping stimluation during SSSE seirure severity varied between stage 1 and 5.

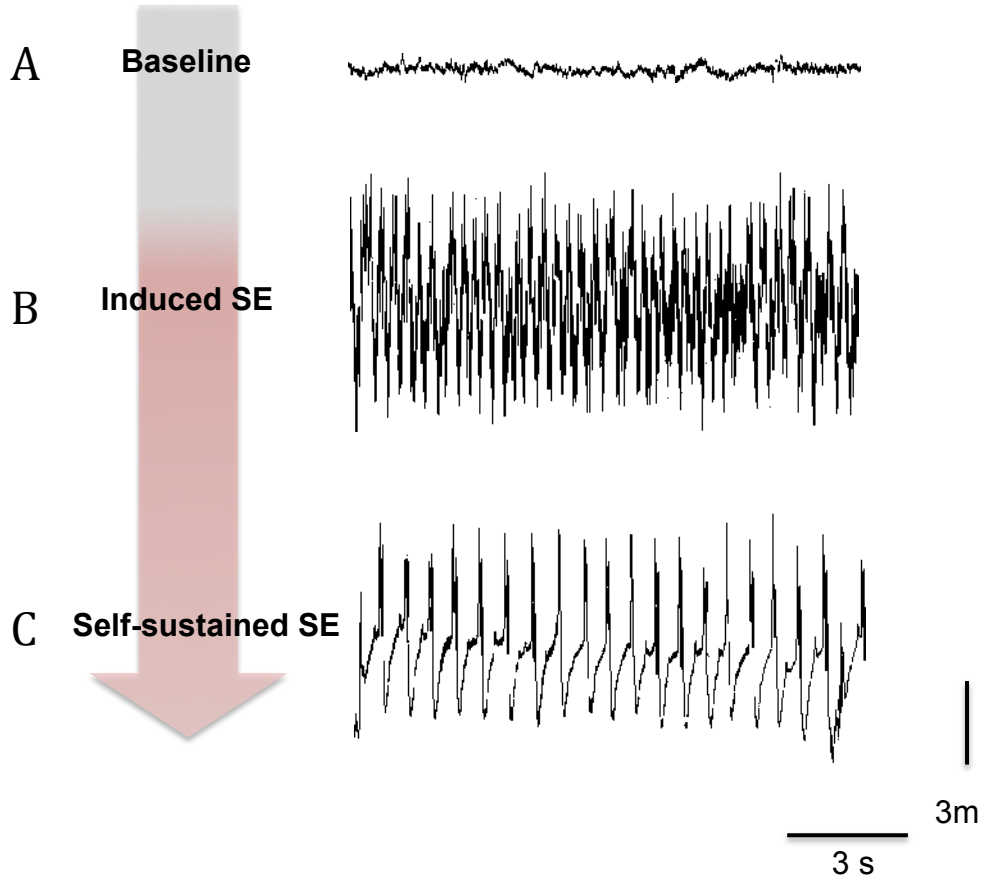

Figure 4.2. Perforant path stimulation.

A sample traces of electrophysiology recordings during**:** baseline activity (**A**), electrically induced status epilepticus (SE) (**B**) and self sustained status epilepticus (SSSE)(**C**).

3.2 Carvacrol had neuroprotective effect in the hilus

The summary of cell count statistics is shown in Table 4.1. The difference in cell density in the hilar region across the three groups was statistically significant [$F\ (2,14) = 7.14$, p = .007, one way ANOVA]. The average cell density in the hilar region (see Table 4.1, **Figure 4.3**) in epileptic animals reduced significantly compared to control animals [p=0.007, One-way ANOVA, Turkey post hoc].

Epileptic animals had ~43 % neuronal cell reduction compared to control animals whereas in epileptic animals treated with TRPM7 channel blocker, only ~13 % cell reduction was observed. Likewise the cell density in epileptic treated animals was also higher compared to epileptic animals [p = .04, post hoc Tukey's test]. However, there was no significant difference in hilar cell density between treated epileptic and control groups. This shows that inhibiting TRPM7 channel by carvacrol significantly rescued cell death in the hilus.

Table 4.1. Summary statistics of cell count in three area of the hippocampus

Groups	Mean* ± SD	SEM	95% Confidence Interval
	Hlius		
Epileptic	0.22±0.02	0.01	0.20 -0.23
Control	0.38±0.04	0.02	0.32 -0.43
Epileptic + Carv	0.33±0.12	0.05	0.21 -0.45
	CA1		
Epileptic	125.15±7.88	3.52	115.37 -134.93
Control	156.95±11.53	5.16	142.64 -171.27
Epileptic + Carv	160.31±4.14	1.85	155.17 -165.45
	CA3		
Epileptic	107.90±9.43	4.22	96.20- 119.60
Control	125.47±18.72	8.37	102.22 -148.72
Epileptic + Carv	120.59±11.42	5.11	106.42 -134.76

SD – standard deviation, SEM – standard error of the mean, Carv- carvacrol, * mean cell density in hilar region and mean cell count in CA1 and CA3 regions.

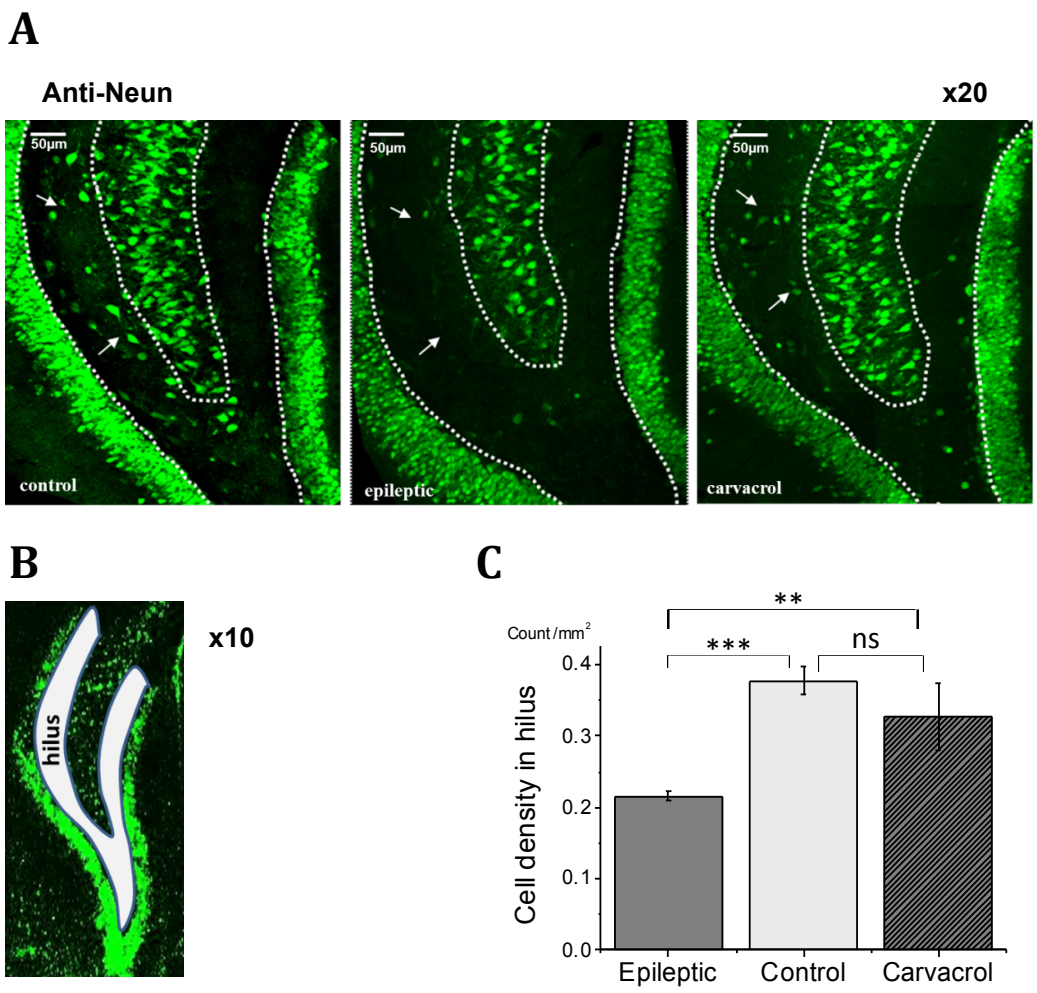

Figure 4.3. Cell count in hilar region of the hippocampus.

A - Confocal images (x20 magnification) showing coronal sections of anti-NeuN stained hilar region in control (left), epileptic (middle) and carvacrol treated (right) animals. **B** – A Confocal image (x10 magnification) of the hilar area showing the region of cell counting. **C**- Bar charts show mean± SEM cell count in three groups of animals. *** $p < 0.007$, ** $p = 0.04$, One-way ANOVA, Tukey's test.

3.1 Carvacrol had neuroprotective effect in CA1

In CA1 area neurons were counted as a number of cells per length of the CA1 region as describe in general methods section due to difficulty in defining borders of CA1. Therefore, cell count per length would give more accurate estimate of cell number per region compared to calculating cell density. Only very few cells were located further apart from CA1 region, whereas most of them within 45 µm distance. Therefore, cells within the distance of 45 µm were also were included.

One way ANOVA showed that cell number in CA1 differed significantly across the three groups [$F\ (2,12) = 26.6,\ p\ \ .0.001$]. Mean neuronal cell count in CA1 region was significantly reduced in epileptic animals compared to control animals [p <.001, post hoc Tukey's test]. A lesser degree of cell loss was observed in CA1 region (by ~ 20 %) compared to hilar region in epileptic rats. This cell loss was completely rescued by blocking TRPM7 channel. There was almost no difference in CA1 cell count between carvacrol treated epileptic and control animals (see **Figure 4.4**) [p >0.05, post hoc Tukey's test] whereas cell count between epileptic and treated epileptic groups was statistically significant [p< .001, post hoc Tukey's test]. In some slices in certain areas of CA1 complete loss was also seen.

3.1 No significant cell death was observed in CA3

No significant cell loss was observed in CA3 area [$F\ (2,12) = 2.16,\ p$ = .16, One way ANOVA]. There was not significant difference in cell number across the three groups. Although epileptic animals had slightly reduced cell number this was not statistically significant.

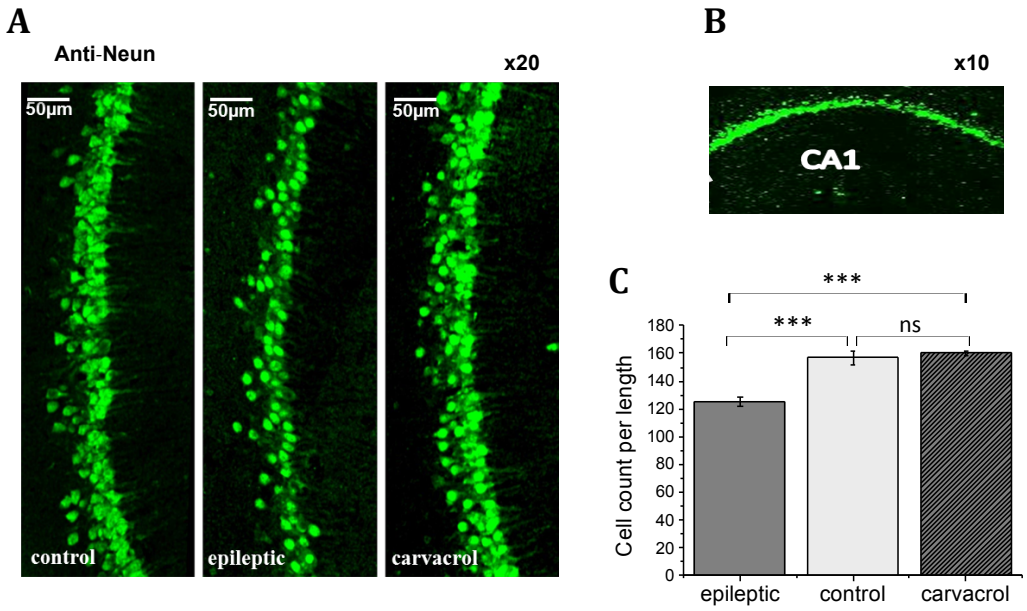

Figure 4.4. Cell count in CA1 region of the hippocampus.

A. - Confocal images (x20 magnification) showing coronal sections of NeuN stained CA1 area from slices in control (left), epileptic (middle) and epileptic animas treated with carvacrol (right). **B** – A confocal image (x10 magnification) of CA1 region showing the region of cell counting. **C** – bar chart represent mean± SEM cell number per length of CA1 in three groups of animals. ****p* <.001, ns – *p*>0.05, One-way ANOVA, post hoc Tukey 's test

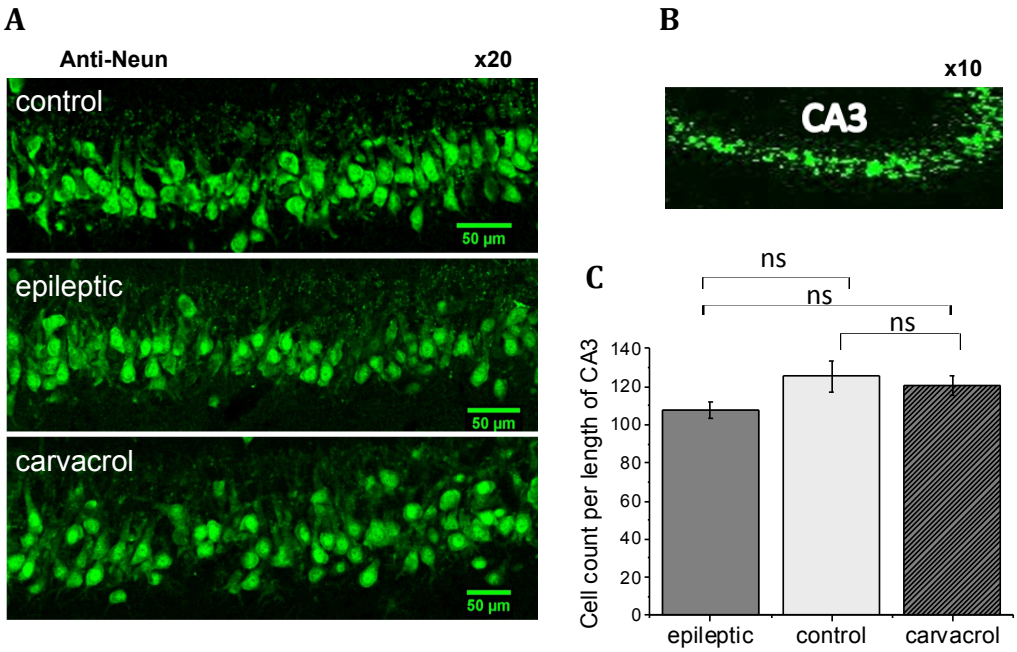

Figure 4.5. Cell count in CA3 region of the hippocampus.

A. - Confocal images (x20 magnification) of CA3 area from slices in control, epileptic and epileptic animas treated with carvacrol. **B** – A confocal image (x10 magnification) of CA3 area showing the region of cell counting. **C** – bar charts represent mean± SEM cell number per length of CA3 in three groups of animals. There is no significant difference in cell count between control, epileptic and treated animals. ns – $p > .05$, One-way ANOVA.

3.2 Expression of TRPM7 channel in the hippocampus

I then was interested to see qualitatively the pattern of expression of TRPM7 channel in the three areas of the hippocampus: CA1, CA3 and the hilus. The example images taken from a heathy control animal in order to assess if the areas where I quantified cell damage TRPM7 channel is present. To exclude non-specific binding of TRPM7 channel, a negative control was performed without adding primary anti-TRPM7 antibody (see chapter 2) and this did not show any staining. Immunostaining pattern shows that TRPM7 channels are expressed widely in the hippocampus. They are expressed in the neuronal cell bodies as well as in dendrites and axons (see **Figure 4.6**). Although I did not quantify the intensity, it seems that greater TRPM7 channel immunoreactivity is present in the CA1, followed by hilus and to a lesser degree in CA3 region.

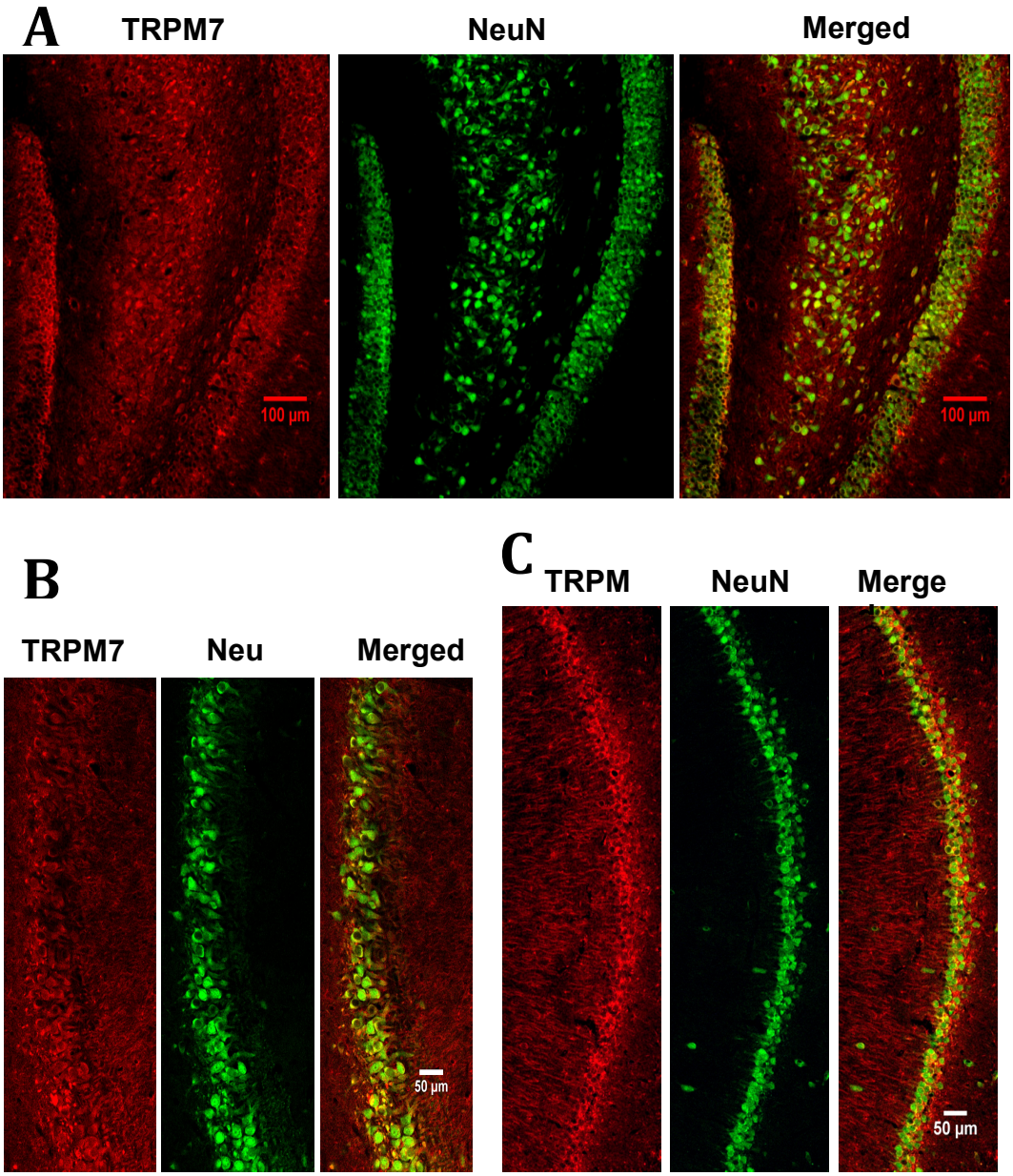

Figure 4.6 Confocal images (20x) showing expression pattern of TRM7 channel in the hippocampus in healthy control animal (A) –hilus, (B) – CA3, (C) – CA1.

4. Discussion

The pattern of cell damage following SE seen here was consistent with what has been observed in PPS model in previous studies, except the absence of damage in CA3 area. The most severe damage was seen in hilar region with almost half of the neurons lost. To a lesser degree damage was observed in CA1 area, about 20% of CA1 neurons were lost in epileptic animals. Blocking TRPM7 channel prevented cell loss in both hilar and CA1 regions; almost no cell loss was observed in CA1 region of epileptic animals treated with carvacrol.

Contrary to previous studies I did not detect cell loss in CA3 region in epileptic rats compared to control animals. Although there was a trend for the cell number in CA3 area in epileptic animals to be lower compared to that in the control group, this did not reach significance. While cell damage in CA3 area was reported in PPS epilepsy model, the cell loss was minimal in this area compared to CA1 and hilus (Pauli et al., 2006). A possible explanation for not detecting cell damage in CA3 area in the current study could be that cell damage was subtle in CA3 area and was not detected with conservative cell counting methods.

Moreover, CA3 region is generally less sensitive to excitotoxic cell damage compared to CA1 area (Gee et al., 2006; Ohmori et al., 1996). CA1 region is more vulnerable to variety of damage such as oxidative stress, ischemia/stroke as well as in neurodegenerative disorders (Butler et al., 2010).This has been explained by lower expression of AMPA and NMDA receptors in CA3 compared to CA1 area (Baltan et al., 2013). AMPA receptors are activated first then depolarised cells trigger NMDA activation. Therefore, in CA3 fewer AMPA and NMDA receptors are activated, hence the region is less vulnerable to excitotoxic damage. As discussed above NMDA receptors are important to induce excitotoxic cell damage. This then could trigger activation of TRPM7 channels.

Blocking TRPM7 channel by carvacrol provided better protection of neuronal cell death in CA1 area compared to hilar region: cell death in CA1 was completely prevented by carvacrol. First, this could be explained by less severe damage to CA1 area (~ 20 % cell loss) compared to hilar region (~ 50 % cell loss) after SE. In addition, cell damage in hilar region is initiated earlier than in CA1 during perforant path stimulation (Norwood et al., 2011). It was shown that 40 minute stimulation already causes damage to hilar region whereas stimulation over 60 min led to damage to other areas of the hippocampus.

Blocking TRPM7 channel with carvacrol prevented initial cascade of processes triggered by excessive neuronal firing that leads to cell damage. Although treatment was given only during the first 24 hour following induced SE this was sufficient to prevent neuronal cell death in the hippocampus. It was shown in previous studies that cell death in PPS model is at peak level during first 24 hour. Carvacrol has short half-life and rapidly excreted by kidneys (Tisserand and Young, 2013; Michiels et al., 2008). Therefore, we proposed administration of carvacrol 3 times during first 24 hour after SE, every 8-10 hour, could provide better neuroprotection than a single injection post SE.

TRPM7 channel inhibition prevented cell death in ischemia/anoxia induced brain damage. Carvacrol has been reported to reduce infarct volume and improve neurological defect after ischemia/reperfusion injury in mice (Yu et al., 2012). Yu et al. showed that carvacrol substantially decreased infarct volume and improved neurological deficits after 75 min of ischemia and 24 h of reperfusion(Yu et al., 2012). This neuroprotection was dose-dependent. This result is consistent with previous studies that have reported a neuroprotective role of blocking TRPM7 in ischemia induced damage in CA1 (Sun et al., 2009). Intrahippocampal injections of viral vectors bearing shRNA against TRPM7 channel made neuronal cells resistant to ischemic death after brain ischemia and prevented ischemia-induced deficits in LTP and preserved memory function (Sun et al., 2009). Here I showed that TRPM7 inhibition also prevented

cell death induced by SE. In both ischemia and SE induced cell death excitotoxicity and Ca^{2+} overload of the cells play an essential role.

However, NMDA blockers alone did not prevent cell death in anoxia induced cell damage. Blocking TRPM7 by sRNAi had significant effect in preventing Ca^{2+} overload and cell death in the absence of NMDA block suggesting its essential role in this pathway for both excitotoxic and non-excitotoxic neuronal damage. TRPM7 is more important in prolonged anoxia induced excitotoxicity because NMDA receptors become desensitised quickly under anoxia conditions. Blocking NMDA receptors did not have protective effects in clinical trials. Further, NMDA antagonists would only block excitotoxicity and unmask the predominant pathway for Ca^{2+} entry -TRPM7 pathway (Nicotera and Bano, 2003).

Possibly in the future concurrent use of NMDA and TRPM7 blockers *in vivo* and in clinical trials could provide better protection against cell death following brain insult that leads to cell damage. Because carvacrol is a food additive and hence a safe compound it can also be transferred easily into clinical research.

5. Summary of the chapter

Perforant path stimulation in 8-9 week old rats produced chronic epilepsy in ~95% of animals. Hippocampal coronal sections 3-4 week following induced SE was immunostained with anti-NeuN followed by counting neurons in three areas of the hippocampus; CA1, CA3 and hilar region. Epileptic rats had 40-50% loss of neurons in hilar region and ~20% loss in CA1 region. No significant difference was observed in cell number in CA3 area between control and epileptic groups. The cell loss was prevented by blocking TRPM7 channels with carvacrol in both CA1 and hilar region, with complete preservation of neuron in CA1 area. This finding suggests an essential role of TRPM7 channels in SE induced hippocampal damage.

Chapter 5. Anti-seizure and antiepileptogenetic effect of TRPM7 channel

1. Introduction

The development of chronic acquired epilepsy has been linked to an initial brain insult. However, it is not clear whether loss of neurons itself is the main contributing factor or downstream pathways that are triggered after an insult or compensatory synaptic modification are important for the development of epilepsy. In previous experiments in the current study TRPM7 channel inhibition with carvacrol prevented cell loss in the hippocampus after SE. Therefore, the next objective was to test whether protecting neuronal cell death will prevent against the development of epilepsy.

Early pharmacological treatment after initial insult can prevent or modify the development of epilepsy. The goal is to prevent or reverse the epileptogenic process in those at risk (Löscher and Brandt, 2010). Three different strategies have been suggested; 1) early treatment after an insult to modify onset of the disease – insult modification, 2) treatment during the latent period, 3) administration of the treatment once the symptoms of disease are manifest. The latter is most likely to be applicable to human epilepsy, however, much longer period of treatment will be needed to assess its effectiveness. The disease modification in epilepsy also aims to decrease seizure severity, if they occur, as well as modify sensitivity to current AEDs and comorbidity onset (Barker-Haliski et al., 2015).

The approach was used in the current study is similar to the first strategy mentioned above - early post-insult treatment to modify the disease i.e. insult modification.

Aim: To test the effect of TRPM7 channel inhibition on epileptogenesis following PPS induced SE.

Hypothesis: Blocking TRPM7 channel after initial insult, i.e. SE prevents neuronal cell loss. Cell death by itself or by triggering downstream mechanisms

can contribute to the development of epilepsy. Therefore, rescuing hippocampal damage would prevent epileptogenesis.

2. Methods

A wireless EEG transmitter and a stimulating electrode were implanted in animals and then SE was induced after one week (see chapter 2). 24 hour EEG recordings for 2 month was analysed in epileptic control (n=6) vs. epileptic treated (carvacrol 75 mg/kg i.p.) animals (n=7). The same carvacrol treatment protocol was used as mentioned in the previous chapter (see chapter 4). Coastline length analysis was used initially to analyse seizure frequency. An event detection library was then created for comprehensive seizure analysis.

In general, definitions of a seizure are not completely satisfactory from both a research and clinical perspective and amendments are needed. Moreover, as suggested separate definitions rather than one unique would be more realistic (Walker and Kovac, 2015). In the current study, I used a conservative approach to define a seizure. Short duration, possible seizures (<15 s), that had low frequency and low amplitude (see **Figure 5.2B**) were challenging sometimes to distinguish from some non-seizure events, such as runs of spikes or certain artefacts. In order to avoid a bias and enable accurate comparison such short and unclear seizures were not included. Therefore the following criteria were used to count seizures: events that show clear evolution over time of frequency and amplitude and that lasted over 20 s (see **Figure 5.2A**).

Shapiro-Wilk and Anderson Darling tests were carried out to check for Gaussian distribution.

3. Results

3.1 Coastline analysis results

I initially examined coastline length, which is a measure of absolute difference in voltage between consecutive data points, and which is increased during seizure activity. However, along with seizures, a high amount of muscle activity such as eating artefacts as well as high frequency events and noise also increased coastline length. Eating artefact was a major problem in many recordings as this was present throughout some recordings and occurred in clusters and if a seizure occurs amongst these events it was impossible to distinguish them using this measure. High frequency oscillations and noise occurred as discrete events. In all these non-seizure events, the coastline increased and the pattern was indistinguishable from seizure activity. This suggested coastline length analysis as a non-specific and unreliable tool to analyse seizure frequency.Therefore, for accurate and comprehensive analysis of seizures, an event detection library was developed.

3.2 Event detection library

An Event Classifier uses an Event detection library to detect events of interest. I created an Event detection library to identify seizures in PPS model. The classifier detected 1 sec epochs of a seizure. Sometimes throughout one seizure multiple epochs were identified (see **Figure 5.1**) or in some occasions only one point in a seizure was detected. The main problem arose when animals exhibited interictal events throughout; these are short events that resembled a fragment of a seizure.

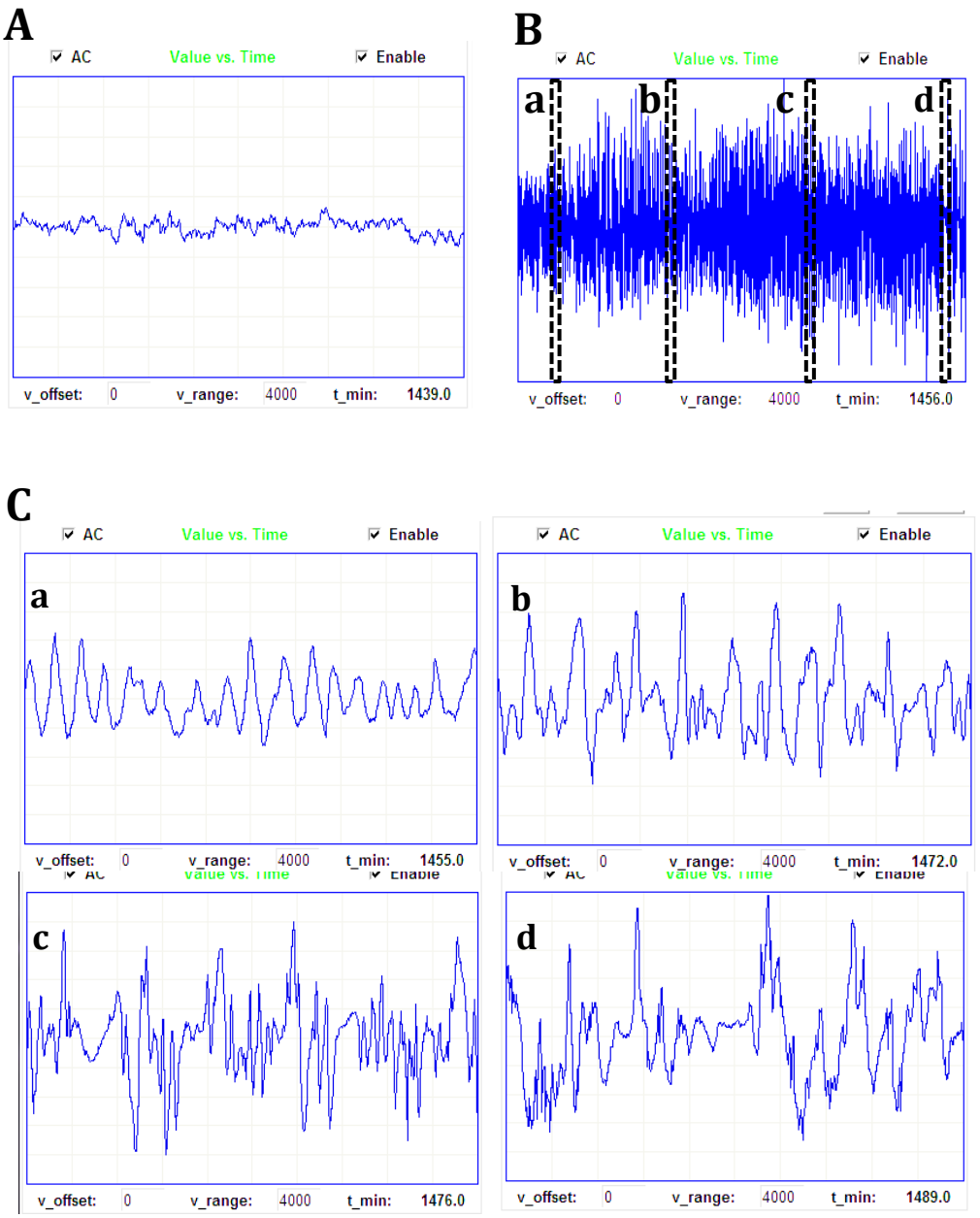

Figure 5.1.Neuroarchiver outputs of seizure fragments identified by the Event detection library.

(**A**) A baseline trace recorded before start of the seizure (1 second) (**B**) a seizure detected by the library in multiple locations (32 second), several examples of which are shown a, b, c and d areas (**C**) expanded 1 second epochs of the seizure (B) detected at various points

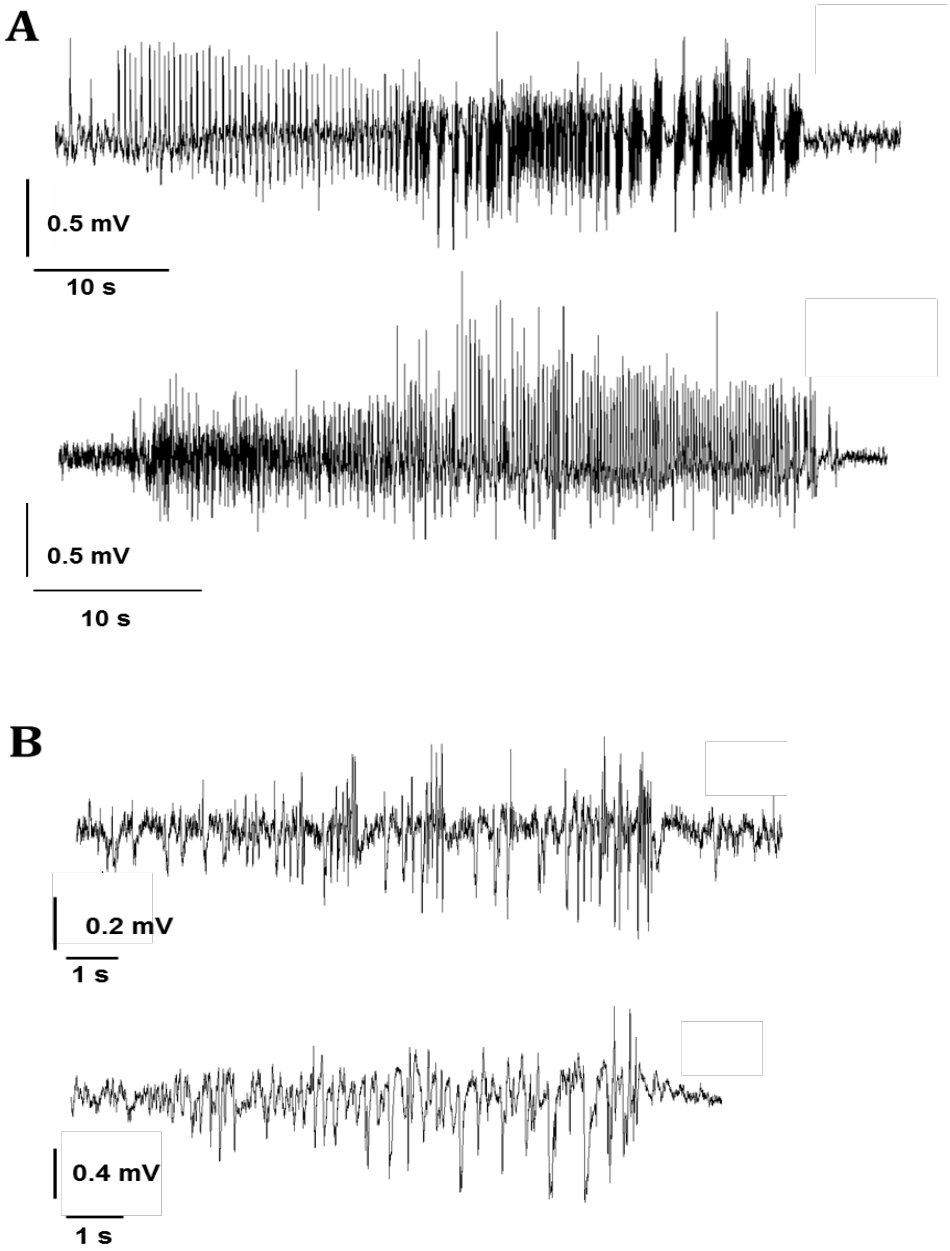

Figure 5.2. EEG seizure examples

(A) Examples of 'long' definite seizures that were used as criteria for determining seizure frequency. (**B**) – examples of 'short' probable seizure activities, that were not included in analysis

Because the library detected only 1 sec epochs it could not distinguish between an interictal event and a seizure fragment. False positives occasionally would also occur, such as non-specific activities, for example runs of spikes, or high amplitude baseline, but these were rare.

In contrast to coastline length analysis, event detection library perfectly distinguished between non seizure events such as eating artifact, high frequency oscillation and noise from seizures; these were not detected as a seizure. All seizures were checked visually; hence this was a semi-automatic tool. In total 1440 hours EEG recording in each animal (n=13) was analysed using Event detection library followed by visual analysis.

3.3 TRPM7 channel inhibition by carvacrol prevents the development of recurrent status epilepticus

The next day following induction of SE some animals developed prolonged seizures, recurrent SE (see **Figure 5.3**). Therefore, I first analysed if blocking TRPM7 channel by carvacrol affected SE rate, i.e. if recurrent SE rate was different in epileptic compared to epileptic treated animals. In addition to 13 animals' with long-term EEG recordings, two animals that had only one week recordings (due to problems with the transmitter battery) were also included in the analysis. SE was defined as prolonged seizures lasting over 30 minute, with a spike frequency of 3 Hz or higher, or recurrent seizures occurring with an interval of less than two minutes between them. Some animals exhibited cyclical pattern of SE (see **Figure 5.3**B). Six out of seven epileptic animals (~85%) had recurrent SE following initial induced SE whereas only 2 in 8 epileptic animals treated with carvacrol (25%) developed recurrent SE (see **Figure 5.4**). This difference was statistically significant (p=0.04, Fisher exact test) suggesting that blocking TRPM7 channel protected against recurrent SE. Analyzing the duration of SE, i.e. to determine when exactly SE stops is

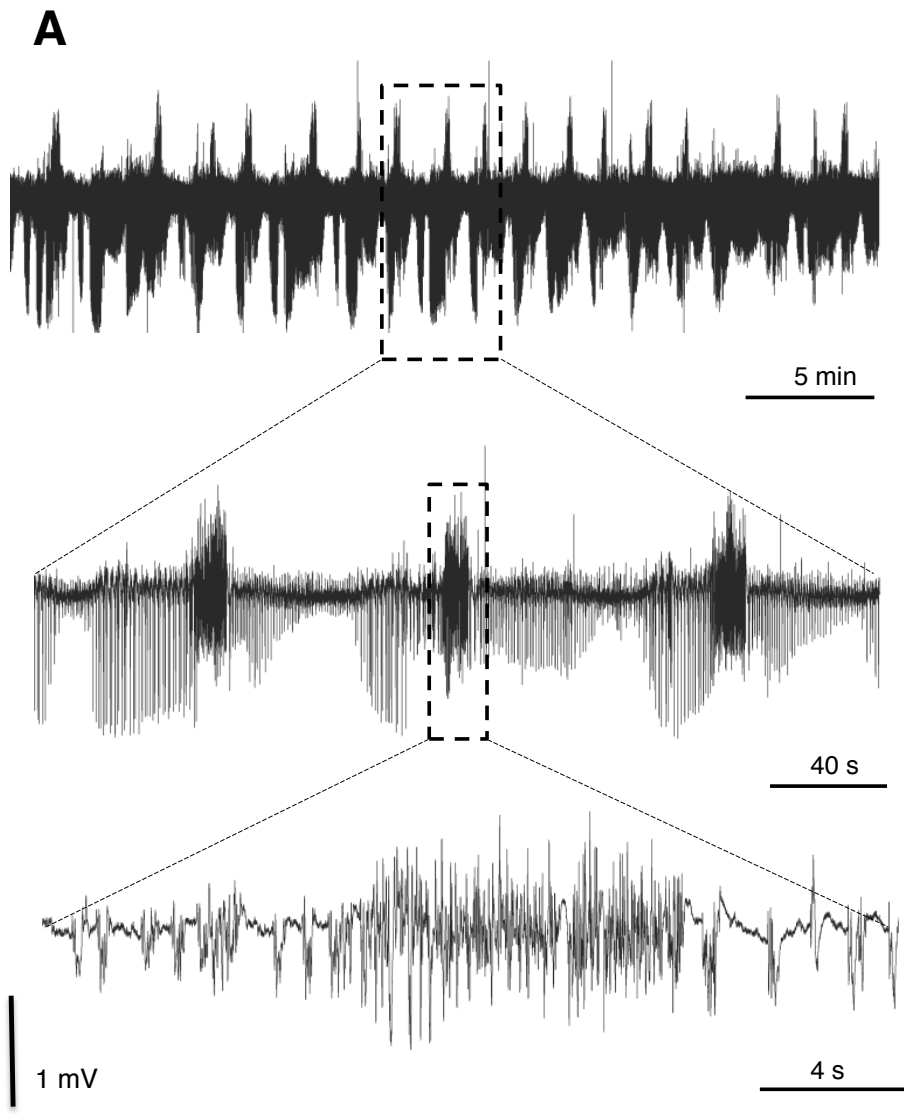
A
5 min
40 s
1 mV
4 s

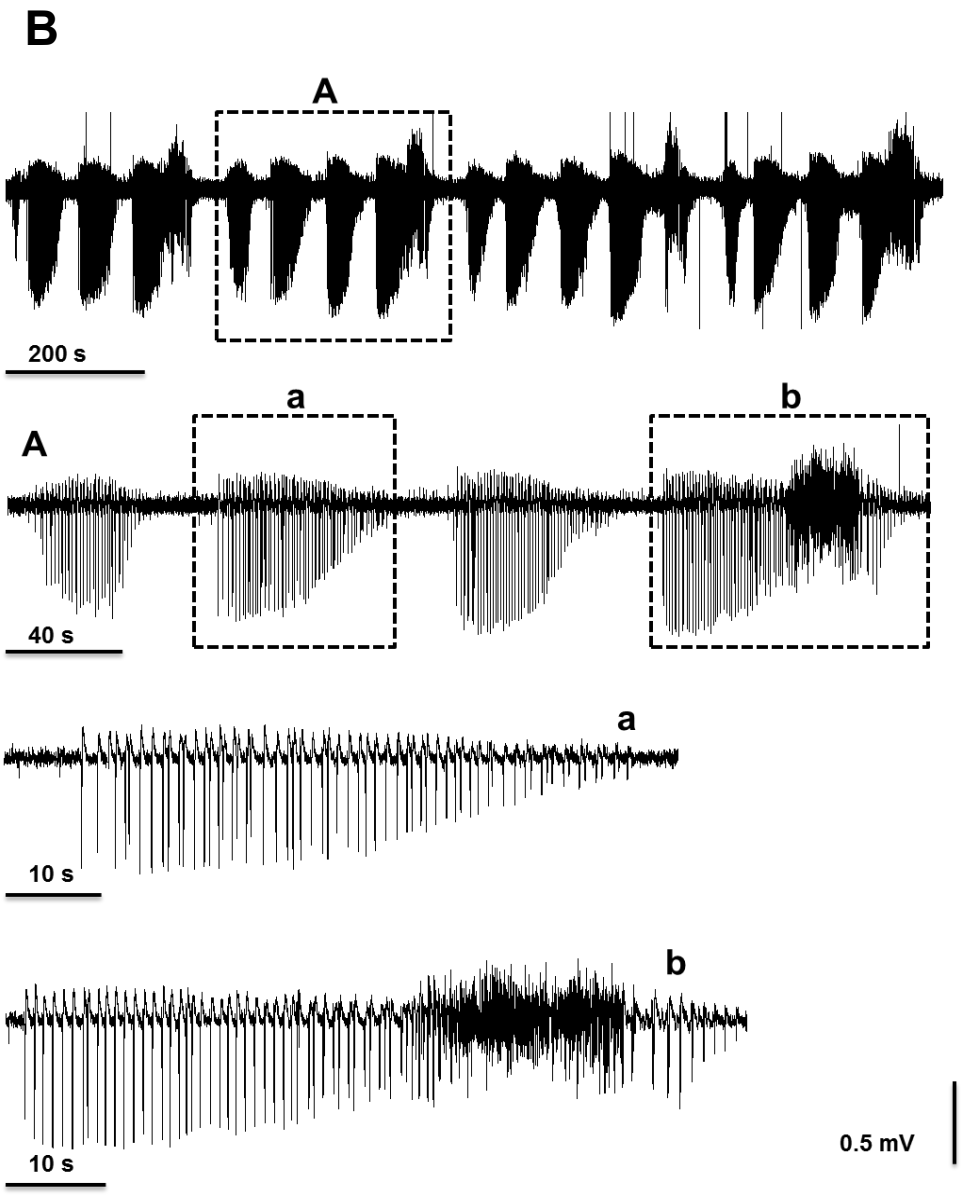

Figure 5.3 Examples traces of status epilepticus.

(**A**) top trace show a ~30 min interval of status epilepticus, middle and bottom traces are zoomed fragments of the top trace showing three consecutive seizures and a single seizure trace respectively. (**B**) a ~22 min fragment of SE that has cyclical pattern.

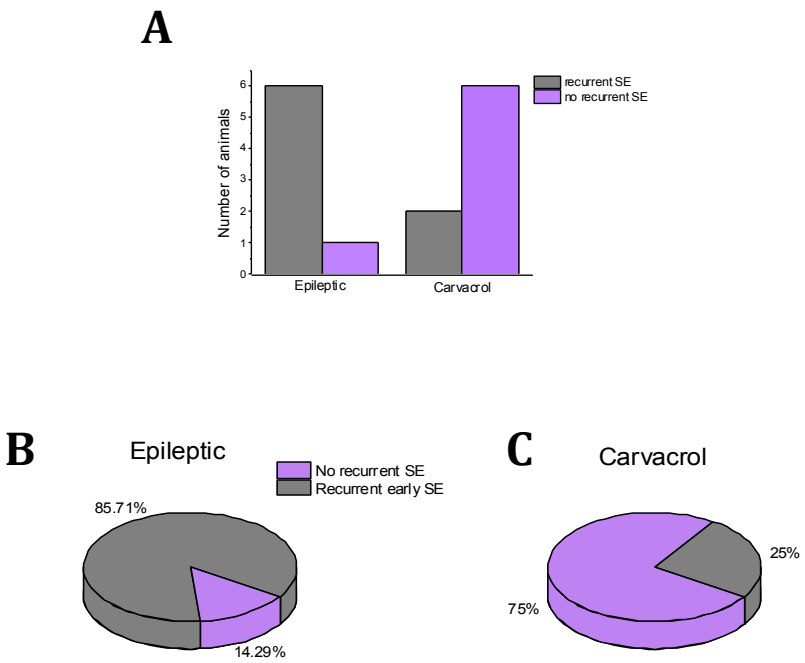

Figure 5.4. Recurrent SE.

(A) – Bar charts show frequency of recurrent SE in each animal group, SPSS output for contingency table. Six out of seven epileptic animals developed recurrent SE and only one animal did not have recurrent SE, whereas in epileptic animals treated with carvacrol only two out of eight animals developed recurrent SE and six animals did not, p=0.04 (Fisher exact test). (**B)** - pie chart illustrates proportion of recurrent SE in epileptic (85.71%) versus (**C**) epileptic animals treated with carvacrol (25%).

challenging although an approximate estimate of SE duration was possible to determine: some animals had continued SE lasting up to 10-12 hours.

3.4 Inhibiting TRPM7 channel by carvacrol prevents early seizures

Seizure frequency was quantified per week for each animal group after one week following induced SE. I did not quantify the first week because some animals continued to have SE in the first week. Some animals had SE, whereas others only single seizures following induced SE, yet others had both SE and then recurrent seizures. Therefore, it would be difficult to compare SE against short single seizures. Also after prolonged SE, some of which continued up to 10 hours, animals would have a period of recovery.

Animals developed spontaneous seizures almost immediately after initial SE. In the following day after induced SE, animals had single seizures and recurrent SE. Analysis of seizure per day revealed that epileptic animals had 1-2 seizure per day occasionally clustering up to 4-6 seizures per day (see **Figure 5.5**). The maximum number of seizures animals had per day was 7. The number of seizures was highest in the second week in epileptic animals (see **Figure 5.5** and **Figure 5.6**). Following this peak seizure frequency abruptly declined in the third week. Epileptic treated animals in contrast had the lowest seizure frequency in the second week following SE induction. Similarly, treated animals had 1-2 seizure per day, with highest seizure count reaching 7 seizures a day in one animal.

To compare seizure frequency per week during seven weeks in the two groups a generalized linear model (with a poisson probability distribution, week as a within-subject effect and treatment as the between-subject factor) was applied (this test was performed with help from my supervisor, Professor Matthew Walker).

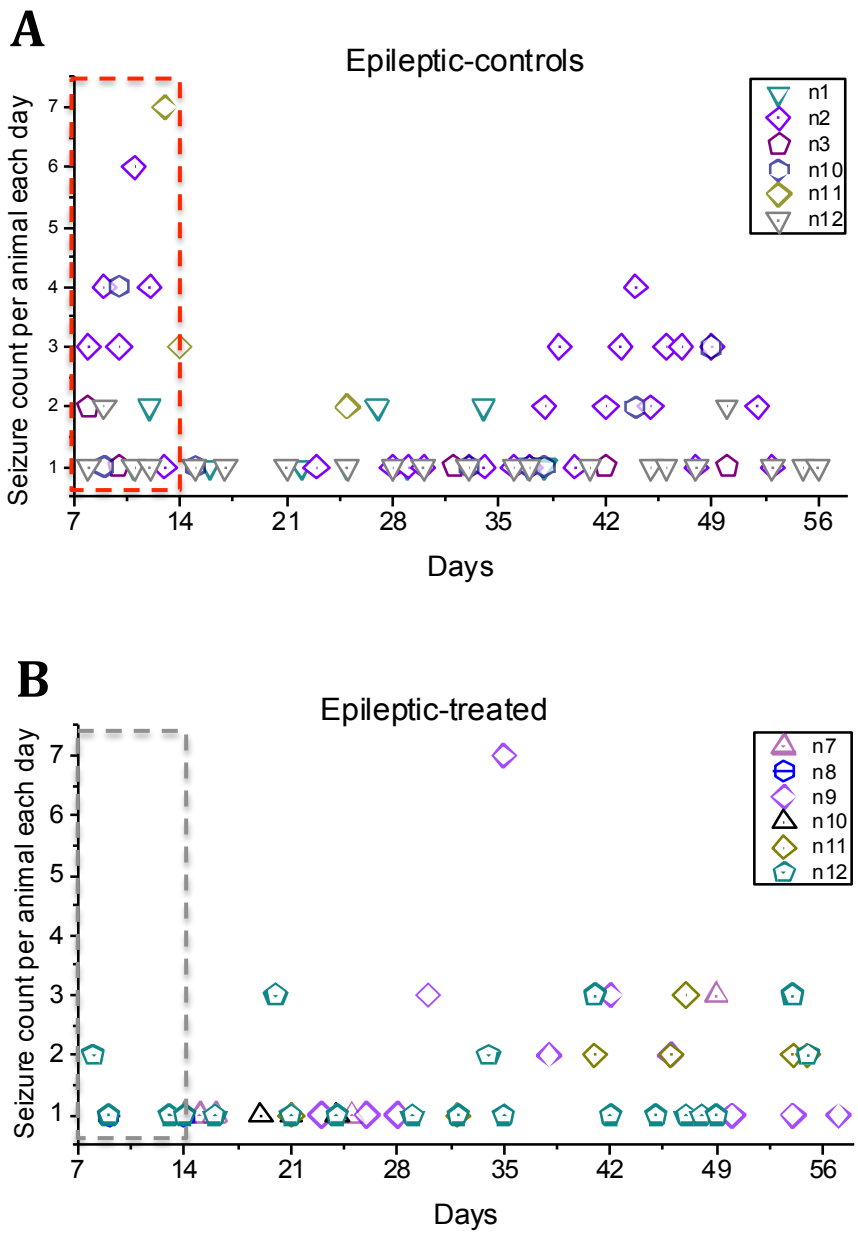

Figure 5.5. Seizure counts in each animal per day.

Number of seizures in epileptic (**A**) and treated (**B**) animals shown separately. Each symbol represents number of seizure in an individual animal in a given day. X axis shows days from the induction of SE: seizure counts starts from day 7 (week 2). Red and grey dashed rectangles indicate the areas with significant difference in seizure number in epileptic control and epileptic treated animals respectively

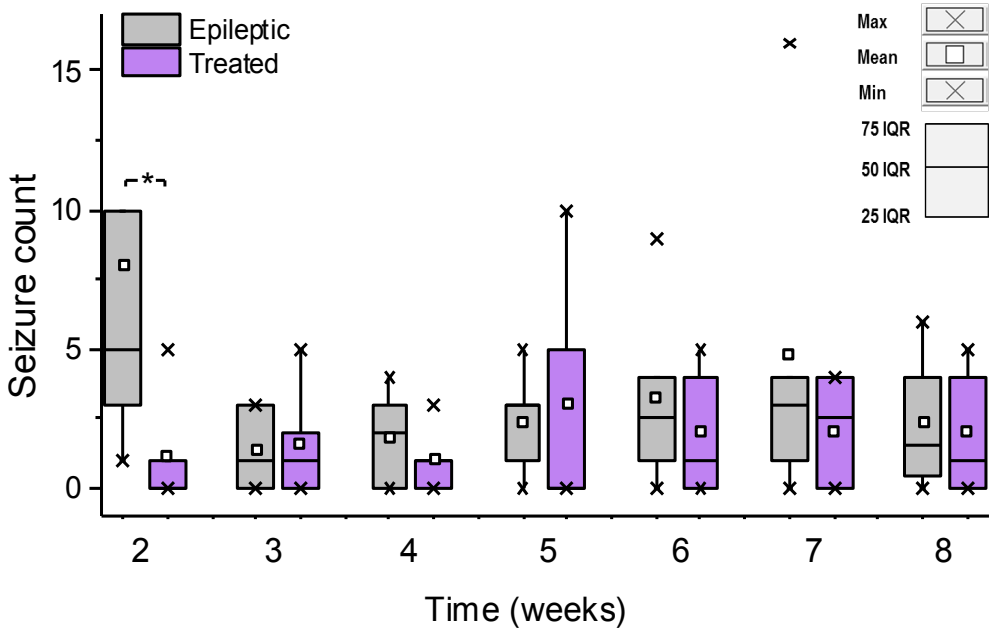

Figure 5.6. Box plots show seizure count per week in two groups of animals, epileptic and treated.

Median, 25th and 75th interquartile ranges (IQR), minimum and maximum data values are shown. There was significant difference in seizure count between epileptic control (n=6) and epileptic treated (n=7) groups in the second week following status epilepticus. * p=0.015 (generalized linear model, post-hoc Mann-Whitney test). One outlier in the week two in epileptic animals not shown in the graph, at point 21.

The test result revealed that overall there were no significant difference between epileptic and epileptic treated groups [Wald-Chi Square 1.77, DF (1), p = 0.18). However, the interaction of treatment with week was significant [Wald-Chi Square 37.8, DF (6), p < 0.001]. This indicates that there is a different effect of treatment depending on week. With a post-hoc Mann-Whitney test, only the second week treatment effect was significantly different p = 0.015 between epileptic (median=5) and treated groups (median=0) (see **Figure 5.6**).This effect was not sustained in the subsequent weeks i.e. no significant difference between the groups in seizure frequency was seen afterwards.

3.5 Seizure duration

Duration of a seizure was counted from the start of an abrupt change in baseline power and until the end when the frequency of spiking was less than 3 Hz. Afterdischarges following seizures were not included. Mean seizure duration was 61±5.2 seconds in epileptic animals versus 51±3.1 seconds in epileptic treated animals. Seizure duration varied from ~30 second to ~100 second across all animals analysed. Seizure duration was measured starting from week two, due to recurrent SE that occurred in animals in the first week. As mentioned above, duration of SE is difficult to determine precisely and also difficult to compare with single short seizures.

To compare difference in seizure duration per week between epileptic-control and epileptic-treated animals two-way ANOVA test was used. There were no significant change in seizure duration over time (between weeks) [$F(6,41)=1.5$, $p=0.2$) and no significant difference in seizure duration between epileptic-control and epileptic-treated animals [$F(1,41)=3.4$, $p=0.07$), and interaction of week and treatment group was not significant [$F(6,41)=0.5$, $p=0.8$) (see **Figure 5.7**).

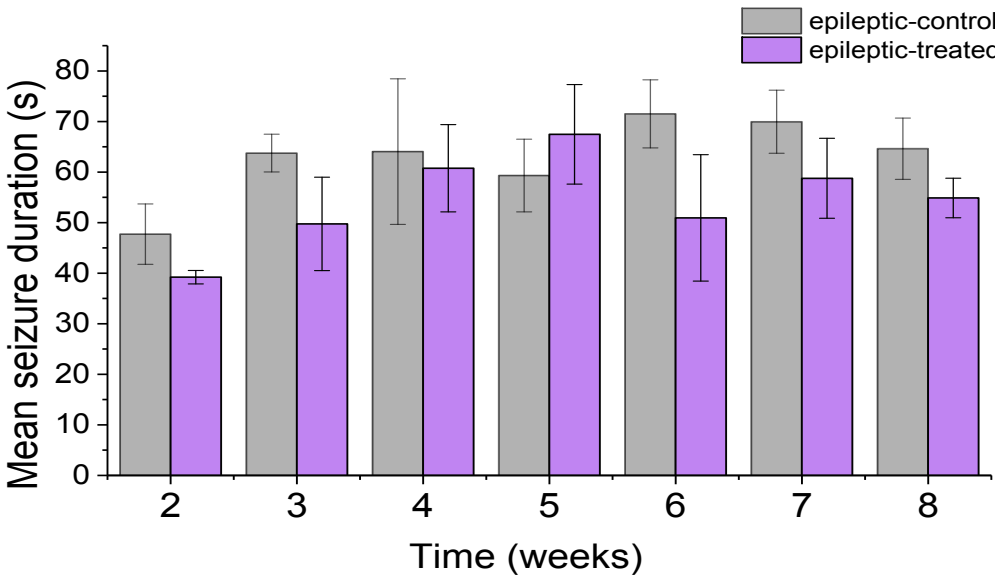

Figure 5.7. Seizure duration.

Seizure duration per week (mean ±SEM) in epileptic and epileptic treated group over during 7 weeks is illustrated as bar charts. Seizure duration was measure started form second week after SE induction. There was no difference in seizure duration over time, as well as between epileptic and treated animal groups, and interaction of time and treatment (p0.05, two-way ANOVA).

4. Discussion

Coastline analysis proved to be a non-specific method for seizure analysis. It detected any event that causes increase in coastline length such as various artifacts from muscle movements, high frequency events, as well as noise. Event detection library could differentiate between those non-seizure events and seizures and reliably detected all seizures. The library had relatively low specificity and interictal events were detected as a seizure in 1 second epochs. However, such automatic detection of seizures by the Event detection library followed by visual checking of each identified epoch provided a robust means of seizure analysis.

The development of spontaneous seizures in PPS model was observed within few days following SE induction (Bumanglag and Sloviter, 2008). The conventional view suggests that from initial insult until development of clinical epilepsy there is a 'latent' period during which a number of structural, molecular and functional changes occur. However, recent animal and human studies suggest that processes leading to epilepsy-epileptogenesis start immediately after an insult. Moreover, subclinical epilepsy can also occur immediately following brain injury suggesting there is no notable 'latent' phase (Löscher et al., 2015). I here observed the development of spontaneous seizures immediately after SE, i.e. the following day after SE induction, which is consistent with the lack of a clear latent period in some epilepsy models.

Recurrent early SE occurred in animals during the first 24 hour following SE induction. Inhibiting TRPM7 channels by carvacrol prevented the development of recurrent status epilepticus and early spontaneous seizures in the second week following SE induction. Thus, seizure severity was prevented by blocking TRPM7 channel during the first two weeks following the initial damage; recurrent SE in the first week and frequency of spontaneous seizures in the second week were prevented. Moreover, blocking TRPM7 channels prevented both generation of seizures (in the second week) and maintenance of sustained

neuronal discharges. Although animals in both epileptic-control and epileptic-treated groups developed seizures in the following day after SE, only a small proportion of animals in treated group (25%) developed recurrent SE as compared to ~85 % in epileptic untreated group. This suggests that blocking TRPM7 channel by carvacrol during the first 24 hour time interval following induced SE reduced or prevented depolarization of neurons and hence excessive neuronal firing which prevented the occurrence of early recurrent SE. However, it is unclear what mechanisms are involved in the prevention of seizures after one week following initial suppression of TRPM7 channels in treated animals.

Nevertheless, inhibiting TRPM7 channels post insult did not have an effect on later - chronic seizures; there was no significant difference in seizure numbers after two weeks between treated and control groups. Thus, preventing recurrent SE and early seizures was sufficient to prevent cell damage but not to prevent development of epilepsy. This supports some early studies suggesting neuroprotection does not always stop the disease development in epilepsy. The relationship between cell loss and development of epilepsy is complex and not well understood yet. Studies reported selective loss of GABA-ergic interneurons and formation of excitatory circuits after death of principal neurons enhance excitability, contributing to epileptogenesis (Ben-Ari and Dudek, 2010). However, neuroprotective treatment did not prevent development of epilepsy in previous studies. In a kainic acid model it was shown that preventing cell death in rats by blocking NMDA receptors did not stop development of epilepsy (Brandt et al., 2003). In a study of a COX2 knock out mouse, status epilepticus resulted in less severe cell damage but no change in behavioural and EEG seizures (Serrano et al., 2011). Similarly, some of the AEDs have shown neuroprotection in epilepsy but they did not have disease modifying effects (Acharya et al., 2008). Maybe markers other than cell death can be used in the future to predict the development of epilepsy or the extent of brain damage and receptor/synaptic modification.

The current research indicates that different mechanisms are involved in the generation of early and late seizures following status epilepticus. Mechanisms that trigger early seizures are linked to neuronal depolarization and excessive neuronal discharge, whereas later seizures are the consequence of synaptic modification in the brain. Possibly processes that can trigger epileptogenesis begin to occur during two hour of perforant path stimulation and involves mechanisms other than neuronal loss. Since blocking TRPM7 channel prevents cell damage and loss, then other factors such as synaptic modification are driving the development of epilepsy. Moreover, some damage in the hilus still occurred in treated animals that can potentially lead to reduction of inhibitory neurons. Furthermore, in 2 hour perforant path stimulation model with high frequency stimulation (20 Hz) in awake animals, that was used in the current study, extrahippocampal brain structures can also be damaged that could potentially be also involved in the development of epilepsy (Sloviter, 1983). However, the role of damage to these structures in the development of TLE is not clear.

I defined a criteria and cut-off to count only long and definite seizures, and not to include short seizures (< 15 s) that also do not show clear evolution of amplitude and frequency. One of the problems with setting such a cut-off for the seizure count could be that seizures may become shorter in the treatment group. However, in such case overall duration of counted seizures would have been shorter in the treated animals but there was no significant difference between groups in seizure duration.

In the current study only short term treatment during first 24 hour following induced SE was employed. This approach assesses the effect of intervention just after an insult, i.e. insult modification. Chronic treatment during latent phase for longer duration, for instance for a week, when cell damage and as a result synaptic reorganisation still continues to occur, could possibly have had a better antiepileptogenic effect. However, from clinical perspective long term treatment during the latent phase could be challenging, because patients not

experiencing any problem after an insult would not always agree to be treated and would not want to be exposed to potentially harmful side effects of a treatment. Moreover, in the PPS model the disease developed almost immediately after the insult without a latent phase. Therefore, in PPS continuing the treatment in the initial phase of the disease could aid to reverse the disease that has already developed. The current study demonstrates that TRPM7 channel can further be investigated as a potential target to be tested for treatment during chronic disease, and may have effect later into disease.

The disease prevention could also be dependent on seizure severity and frequency during perforant path stimulation and afterwards, depending which parts of the hippocampus and other brain regions are recruited and this can vary substantially. Bigger variety from animal to animal may require a much larger sample size to assess the true effect. In addition, we only monitored seizures for 2 month therefore it is difficult to say whether in those animals with rescued cell damage seizures would discontinue or seizure frequency would substantially decrease later or not. On the other hand, it is not clear for how long after treatment individuals need to be evaluated, to conclude that there is or is not a disease modifying effect. Evaluation of true antiepileptogenic effect can require much longer time and a more thorough analysis. It is difficult to say when is the appropriate time to stop observation. Moreover, another issue in disease modification is that treatment needs to be administered as a prophylaxis; not all patients will go on to develop disease after insult, this figure is less than 50%. Instead, biomarkers such as cognitive decline and neurodegeneration have been proposed as a good alternative (Barker-Haliski et al., 2015).

5. Summary of the chapter

8-9 week old SD rats were implanted wireless EEG transmitter followed by were perforant path stimulation after one week to induced SE. EEG was recorded for 2 month. Based on EEG, animals developed spontaneous seizures almost immediately following initial SE. Some animals developed recurrent early SE and this was prevented by blocking TRPM7 channel with carvacrol. Moreover, early seizures, in the second week after initial damage were prevented by inhibiting TRPM7 channels. However, later seizures, i.e. development of epilepsy was not prevented by carvacrol. There was no difference in seizure frequency after 2 weeks and in seizure duration overall between epileptic-control and epileptic-treated animals.

Chapter 6. Cognitive decline in epilepsy: the role of TRPM7 channels

1. Introduction

Cognitive decline is one of the major comorbidities affecting patients' quality of life in TLE, in particular in MTLE, where hippocampal sclerosis is the hallmark of the disease. Hippocampus has a central role in variety types of memory function. Hippocampus and medial temporal lobes are the principal locations responsible for spatial memory (Burgess et al., 2002). Loss of visual spatial memory has been described in MTLE (Lv et al., 2014; Pereira et al., 2010). Moreover, patients with TLE who underwent selective amygdalohippocampectomy showed impaired spatial memory in virtual Morris water maze task (Astur et al., 2002; Barkas et al., 2010). Spatial memory impairment has also been shown in pilocarpine and PPS animal models (Kalemenev et al., 2015; Chauvière et al., 2009; Kelsey et al., 2000). Cell loss in hippocampus is associated with cognitive dysfunction in various neurological disorders including epilepsy. Correlation of memory dysfunction with cell loss in CA1, CA3 and CA4, DG has been shown in specimens obtained from patients who underwent TLE surgery (Pauli et al., 2006). Cell death in CA1 in particular was linked to cognitive and memory impairment (Sun et al., 2009).

In previous chapters I showed that Inhibiting TRPM7 channels by carvacrol prevented recurrent status epilepticus and early seizures following initial damage (SE). As a consequence carvacrol prevented cell loss in the hilar and CA1 region of the hippocampus. One of the goals in disease modification in epilepsy is to identify drugs that can prevent or improve comorbidities associated with epilepsy, amongst which cognitive decline is one of the most important. Therefore, the final question was whether rescuing neuronal cell death, preventing recurrent SE and early seizures by blocking TRPM7 channels will improve cognitive function in animals treated with carvacrol after SE. Blocking TRPM7 channel and as a result prevention of cell damage in CA1 region in a stroke model prevented spatial-navigational memory deficit in rats (Sun et al., 2009).

Aim: To assess effect of blocking TRPM7 channel on memory dysfunction in animals following SE induced chronic epilepsy

Hypothesis: Cell death in the hippocampus is linked to memory impairment. Blocking TRPM7 channel with carvacrol prevents cell damage in hilar and CA1 region of the hippocampus. Therefore, rescuing cell death would prevent memory impairment in animals treated with TRPM7 antagonist, carvacrol.

2. Methods

Cognitive function was assessed in epileptic (n=5), epileptic-treated (75 mg/kg carvacrol) (n=6) and in control animals (n=6). The same PPS and carvacrol treatment protocol as for previous experiments (see chapter 2 and 4) was used, except EEG was not recorded. In addition, animals kept for longer time before assessing for a cognitive dysfunction (3-4 month) following SE induction. The longer time was speculated to allow for the damage to influence the cognitive function. I was blinded to the treatment groups. Alternating reward T-maze test was used. T-maze training steps are described in the general methods section (see chapter 2). The diagram below (see **Figure 6.1**) shows steps of the main test. During the main test animals initially were given 5 sec delay and then 60 s delay before making choice after the first run in the T-maze. One animal in the epileptic group that was not possible to train, was very aggressive and not moving in the T-maze was excluded.

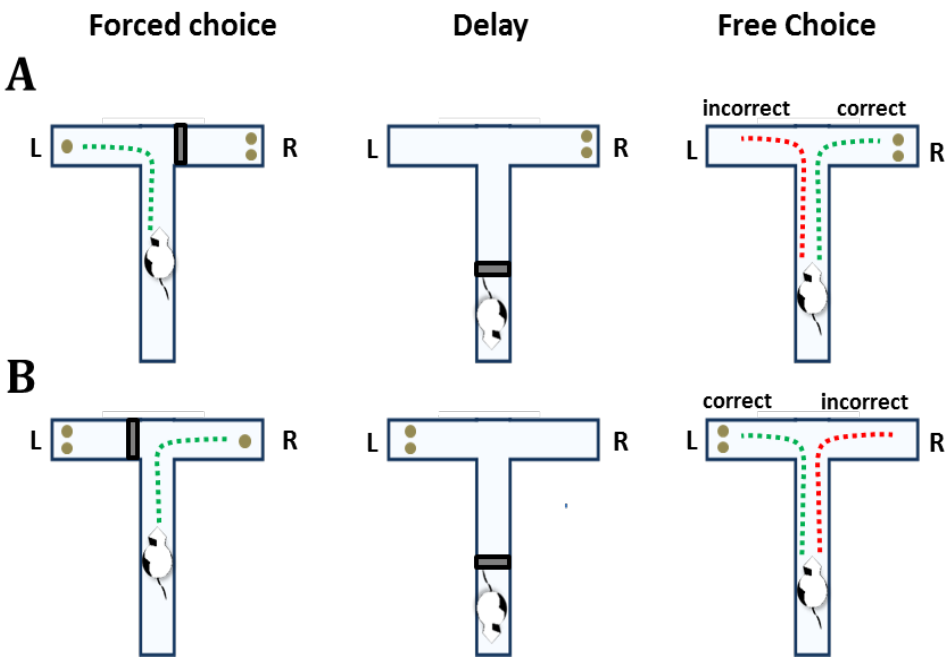

Figure 6.1. Delayed alteration reward T-maze steps in (A) right and (B) left correct choice arm.

In step 'forced choice' the choice arm is blocked and both arms baited with reward pellets, one in sample arm and 2 pellets in the correct choice arm. After entering the sample arm animal eats a pellet, then animals returned back to start arm (not facing T junction) which will be blocked to introduce 5/60 s 'delay', and the block to enter choice arm will be removed. Then in step 'free choice' animal choose which arm to enter. Rats typically alternate location – correct arm. If they enter the same side this is incorrect choice. Left/Right (R/L) arm sequences during experiments were randomised so that all rats receive the same number of both left and right arm.

3. Results

3.1 Habituation and training

Epileptic animals tend to exhibit aggressive behavior ('jumpy') frequently during the training and the main test: they were difficult to handle initially and would frequently jump out of the cage and sometimes t-maze. However, such behavior was observed very rarely in the control and treated groups. However, all groups of animals spent similar time to reach goal arm and the time required to fully habituate animals was similar in all groups. Habitation, i.e. to train animals to run freely run in the t-maze and eat several reward pellets in both goal arms was achieved in one week. Animals were anxious initially and reluctant to eat pellets in the t-maze in the first 4-5 days. Once they consumed at least 1 pellet they could continue each time consume more and were less hesitant with each trial. This was important step to initiate stepwise training. Initial stepwise training and the main training required 7-8 days. After a successful training, i.e. each animal eat 5-6 pellets in both arms and move towards the goal arm quickly and without hesitation the main training was initiated. During trainings after several trials animals would fall asleep and be lazy, and thus they would not move in the T-maze. Therefore, after 3-4 trials animals were taken back to their room, either to continue later in the day or the following day. Occasionally rats would not move in the t-maze, and stayed motionless during the trial. If this happened after 2-3 minute animal was returned back to the cage to try later.

3.2 The main test

During the main test when all four limbs of the animal were on a goal arm this was considered a choice arm. Sometimes animals turn head to both sides before making a choice. Occasionally animals had seizures during the training

as well as the main test. If a seizure occurred in the start arm or at the T-junction before making a choice, the animal was returned back to the home cage and left for about 20-30 minutes to recover before starting the next trial. This would allow sufficient time to recover from post ictal confusion and lethargy. Animals are more aggressive ('jumpy') postictally for a while. If a seizure occurred after animal entered a choice arm that trial would be counted however animal again would rest 20-30 min before the next trial.

Animals were initially tested with 5 second delay then with 60 second delay, no significant difference was observed between these trials. Total percentages of correct choice for all trials per animals were calculated (18 trials for each animal). To compare difference of correct arm choice between the three groups of animals one way ANOVA was used. There was significant difference between the three groups in the percentage of correct arm choice [$F(2,14) = 9.7$; $p=0.002$] (see **Figure 6.2**).

Table 6.1. Summary of correct arm choice (%) in reward alternation T- maze test

Groups	Mean ± SD (%)	SEM	95% Confidence Interval
Control	95.3±3.9	1.6	91.2 -99.5
Epileptic	63.4±14.5	6.5	45.4 -81.4
Epileptic + Carv	86.5±15.3	6.2	70.4 -100

SD- standard deviation, SEM- standard error of mean, Carv - carvacrol

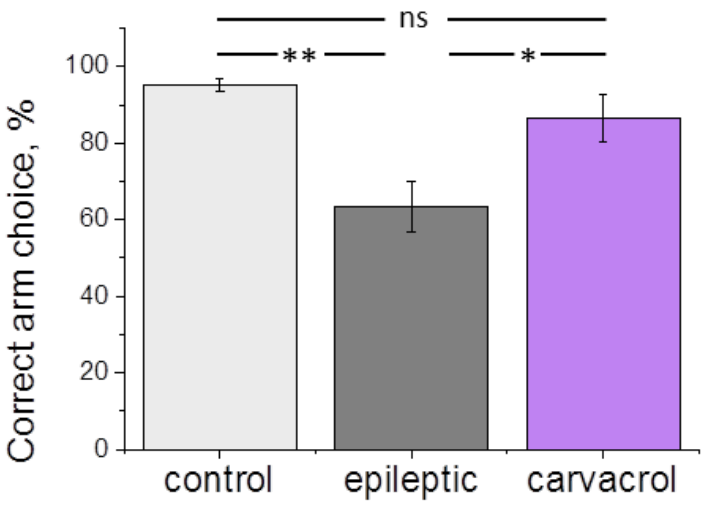

Figure 6.2. **Bar charts illustrate correct arm choice percentage**

in control (n=6), epileptic (n=5), and epileptic animals treated with carvacrol (n=6). The correct arm choice in epileptic animals significantly lower compared to control (healthy) animals and epileptic –treated animals, ***p*=0.002 and **p*=0.02 respectively. No significant difference between control and epeileptic-treated animas in the percent of correct arm choice, *p*=0.44.

The mean percentage of correct arm choice in the T-maze was 95.3±3.9% in control animals versus 63.4±14.5 % in epileptic animals (see Table 6.1). This difference was statistically significant (post hoc Tukey's test, p=0.002) suggesting that spatial memory was impaired in epileptic animals. Whereas animals treated by carvacrol performed 86.5±15.3 % correct which was significantly higher compared to epileptic animals (post hoc Tukey's test p=0.02) and not significantly different from control animals (post hoc Tukey's test p=0.44) suggesting that carvacrol was able to prevent status epilepticus and seizure induced memory dysfunction.

4. Discussion

Alternating T-maze test is a measure of working spatial memory function. The terms working and short-term memory have been used interchangeably and are not very distinct. Short-term memory has been defined as a limited amount of information that can be stored temporarily in an assessable way. In contrast to long-term memory this type of memory has limited capacity and decays in time. Whereas working memory is referred to the short-term memory that in addition includes other mechanisms that are necessary to plan and conduct certain tasks. Tests measuring working memory have been shown better associated with intellectual capacity than tests for a short-term memory (Cowan, 2008). Rats have remarkable ability to alternate spatial location, this can be spontaneous or by using reinforcement. For alternation rats use short-term memory, so that they remember which part of the maze they entered first (Dudchenko, 2004).

Here I observed substantial impairment of spatial working memory in epileptic rats in delayed T-maze alternating test. Following 3-4 months from the development of chronic epilepsy animals had substantial impairment of spatial memory. However, it is not clear how this time interval in animals can be compared with cognitive impairment in human epilepsy. Memory impairment in

PPS model of TLE is substantial. Epileptic animals made ~63 % correct arm choice (almost down to chance) compared to ~95% in control animals. This is consistent with the observation that in rats hippocampal damage leads to selective spatial memory deficit (O'Keefe and Burgess, 1996). 'Place cells' located in CA1/CA3 regions of the hippocampus encode the rat's location within an open environment and have an important role in spatial memory; in freely moving rats place cells respond whenever a rats enter a specific portion of its environment independent of rats orientation (Burgess et al., 2002). Damage to place cells in CA1 region could be responsible for the impairment of spatial memory in the current study. Inhibiting TRPM7 channel by carvacrol significantly improved memory function. This suggests that preventing cell damage in CA1 and hilus had robust effect to prevent memory impairment in PPS model. In previous chapters I showed that cell loss in CA1 region was completely rescued by blocking TRPM7 channel after SE. The CA1 region is particularly important in spatial memory function. Prevention of this region from damage in treated animals could explain preserved memory function. Involvement of CA1/CA3 regions in memory is well known. Selective impairment of spatial memory was observed in CA1 NMDA receptor knockdown mice (Tsien et al., 1996). In addition, the role of hilar GABAergic interneurons in spatial memory and learning have been demonstrated in Morris water maze test (Andrews-Zwilling et al., 2012). These findings highlight the importance of hippocampal pyramidal and as well as inhibitory neurons in the spatial memory.

Along with disease modification e.g. preventing development of epilepsy, a comorbidity modification is another important goal in epilepsy. In fact, often patients describe comorbidities being more troublesome and affecting quality of life more than seizures themselves (Barker-Haliski et al., 2015). Therefore, this highlights the important role of TRPM7 channels as a target for cognitive comorbidity modification in epilepsy. This is worthy of further studied for consideration of translation into clinical trials.

5. Summary of the chapter

Three to four month following PPS induced chronic epilepsy animals were assessed for memory impairment using delayed reward alternation T-maze test. Performance on T-maze was compared in three groups of animals: healthy controls, epileptic and epileptic animals treated with TRPM7 channel blocker, carvacrol. Epileptic animals had significant spatial memory impairment compared to control animals suggesting substantial memory deficit in PPS model. Whereas animal treated with carvacrol had significantly improved short term memory function compared to epileptic animals suggesting protective role of blocking TRPM7 channel against cognitive impairment in chronic epilepsy.

Chapter 7. General discussion

1. Summary of in vitro findings

The current study provides evidence that stress activated TRPM7 channels are involved in seizure generation in epilepsy and blocking these channels stops seizure activity *in vitro*. Activation of TRPM7 channels can be the consequence of molecular alterations that occur during seizure activity such as electrolyte disturbance (low intracellular Mg^{2+} and extracellular Ca^{2+}, decreased pH) or increased ROS production (Kozak and Cahalan, 2003; Monteilh-Zoller et al., 2003; Jiang et al. 2005; Lipski et al. 2006). These conditions promote TRPM7 channel activation, and Na^{+} and Ca^{2+} entering cells through the channel can exacerbate seizure activity. It has been shown that in acidic conditions the inward rectification in TRPM7 channels is much greater than under physiological conditions (Jiang et al., 2005). Prominent intracellular acidification occurs with seizure activity (Xiong et al., 2000), suggesting that there may be a positive feedback whereby acidification due to seizure activity contributes to TRPM7 channel opening which in turn further promotes seizure activity.

The following hypotheses were tested in *in vitro* studies: **Hypothesis 1.** TRPM7 current will increase during low Mg^{2+} induced seizure activity and blocking TRPM7 channel by antagonists added to the extracellular medium would decrease or abolish *in vitro* epileptiform activity by reducing influx of cations, such as Na^{+} and Ca^{2+} to cells and thus decrease cell depolarisation; **Hypothesis 2.** TRPM7 channels will also be activated during seizure activity induced in physiological Mg^{2+} concentrations, under the influence of other

mechanism that open the channel and occur during seizure activity, such as decreased low extracellular Ca^{2+}, low pH and ROS formation. The two models of seizure that were used in the current study relied on different mechanisms to induce seizure activity; increasing excitability of cells by decreasing Mg^{2+} concentrations in the perfusion solution and via blocking inhibitory pathways by a $GABA_A$ receptor antagonist. Here, I showed that TRPM7 channels are involved in seizure generation in both conditions. Carvacrol, a non-selective blocker of TRPM7 channel completely abolished *in vitro* seizure activity within 10 min of administration in both seizure models. Similarly, Waxiencin A, a potentially selective TRPM7 blocker significantly decreased seizure-like activity within 5 min of addition to the perfusion solution and completely blocked the activity by 20 min in both seizure models. PTZ and low Mg^{2+} generated distinct type of seizure-like activity, low Mg^{2+} mainly ictal-like whereas PTZ principally interictal-like seizure activity. This enabled me to test the effect of TRPM7 blockers on both types of epileptiform discharges; inhibiting TRPM7 channel abolished both ictal-like and interictal-like activity. **Hyothesis 3.** A study published by Joca et al. suggested that carvacrol inhibited peripheral sodium channels (Joca et al., 2012). Therefore, to determine whether carvacrol has relevant effects on sodium channels that would reduce it's potential to be used as a specific inhibitor of TRPM7 channels I tested the effect of carvacrol on fEPSP. In contrast to the previous study, carvacrol did not affect slope of fibre volley and interestingly increased the slope of fEPSP, suggesting no inhibition of sodium channels in the hippocampus occurred. This could possibly be explained by different variants of sodium channels in peripheral nerves and CNS.

2. Summary of in vivo findings

The following hypotheses were tested in *in vivo* studies: **Hypothesis 1.** TRPM7 channel activation during excessive neuronal firing will contribute to cell depolarisation, and Ca^{2+} entry via the channel can trigger a cascade of

processes contributing to cell toxicity and death. Moreover, Zn^{2+} as well as other trace metals entering the cells in stress conditions via TRPM7 channel can play a role in cell death (Montell, 2005; Nadler et al., 2001). Influx of Ca^{2+} via TRPM7 channel can further increase ROS production and then trigger downstream mechanisms that may also contribute to cell death. Activation of TRPM7 may therefore contribute to neuronal death after a brain insult. Therefore, blocking TRPM7 channel would prevent or reduce excitotoxicity induced cell damage in vulnerable areas of the hippocampus. TRPM7 inhibition in hippocampal CA1 area has been shown to prevent cell death after ischemia in animal studies (Chen et al., 2015; Yu et al., 2012; Sun et al., 2009). Here I showed that blocking TRPM7 channel completely prevented cell damage in CA1 area and significantly reduced cell loss in hilar region. This effect was achieved only by short time treatment with carvacrol after SE (24 hours). This suggests a strong potential of TRPM7 channel inhibition in preventing excitotoxicity induced neuronal cell death. Possibly synergy between opening of NMDA receptors and TRPM7 channels are responsible for cell damage mechanisms post SE initially. However, TRPM7 channels are principally responsible for sustaining the processes leading to neuronal cell loss (Nicotera and Bano, 2003).

CA1 and hilus are the most commonly affected areas in hippocampal sclerosis in animal models as well as in humans: both principal neuron and interneuron degeneration have been described. In the current study I did not investigate for cell type specific cell loss, this was out of scope of the study. However, loss of various type of neurons were suggested by others, and pattern of cell loss varies among species and epilepsy models (Houser, 2014). Although certain patterns of cell loss has been described it is not clear if those cell types are particularly vulnerable or corresponding to overall cell loss (Matthew et al., 2006). Loss of excitatory mossy cells and various interneurons types in hilar region was reported (Schwarcz and Witter, 2002). Although both parvalbumin and somatostatin cell loss has been described in hippocampal sclerosis the loss of somatisation expressing interneurons in hilar and CA1 region is more

prominent and has been most common finding in animal models and human epilepsy. Somatostatin neurons in these regions provide inhibitory innervation of granule cell and pyramidal cell dendrites; they control excitability of the principal cells directly at the sites of their main excitatory inputs and are therefore implicated in epileptogenesis (Houser, 2014).

Hypothesis 2. Cell death by itself or by triggering downstream mechanisms can contribute to the development of epilepsy. Therefore, rescuing hippocampal damage may prevent epileptogenesis. Here I showed that blocking TRPM7 channel by carvacrol reduced the disease severity in the first two weeks following initial damage. Blocking TRPM7 channels inhibited early recurrent SE in the first week and early seizures in the second week. However, blocking TRPM7 channel in the first 24 hour post insult did not prevent the development of late seizures, i.e. chronic epilepsy. I did not analyse short seizures; it could be speculated that with carvacrol treatment seizures could become shorter and those were not included in analysis. However, in such case overall duration of counted seizures would have been shorter in treated animals compared to control group but no significant difference was observed in seizure duration between treated and control groups. This highlights the importance of understanding the relationship between initial neuronal cell damage and epileptogenesis. Many studies that reported neuroprotection in epilepsy failed to show antiepileptogenic effects (Serrano et al., 2011; Acharya et al., 2008; Brandt et al., 2003). Possibly markers other than cell death can be used in the future to reliably predict development of epilepsy after an insult.

Blocking TRPM7 channel in the first 24 hour following SE was sufficient to prevent recurrent status epilepticus and related neuronal cell death. It was reported that cell death in PPS model mainly occurs in the first 1-2 days after initial damage (Gorter et al., 2003). Here I observed recurrent SE the next day following perforant path stimulation that would lead to more extensive cell damage. This could explain the peak of cell death during this time interval in PPS model. The correlation between duration of SE and extent of cell damage

has been shown previously (Norwood et al., 2011). This highlights the importance of stopping SE early to prevent cell damage and related cognitive deficit.

Hypothesis 3. Cell death in the hippocampus is linked to memory impairment in humans as well as in animals (Kalemenev et al., 2015; Lv et al., 2014; Pereira et al., 2010; Chauvière et al., 2009; Pauli et al., 2006; Kelsey et al., 2000). Therefore, I tested if rescuing cell death would prevent memory impairment in animals treated with TRPM7 antagonist, carvacrol. The association between cell damage and memory deficit is well established, in particular spatial memory impairment was linked to cell loss in CA1 area (Sun et al., 2009;Tsien et al., 1996). Here I showed significant preservation of memory function in animals treated with a TRPM7 channel antagonist. This suggests that prevention of cell death in CA1 and hilus rescued memory impairment in these animals.

Although blocking TRPM7 channels did not modify the disease development, i.e. development of recurrent spontaneous seizures, this prevented the development of cognitive comorbidity associated with epilepsy which is a remarkable effect. Cognitive comorbidity is a major challenge in epilepsy that hugely affects patients' quality of life and is not possible to reverse or treat (Fisher et al., 2000; Thompson and Corcoran, 1992). Therefore, development of therapies that can prevent cognitive impairment is crucial.

Activation of inflammatory processes in the brain following injury and excitotoxicity, and presence of inflammation in the brain during the period prior to the development of epilepsy and in chronic epilepsy led to suggestion that inflammation can play a role in the development of epilepsy. Although certain anti-inflammatory compounds demonstrated anti-seizure effect in animal models, the role of such immunosuppressive treatment in the prevention of epileptogenesis is unclear (Vezzani et al., 2013). While anti-inflammatory treatment can have anti-seizure effect in chronic epilepsy, there is a concern

about harmful effect of long term immunosuppression use. TRPM channel subfamily, including TRPM7 channels have been suggested to play a role in inflammatory processes, in innate and adaptive immunity. TRPM7 channels modulate the entry of Ca^{2+} during receptor stimulation and other Ca^{2+}-dependent cellular functions and being one of the main routes for the entry of divalent cations into immune cells can act as immunomodulator (Massullo et al., 2006). Blocking TRPM7 channel could therefore be potent alternative anti-inflammatory target in the treatment of epilepsy.

The main limitation of this study is that carvacrol, a non-specific blocker of TRPM7 channel was used for *in vivo* experiments. Carvacrol was chosen as relatively more specific antagonist of TRPM7 channel that has a simple structure and is a safe compound to use *in vivo.* Waixenicin A which we only could obtain recently and only in small quantities could possibly be a good alternative. Waixenicin A has not been yet tested for *in vivo* use *w*hereas carvacrol has been used extensively for *in vivo* research.

3. Future perspectives

Cell death prevention by blocking TRPM7 channel as well as prevention of cognitive impairment in epilepsy can be transferred in the future into clinical trials. Concurrent use of TRPM7 channel and NMDA receptors blockers can also be tested for better neuroprotection and possibly prevention of the disease development after an insult. Agents to block TRPM7 channel can be tested in the future for use after clinical refractory SE to prevent potential cell damage. Possibly longer treatment period with TRPM7 channel blockers after an insult or even when the disease has developed can decrease the disease severity or provide better seizure control. Third of patients with epilepsy and even higher proportion in TLE do not respond to currently available AEDs, this can offer a new and possibly more effective symptomatic treatment. Blocking TRPM7 channel can offer a novel target that acts through a different mechanism. Here

blocking the channel prevented prolonged seizures as well as neuronal cell loss and hence such target can reduce severity of epilepsy and associated neurodegeneration. Moreover, suggested anti-inflammatory effect of blocking TRPM7 channels could have additional beneficial effect and increase seizure threshold. By acting on multiple pathways such as prevention of inflammation, neuronal cell death and seizure generation targeting TRPM7 channel may offer not only antiseizure effects but also the possibility of disease modification which has not been seen with other AEDs. Moreover, a new target may overcome resistance to drugs that act on other targets (e.g. sodium channels). Perhaps the best approaches will be those that target multiple mechanisms and pathways.

Carvacrol is a food additive and therefore is a safe compound to be tested in clinical research. However, In order to confirm that the effect I have seen here is exclusively due to TRPM7 channel inhibition an shRNA study has to be conducted in a larger animal cohort. On the other hand, whole cell patching can provide better understanding of mechanism of action of carvacrol. Possibly Waxiencin A can further be tested for *in vivo* safety or new compounds specifically targeting TRPM7 channel that can also be developed and tested for *in vivo* use.

Analysing cell death in animals that underwent behavioural experiments could provide useful information in respect to correlation between cell death and cognitive impairment and seizure frequency. This could identify whether there is a correlation between degree of cognitive impairment and cell loss, as well as a correlation between cell death and seizure frequency. Moreover, investigating cell death in animals 3-4 month following induction of SE (i.e. in animals that underwent behavioural experiments) versus 3-4 weeks post SE that was analysed in the current study, could provide information on how cell degeneration changes over time, whether cell number remains the same, increases or decrease. Evidence suggests that in earlier stage cell death can be more prominent, thereafter neurogenesis can take place and lost cells can

be replaced. However, the process of neurogenesis is aberrant in chronic epilepsy and the new cells do not provide adequate function for memory and learning (Scharfman and Gray, 2007).

4. Conclusion

The current study, for the first time, provides valuable information about the role of stress activated TRPM7 channels in epilepsy. Here I showed that inhibiting TRPM7 channel *in vitro* significantly reduced seizure-like activity in two different in vitro seizure models, both that relies on reduced Mg^{2+} concentration to activate TRPM7 channel and the model independent of Mg^{2+} concentrations. First, this indicates that TRPM7 channel are involved in seizure generation. Moreover, opening of TRPM7 channel during seizure activity occurs also independent of reduced Mg^{2+} levels suggesting other mechanisms that occur during seizure activity can also open TRPM7 channels. *In vivo* results suggest that TRPM7 channel activation contributes to seizure induced cell death and cell loss can be prevented by blocking TRPM7 channels. Blocking TRPM7 channel affected early post damage disease severity, recurrent SE and frequency of early seizures were prevented. However, blocking TRPM7 channels *in vivo* did not prevent the development of epilepsy, at least in two month post initial damage monitoring. Nevertheless, preventing cell death and early disease severity was protective against cognitive comorbidity. These results indicate that TRPM7 is a good candidate to study further and be translated into clinical research.

Chapter 8. References

Aarts, M., Iihara, K., Wei, W.-L., Xiong, Z.-G., Arundine, M., Cerwinski, W., MacDonald, J.F., Tymianski, M., 2003. A Key Role for TRPM7 Channels in Anoxic Neuronal Death. Cell 115, 863–877. doi:10.1016/S0092-8674(03)01017-1

Acharya, M.M., Hattiangady, B., Shetty, A.K., 2008. Progress in neuroprotective strategies for preventing epilepsy. Prog. Neurobiol. 84, 363–404. doi:10.1016/j.pneurobio.2007.10.010

Agrawal, N., Govender, S., 2011. Epilepsy and neuropsychiatric comorbidities. Adv. Psychiatr. Treat. 17, 44–53. doi:10.1192/apt.bp.108.006510

Amaral, D.G., Scharfman, H.E., Lavenex, P., 2007. The dentate gyrus: fundamental neuroanatomical organization (dentate gyrus for dummies). Prog. Brain Res. 163, 3–22. doi:10.1016/S0079-6123(07)63001-5

Andersen, P., Bliss, T.V., Skrede, K.K., 1971. Lamellar organization of hippocampal pathways. Exp. Brain Res. 13, 222–238.

Andersen, P., Holmqvist, B., Voorhoeve, P.E., 1966. Entorhinal Activation of Dentate Granule Cells. Acta Physiol. Scand. 66, 448–460. doi:10.1111/j.1748-1716.1966.tb03223.x

Andrews-Zwilling, Y., Gillespie, A.K., Kravitz, A.V., Nelson, A.B., Devidze, N., Lo, I., Yoon, S.Y., Bien-Ly, N., Ring, K., Zwilling, D., Potter, G.B.,

Rubenstein, J.L.R., Kreitzer, A.C., Huang, Y., 2012. Hilar GABAergic interneuron activity controls spatial learning and memory retrieval. PloS One 7, e40555. doi:10.1371/journal.pone.0040555

Astur, R.S., Taylor, L.B., Mamelak, A.N., Philpott, L., Sutherland, R.J., 2002. Humans with hippocampus damage display severe spatial memory impairments in a virtual Morris water task. Behav. Brain Res. 132, 77–84.

Baaij, J.H.F. de, Hoenderop, J.G.J., Bindels, R.J.M., 2015. Magnesium in Man: Implications for Health and Disease. Physiol. Rev. 95, 1–46. doi:10.1152/physrev.00012.2014

Baltan, S., Carmichael, S.T., Matute, C., Xi, G., Zhang, J.H., 2013. White Matter Injury in Stroke and CNS Disease. Springer Science & Business Media.

Barkas, L.J., Henderson, J.L., Hamilton, D.A., Redhead, E.S., Gray, W.P., 2010. Selective temporal resections and spatial memory impairment: cue dependent lateralization effects. Behav. Brain Res. 208, 535–544. doi:10.1016/j.bbr.2009.12.035

Barker-Haliski, M.L., Friedman, D., French, J.A., White, H.S., 2015. Disease modification in epilepsy: from animal models to clinical applications. Drugs 75, 749–767. doi:10.1007/s40265-015-0395-9

Baxendale, S.A., van Paesschen, W., Thompson, P.J., Connelly, A., Duncan, J.S., Harkness, W.F., Shorvon, S.D., 1998. The relationship between quantitative MRI and neuropsychological functioning in temporal lobe epilepsy. Epilepsia 39, 158–166.

Ben-Ari, Y., Dudek, F.E., 2010. Primary and secondary mechanisms of epileptogenesis in the temporal lobe: there is a before and an after.

Epilepsy Curr. Am. Epilepsy Soc. 10, 118–125. doi:10.1111/j.1535-7511.2010.01376.x

Brandt, C., Potschka, H., Löscher, W., Ebert, U., 2003. N-methyl-D-aspartate receptor blockade after status epilepticus protects against limbic brain damage but not against epilepsy in the kainate model of temporal lobe epilepsy. Neuroscience 118, 727–740.

Briellmann, R.S., Newton, M.R., Wellard, R.M., Jackson, G.D., 2001. Hippocampal sclerosis following brief generalized seizures in adulthood. Neurology 57, 315–317. doi:10.1212/WNL.57.2.315

Brito, V.B., Folmer, V., Puntel, G.O., Fachinetto, R., Soares, J.C.M., Zeni, G., Nogueira, C.W., Rocha, J.B.T., 2006. Diphenyl diselenide and 2,3-dimercaptopropanol increase the PTZ-induced chemical seizure and mortality in mice. Brain Res. Bull. 68, 414–418. doi:10.1016/j.brainresbull.2005.09.007

Brophy, G.M., Bell, R., Claassen, J., Alldredge, B., Bleck, T.P., Glauser, T., LaRoche, S.M., Jr, J.J.R., Shutter, L., Sperling, M.R., Treiman, D.M., Vespa, P.M., Committee, N.C.S.S.E.G.W., 2012. Guidelines for the Evaluation and Management of Status Epilepticus. Neurocrit. Care 17, 3–23. doi:10.1007/s12028-012-9695-z

Bumanglag, A.V., Sloviter, R.S., 2008. Minimal latency to hippocampal epileptogenesis and clinical epilepsy after perforant pathway stimulation-induced status epilepticus in awake rats. J. Comp. Neurol. 510, 561–580. doi:10.1002/cne.21801

Burgess, N., Maguire, E.A., O'Keefe, J., 2002. The Human Hippocampus and Spatial and Episodic Memory. Neuron 35, 625–641. doi:10.1016/S0896-6273(02)00830-9

Butler, C.R., Zeman, A.Z., 2008. Recent insights into the impairment of memory in epilepsy: transient epileptic amnesia, accelerated long-term forgetting and remote memory impairment. Brain 131, 2243–2263. doi:10.1093/brain/awn127

Butler, T.R., Self, R.L., Smith, K.J., Sharrett-Field, L.J., Berry, J.N., Littleton, J.M., Pauly, J.R., Mulholland, P.J., Prendergast, M.A., 2010. Selective vulnerability of hippocampal cornu ammonis 1 pyramidal cells to excitotoxic insult is associated with the expression of polyamine-sensitive N-methyl-D-asparate-type glutamate receptors. Neuroscience 165, 525–534. doi:10.1016/j.neuroscience.2009.10.018

Carletti, F., Ferraro, G., Rizzo, V., Cannizzaro, C., Sardo, P., 2013. Antiepileptic effect of dimethyl sulfoxide in a rat model of temporal lobe epilepsy. Neurosci. Lett. doi:10.1016/j.neulet.2013.04.031

Chang, P., Hashemi, K.S., Walker, M.C., 2011. A novel telemetry system for recording EEG in small animals. J. Neurosci. Methods 201, 106–115. doi:10.1016/j.jneumeth.2011.07.018

Chauvière, L., Rafrafi, N., Thinus-Blanc, C., Bartolomei, F., Esclapez, M., Bernard, C., 2009. Early Deficits in Spatial Memory and Theta Rhythm in Experimental Temporal Lobe Epilepsy. J. Neurosci. 29, 5402–5410. doi:10.1523/JNEUROSCI.4699-08.2009

Chen, W., Xu, B., Xiao, A., Liu, L., Fang, X., Liu, R., Turlova, E., Barszczyk, A., Zhong, X., Sun, C.L.F., Britto, L.R.G., Feng, Z.-P., Sun, H.-S., 2015. TRPM7 inhibitor carvacrol protects brain from neonatal hypoxic-ischemic injury. Mol. Brain 8. doi:10.1186/s13041-015-0102-5

Chen, X., Numata, T., Li, M., Mori, Y., Orser, B.A., Jackson, M.F., Xiong, Z.-G., MacDonald, J.F., 2010. The modulation of TRPM7 currents by

nafamostat mesilate depends directly upon extracellular concentrations of divalent cations. Mol. Brain 3, 38. doi:10.1186/1756-6606-3-38

Chokshi, R., Fruasaha, P., Kozak, J.A., 2012. 2-Aminoethyl diphenyl borinate (2-APB) inhibits TRPM7 channels through an intracellular acidification mechanism. Channels 6. doi:10.4161/chan.21628

Chubanov, V., Mederos y Schnitzler, M., Wäring, J., Plank, A., Gudermann, T., 2005. Emerging roles of TRPM6/TRPM7 channel kinase signal transduction complexes. Naunyn. Schmiedebergs Arch. Pharmacol. 371, 334–341. doi:10.1007/s00210-005-1056-4

Clapham, D.E., Runnels, L.W., Strübing, C., 2001. The TRP ion channel family. Nat. Rev. Neurosci. 2, 387–396. doi:10.1038/35077544

Cook, N.L., Van Den Heuvel, C., Vink, R., 2009. Are the transient receptor potential melastatin (TRPM) channels important in magnesium homeostasis following traumatic brain injury? Magnes. Res. Off. Organ Int. Soc. Dev. Res. Magnes. 22, 225–234. doi:10.1684/mrh.2009.0189

Cowan, N., 2008. What are the differences between long-term, short-term, and working memory? Prog. Brain Res. 169, 323–338. doi:10.1016/S0079-6123(07)00020-9

Deacon, R.M.J., Rawlins, J.N.P., 2006. T-maze alternation in the rodent. Nat. Protoc. 1, 7–12. doi:10.1038/nprot.2006.2

Demeuse, P., Penner, R., Fleig, A., 2006. TRPM7 channel is regulated by magnesium nucleotides via its kinase domain. J. Gen. Physiol. 127, 421–434. doi:10.1085/jgp.200509410

Devinsky, O., 2003. Psychiatric comorbidity in patients with epilepsy: implications for diagnosis and treatment. Epilepsy Behav.,

Comorbidities of Epilepsy: Special Topics 4, Supplement 4, 2–10. doi:10.1016/j.yebeh.2003.10.002

Dingledine, R., Varvel, N.H., Dudek, F.E., 2014. When and how do seizures kill neurons, and is cell death relevant to epileptogenesis? Adv. Exp. Med. Biol. 813, 109–122. doi:10.1007/978-94-017-8914-1_9

Dreier, J.P., Heinemann, U., 1991. Regional and time dependent variations of low Mg2+ induced epileptiform activity in rat temporal cortex slices. Exp. Brain Res. Exp. Hirnforsch. Expérimentation Cérébrale 87, 581–596.

Dreier, J.P., Zhang, C.L., Heinemann, U., 1998. Phenytoin, phenobarbital, and midazolam fail to stop status epilepticus-like activity induced by low magnesium in rat entorhinal slices, but can prevent its development. Acta Neurol. Scand. 98, 154–160.

Dudchenko, P.A., 2004. An overview of the tasks used to test working memory in rodents. Neurosci. Biobehav. Rev. 28, 699–709. doi:10.1016/j.neubiorev.2004.09.002

Elizondo, M.R., Arduini, B.L., Paulsen, J., MacDonald, E.L., Sabel, J.L., Henion, P.D., Cornell, R.A., Parichy, D.M., 2005. Defective skeletogenesis with kidney stone formation in dwarf zebrafish mutant for trpm7. Curr. Biol. CB 15, 667–671. doi:10.1016/j.cub.2005.02.050

Elliott, B., Joyce, E., Shorvon, S., 2009. Delusions, illusions and hallucinations in epilepsy: 2. Complex phenomena and psychosis. Epilepsy Res. 85, 172–186. doi:10.1016/j.eplepsyres.2009.03.017

Fisher, R.S., Vickrey, B.G., Gibson, P., Hermann, B., Penovich, P., Scherer, A., Walker, S., 2000. The impact of epilepsy from the patient's perspective I. Descriptions and subjective perceptions. Epilepsy Res. 41, 39–51.

Fleig, A., Penner, R., 2004. The TRPM ion channel subfamily: molecular, biophysical and functional features. Trends Pharmacol. Sci. 25, 633–639. doi:10.1016/j.tips.2004.10.004

Gee, C.E., Benquet, P., Raineteau, O., Rietschin, L., Kirbach, S.W., Gerber, U., 2006. NMDA receptors and the differential ischemic vulnerability of hippocampal neurons. Eur. J. Neurosci. 23, 2595–2603. doi:10.1111/j.1460-9568.2006.04786.x

Gleissner, U., Helmstaedter, C., Elger, C., 1998. Right hippocampal contribution to visual memory: a presurgical and postsurgical study in patients with temporal lobe epilepsy. J. Neurol. Neurosurg. Psychiatry 65, 665–669.

Gorter, J.A., Gonçalves Pereira, P.M., van Vliet, E.A., Aronica, E., Lopes da Silva, F.H., Lucassen, P.J., 2003. Neuronal cell death in a rat model for mesial temporal lobe epilepsy is induced by the initial status epilepticus and not by later repeated spontaneous seizures. Epilepsia 44, 647–658.

Guidelines for Epidemiologic Studies on Epilepsy, 1993. . Epilepsia 34, 592–596. doi:10.1111/j.1528-1157.1993.tb00433.x

Harteneck, C., 2005. Function and pharmacology of TRPM cation channels. Naunyn. Schmiedebergs Arch. Pharmacol. 371, 307–314. doi:10.1007/s00210-005-1034-x

Hermann, B.P., Seidenberg, M., Schoenfeld, J., Davies, K., 1997. Neuropsychological characteristics of the syndrome of mesial temporal lobe epilepsy. Arch. Neurol. 54, 369–376.

Houser, C.R., 2014. Do Structural Changes in GABA Neurons Give Rise to the Epileptic State?, in: Scharfman, H.E., Buckmaster, P.S. (Eds.), Issues

in Clinical Epileptology: A View from the Bench, Advances in Experimental Medicine and Biology. Springer Netherlands, pp. 151–160.

Hu, H.-Z., Gu, Q., Wang, C., Colton, C.K., Tang, J., Kinoshita-Kawada, M., Lee, L.-Y., Wood, J.D., Zhu, M.X., 2004. 2-Aminoethoxydiphenyl Borate Is a Common Activator of TRPV1, TRPV2, and TRPV3. J. Biol. Chem. 279, 35741–35748. doi:10.1074/jbc.M404164200

Inoue, K., Branigan, D., Xiong, Z.-G., 2010. Zinc-induced neurotoxicity mediated by transient receptor potential melastatin 7 channels. J. Biol. Chem. 285, 7430–7439. doi:10.1074/jbc.M109.040485

Jefferys, J.G.R., Jiruska, P., de Curtis, M., Avoli, M., 2012. Limbic Network Synchronization and Temporal Lobe Epilepsy, in: Noebels, J.L., Avoli, M., Rogawski, M.A., Olsen, R.W., Delgado-Escueta, A.V. (Eds.), Jasper's Basic Mechanisms of the Epilepsies. National Center for Biotechnology Information (US), Bethesda (MD).

Jiang, J., Li, M., Yue, L., 2005. Potentiation of TRPM7 inward currents by protons. J. Gen. Physiol. 126, 137–150. doi:10.1085/jgp.200409185

Jiang, X., Newell, E.W., Schlichter, L.C., 2003. Regulation of a TRPM7-like current in rat brain microglia. J. Biol. Chem. 278, 42867–42876. doi:10.1074/jbc.M304487200

Jin, J., Desai, B.N., Navarro, B., Donovan, A., Andrews, N.C., Clapham, D.E., 2008. Deletion of Trpm7 Disrupts Embryonic Development and Thymopoiesis Without Altering Mg2+ Homeostasis. Science 322, 756–760. doi:10.1126/science.1163493

Joca, H.C., Cruz-Mendes, Y., Oliveira-Abreu, K., Maia-Joca, R.P.M., Barbosa, R., Lemos, T.L., Lacerda Beirão, P.S., Leal-Cardoso, J.H., 2012.

Carvacrol decreases neuronal excitability by inhibition of voltage-gated sodium channels. J. Nat. Prod. 75, 1511–1517. doi:10.1021/np300050g

JOHNSON, M., JOHNSON, M., SANDER, J., SANDER, J., 2001. The clinical impact of epilepsy genetics. J. Neurol. Neurosurg. Psychiatry 70, 428–430. doi:10.1136/jnnp.70.4.428

Kaitsuka, T., Katagiri, C., Beesetty, P., Nakamura, K., Hourani, S., Tomizawa, K., Kozak, J.A., Matsushita, M., 2014. Inactivation of TRPM7 kinase activity does not impair its channel function in mice. Sci. Rep. 4. doi:10.1038/srep05718

Kalemenev, S.V., Zubareva, O.E., Frolova, E.V., Sizov, V.V., Lavrentyeva, V.V., Lukomskaya, N.Y., Kim, K.K., Zaitsev, A.V., Magazanik, L.G., 2015. Impairment of exploratory behavior and spatial memory in adolescent rats in lithium-pilocarpine model of temporal lobe epilepsy. Dokl. Biol. Sci. 463, 175–177. doi:10.1134/S0012496615040055

Kelsey, J.E., Sanderson, K.L., Frye, C.A., 2000. Perforant path stimulation in rats produces seizures, loss of hippocampal neurons, and a deficit in spatial mapping which are reduced by prior MK-801. Behav. Brain Res. 107, 59–69.

Kienzler, F., Jedlicka, P., Vuksic, M., Deller, T., Schwarzacher, S.W., 2006. Excitotoxic hippocampal neuron loss following sustained electrical stimulation of the perforant pathway in the mouse. Brain Res. 1085, 195–198. doi:10.1016/j.brainres.2006.02.055

Kovac, S., Domijan, A.-M., Walker, M.C., Abramov, A.Y., 2012. Prolonged seizure activity impairs mitochondrial bioenergetics and induces cell death. J. Cell Sci. 125, 1796–1806. doi:10.1242/jcs.099176

Kow, R.L., Jiang, K., Naydenov, A.V., Le, J.H., Stella, N., Nathanson, N.M., 2014. Modulation of Pilocarpine-Induced Seizures by Cannabinoid Receptor 1. PLoS ONE 9, e95922. doi:10.1371/journal.pone.0095922

Kozak, J.A., Cahalan, M.D., 2003. MIC channels are inhibited by internal divalent cations but not ATP. Biophys. J. 84, 922–927. doi:10.1016/S0006-3495(03)74909-1

Kucherenko, Y.V., Lang, F., 2010. Inhibition of cation channels in human erythrocytes by spermine. J. Membr. Biol. 237, 93–106. doi:10.1007/s00232-010-9310-1

Lencz, T., McCarthy, G., Bronen, R.A., Scott, T.M., Inserni, J.A., Sass, K.J., Novelly, R.A., Kim, J.H., Spencer, D.D., 1992. Quantitative magnetic resonance imaging in temporal lobe epilepsy: relationship to neuropathology and neuropsychological function. Ann. Neurol. 31, 629–637. doi:10.1002/ana.410310610

Lévesque, M., Avoli, M., 2013. The kainic acid model of temporal lobe epilepsy. Neurosci. Biobehav. Rev. 37, 2887–2899. doi:10.1016/j.neubiorev.2013.10.011

Li, M., Jiang, J., Yue, L., 2006. Functional characterization of homo- and heteromeric channel kinases TRPM6 and TRPM7. J. Gen. Physiol. 127, 525–537. doi:10.1085/jgp.200609502

Lipski, J., Park, T.I.H., Li, D., Lee, S.C.W., Trevarton, A.J., Chung, K.K.H., Freestone, P.S., Bai, J.-Z., 2006. Involvement of TRP-like channels in the acute ischemic response of hippocampal CA1 neurons in brain slices. Brain Res. 1077, 187–199. doi:10.1016/j.brainres.2006.01.016

Löscher, W., 2012. Strategies for antiepileptogenesis: Antiepileptic drugs versus novel approaches evaluated in post-status epilepticus models of

temporal lobe epilepsy [WWW Document]. URL http://www.ncbi.nlm.nih.gov/books/NBK98148/ (accessed 1.9.13).

Löscher, W., 2011. Critical review of current animal models of seizures and epilepsy used in the discovery and development of new antiepileptic drugs. Seizure J. Br. Epilepsy Assoc. 20, 359–368. doi:10.1016/j.seizure.2011.01.003

Löscher, W., Brandt, C., 2010. Prevention or Modification of Epileptogenesis after Brain Insults: Experimental Approaches and Translational Research. Pharmacol. Rev. 62, 668–700. doi:10.1124/pr.110.003046

Löscher, W., Hirsch, L.J., Schmidt, D., 2015. The enigma of the latent period in the development of symptomatic acquired epilepsy - Traditional view versus new concepts. Epilepsy Behav. EB 52, 78–92. doi:10.1016/j.yebeh.2015.08.037

Löscher, W., Klitgaard, H., Twyman, R.E., Schmidt, D., 2013. New avenues for anti-epileptic drug discovery and development. Nat. Rev. Drug Discov. 12, 757–776. doi:10.1038/nrd4126

Lv, Z., Huang, D., Ye, W., Chen, Z., Huang, W., Zheng, J., 2014. Alteration of functional connectivity within visuospatial working memory-related brain network in patients with right temporal lobe epilepsy: A resting-state fMRI study. Epilepsy Behav. 35, 64–71. doi:10.1016/j.yebeh.2014.04.001

Manford, M., Hart, Y.M., Sander, J.W., Shorvon, S.D., 1992. The National General Practice Study of Epilepsy. The syndromic classification of the International League Against Epilepsy applied to epilepsy in a general population. Arch. Neurol. 49, 801–808.

Massullo, P., Sumoza-Toledo, A., Bhagat, H., Partida-Sánchez, S., 2006. TRPM channels, calcium and redox sensors during innate immune responses. Semin. Cell Dev. Biol. 17, 654–666. doi:10.1016/j.semcdb.2006.11.006

Matthew, W., Dennis, C., Maria, T., 2006. Hippocampus and Human Disease, in: Andersen, P., Morris, R., Amaral, D., Bliss, T., O'Keefe, J. (Eds.), The Hippocampus Book. Oxford University Press, pp. 769–812.

McNulty, S., Fonfria, E., 2005. The role of TRPM channels in cell death. Pflüg. Arch. Eur. J. Physiol. 451, 235–242. doi:10.1007/s00424-005-1440-4

Menon, B., Ramalingam, K., Kumar, R.V., 2012. Oxidative stress in patients with epilepsy is independent of antiepileptic drugs. Seizure J. Br. Epilepsy Assoc. 21, 780–784. doi:10.1016/j.seizure.2012.09.003

Michiels, J., Missotten, J., Dierick, N., Fremaut, D., Maene, P., De Smet, S., 2008. In vitro degradation and in vivo passage kinetics of carvacrol, thymol, eugenol and trans-cinnamaldehyde along the gastrointestinal tract of piglets. J. Sci. Food Agric. 88, 2371–2381. doi:10.1002/jsfa.3358

Monteilh-Zoller, M.K., Hermosura, M.C., Nadler, M.J.S., Scharenberg, A.M., Penner, R., Fleig, A., 2003. TRPM7 provides an ion channel mechanism for cellular entry of trace metal ions. J. Gen. Physiol. 121, 49–60.

Montell, C., 2005. The TRP superfamily of cation channels. Sci. STKE Signal Transduct. Knowl. Environ. 2005, re3. doi:10.1126/stke.2722005re3

Moser, E.I., Roudi, Y., Witter, M.P., Kentros, C., Bonhoeffer, T., Moser, M.-B., 2014. Grid cells and cortical representation. Nat. Rev. Neurosci. 15, 466–481. doi:10.1038/nrn3766

Mosfeldt Laursen, A., 1984. The contribution of in vitro studies to the understanding of epilepsy. Acta Neurol. Scand. 69, 367–375.

Nadkarni, S., Arnedo, V., Devinsky, O., 2007. Psychosis in epilepsy patients. Epilepsia 48, 17–19. doi:10.1111/j.1528-1167.2007.01394.x

Nadler, M.J., Hermosura, M.C., Inabe, K., Perraud, A.L., Zhu, Q., Stokes, A.J., Kurosaki, T., Kinet, J.P., Penner, R., Scharenberg, A.M., Fleig, A., 2001. LTRPC7 is a Mg.ATP-regulated divalent cation channel required for cell viability. Nature 411, 590–595. doi:10.1038/35079092

Neligan, A., Hauser, W.A., Sander, J.W., 2012. The epidemiology of the epilepsies. Handb. Clin. Neurol. 107, 113–133. doi:10.1016/B978-0-444-52898-8.00006-9

Nicotera, P., Bano, D., 2003. The Enemy at the Gates: Ca2+ Entry through TRPM7 Channels and Anoxic Neuronal Death. Cell 115, 768–770. doi:10.1016/S0092-8674(03)01019-5

Nilius, B., Voets, T., 2005. TRP channels: a TR(I)P through a world of multifunctional cation channels. Pflüg. Arch. Eur. J. Physiol. 451, 1–10. doi:10.1007/s00424-005-1462-y

Norwood, B.A., Bauer, S., Wegner, S., Hamer, H.M., Oertel, W.H., Sloviter, R.S., Rosenow, F., 2011. Electrical stimulation-induced seizures in rats: a “dose-response” study on resultant neurodegeneration. Epilepsia 52, e109–112. doi:10.1111/j.1528-1167.2011.03159.x

Numata, T., Shimizu, T., Okada, Y., 2007. TRPM7 is a stretch- and swelling-activated cation channel involved in volume regulation in human epithelial cells. Am. J. Physiol. Cell Physiol. 292, C460–467. doi:10.1152/ajpcell.00367.2006

Ohmori, T., Hirashima, Y., Kurimoto, M., Endo, S., Takaku, A., 1996. In vitro hypoxia of cortical and hippocampal CA1 neurons: glutamate, nitric oxide, and platelet activating factor participate in the mechanism of selective neural death in CA1 neurons. Brain Res. 743, 109–115. doi:10.1016/S0006-8993(96)01034-7

Ojo, B., Davies, H., Rezaie, P., Gabbott, P., Colyer, F., Kraev, I., Stewart, M.G., 2013. Age-Induced Loss of Mossy Fibre Synapses on CA3 Thorns in the CA3 Stratum Lucidum. Neurosci. J. 2013, 839535. doi:10.1155/2013/839535

O'Keefe, J., Burgess, N., 1996. Geometric determinants of the place fields of hippocampal neurons. Nature 381, 425–428. doi:10.1038/381425a0

Olney, J.W., deGubareff, T., Sloviter, R.S., 1983. "Epileptic" brain damage in rats induced by sustained electrical stimulation of the perforant path. II. Ultrastructural analysis of acute hippocampal pathology. Brain Res. Bull. 10, 699–712.

Ottman, R., Annegers, J.F., Risch, N., Hauser, W.A., Susser, M., 1996. Relations of Genetic and Environmental Factors in the Etiology of Epilepsy. Ann. Neurol. 39, 442–449. doi:10.1002/ana.410390406

Paravicini, T.M., Chubanov, V., Gudermann, T., 2012. TRPM7: A unique channel involved in magnesium homeostasis. Int. J. Biochem. Cell Biol. 44, 1381–1384. doi:10.1016/j.biocel.2012.05.010

Parnas, M., Peters, M., Dadon, D., Lev, S., Vertkin, I., Slutsky, I., Minke, B., 2009. Carvacrol is a novel inhibitor of Drosophila TRPL and mammalian TRPM7 channels. Cell Calcium 45, 300–309. doi:10.1016/j.ceca.2008.11.009

Pauli, E., Hildebrandt, M., Romstöck, J., Stefan, H., Blümcke, I., 2006. Deficient memory acquisition in temporal lobe epilepsy is predicted by hippocampal granule cell loss. Neurology 67, 1383–1389. doi:10.1212/01.wnl.0000239828.36651.73

Pedersen, S.F., Owsianik, G., Nilius, B., 2005. TRP channels: an overview. Cell Calcium 38, 233–252. doi:10.1016/j.ceca.2005.06.028

Peinelt, C., Lis, A., Beck, A., Fleig, A., Penner, R., 2008. 2-Aminoethoxydiphenyl borate directly facilitates and indirectly inhibits STIM1-dependent gating of CRAC channels. J. Physiol. 586, 3061–3073. doi:10.1113/jphysiol.2008.151365

Pereira, F.R.S., Alessio, A., Sercheli, M.S., Pedro, T., Bilevicius, E., Rondina, J.M., Ozelo, H.F.B., Castellano, G., Covolan, R.J.M., Damasceno, B.P., Cendes, F., 2010. Asymmetrical hippocampal connectivity in mesial temporal lobe epilepsy: evidence from resting state fMRI. BMC Neurosci. 11, 66. doi:10.1186/1471-2202-11-66

Pitkänen, A., Lukasiuk, K., 2009. Molecular and cellular basis of epileptogenesis in symptomatic epilepsy. Epilepsy Behav. EB 14 Suppl 1, 16–25. doi:10.1016/j.yebeh.2008.09.023

Pitkänen, A., Nissinen, J., Nairismägi, J., Lukasiuk, K., Gröhn, O.H.J., Miettinen, R., Kauppinen, R., 2002. Progression of neuronal damage after status epilepticus and during spontaneous seizures in a rat model of temporal lobe epilepsy. Prog. Brain Res. 135, 67–83. doi:10.1016/S0079-6123(02)35008-8

Pitkänen, A., Schwartzkroin, P.A., Moshé, S.L., 2005. Models of Seizures and Epilepsy. Academic Press.

Porter, R.J., Dhir, A., Macdonald, R.L., Rogawski, M.A., 2012. Chapter 39 - Mechanisms of action of antiseizure drugs, in: Theodore, H.S. and W.H. (Ed.), Handbook of Clinical Neurology, Epilepsy. Elsevier, pp. 663–681.

Pun, R.Y.K., Rolle, I.J., Lasarge, C.L., Hosford, B.E., Rosen, J.M., Uhl, J.D., Schmeltzer, S.N., Faulkner, C., Bronson, S.L., Murphy, B.L., Richards, D.A., Holland, K.D., Danzer, S.C., 2012. Excessive activation of mTOR in postnatally generated granule cells is sufficient to cause epilepsy. Neuron 75, 1022–1034. doi:10.1016/j.neuron.2012.08.002

Racine, R.J., 1972. Modification of seizure activity by electrical stimulation. II. Motor seizure. Electroencephalogr. Clin. Neurophysiol. 32, 281–294.

Ramaswamy, S., 2015. Exciting times for inhibition: GABAergic synaptic transmission in dentate gyrus interneuron networks. Front. Neural Circuits 9, 13. doi:10.3389/fncir.2015.00013

Ramsey, I.S., Delling, M., Clapham, D.E., 2006. An introduction to TRP channels. Annu. Rev. Physiol. 68, 619–647. doi:10.1146/annurev.physiol.68.040204.100431

Rausch, R., Babb, T.L., 1993. Hippocampal neuron loss and memory scores before and after temporal lobe surgery for epilepsy. Arch. Neurol. 50, 812–817.

Reddy, D.S., Kuruba, R., 2013. Experimental models of status epilepticus and neuronal injury for evaluation of therapeutic interventions. Int. J. Mol. Sci. 14, 18284–18318. doi:10.3390/ijms140918284

Rogawski, M.A., Löscher, W., 2004. The neurobiology of antiepileptic drugs. Nat. Rev. Neurosci. 5, 553–564. doi:10.1038/nrn1430

Rozsa, E., Robotka, H., Nagy, D., Farkas, T., Sas, K., Vecsei, L., Toldi, J., 2008. The pentylenetetrazole-induced activity in the hippocampus can

be inhibited by the conversion of l-kynurenine to kynurenic acid: An in vitro study. Brain Res. Bull. 76, 474–479. doi:10.1016/j.brainresbull.2007.12.001

Rubio, C., Rubio-Osornio, M., Retana-Márquez, S., Verónica Custodio, M.L., Paz, C., 2010. In vivo experimental models of epilepsy. Cent. Nerv. Syst. Agents Med. Chem. 10, 298–309.

Rugg-Gunn, F., Smalls, J. (Eds.), 2013. Epilepsy 2013 from Membranes to Mankind: A Practical Guide to Epilepsy, 14th edition edition. ed. Epilepsy Society.

Runnels, L.W., Yue, L., Clapham, D.E., 2002. The TRPM7 channel is inactivated by PIP(2) hydrolysis. Nat. Cell Biol. 4, 329–336. doi:10.1038/ncb781

Runnels, L.W., Yue, L., Clapham, D.E., 2001. TRP-PLIK, a Bifunctional Protein with Kinase and Ion Channel Activities. Science 291, 1043–1047. doi:10.1126/science.1058519

Savanthrapadian, S., Meyer, T., Elgueta, C., Booker, S.A., Vida, I., Bartos, M., 2014. Synaptic Properties of SOM- and CCK-Expressing Cells in Dentate Gyrus Interneuron Networks. J. Neurosci. 34, 8197–8209. doi:10.1523/JNEUROSCI.5433-13.2014

Scharfman, H.E., Gray, W.P., 2007. Relevance of seizure-induced neurogenesis in animal models of epilepsy to the etiology of temporal lobe epilepsy. Epilepsia 48 Suppl 2, 33–41.

Schmidt, D., Schachter, S.C., 2014. Drug treatment of epilepsy in adults. BMJ 348. doi:10.1136/bmj.g254

Schmitz, C., Deason, F., Perraud, A.-L., 2007. Molecular components of vertebrate Mg2+-homeostasis regulation. Magnes. Res. Off. Organ Int. Soc. Dev. Res. Magnes. 20, 6–18.

Schmitz, C., Perraud, A.-L., Johnson, C.O., Inabe, K., Smith, M.K., Penner, R., Kurosaki, T., Fleig, A., Scharenberg, A.M., 2003. Regulation of Vertebrate Cellular Mg2+ Homeostasis by TRPM7. Cell 114, 191–200. doi:10.1016/S0092-8674(03)00556-7

Schwarcz, R., Witter, M.P., 2002. Memory impairment in temporal lobe epilepsy: the role of entorhinal lesions. Epilepsy Res. 50, 161–177. doi:10.1016/S0920-1211(02)00077-3

Scimemi, A., Schorge, S., Kullmann, D.M., Walker, M.C., 2006. Epileptogenesis is associated with enhanced glutamatergic transmission in the perforant path. J. Neurophysiol. 95, 1213–1220. doi:10.1152/jn.00680.2005

Semah, F., Picot, M.C., Adam, C., Broglin, D., Arzimanoglou, A., Bazin, B., Cavalcanti, D., Baulac, M., 1998. Is the underlying cause of epilepsy a major prognostic factor for recurrence? Neurology 51, 1256–1262.

Serrano, G.E., Lelutiu, N., Rojas, A., Cochi, S., Shaw, R., Makinson, C.D., Wang, D., FitzGerald, G.A., Dingledine, R., 2011. Ablation of cyclooxygenase-2 in forebrain neurons is neuroprotective and dampens brain inflammation after status epilepticus. J. Neurosci. Off. J. Soc. Neurosci. 31, 14850–14860. doi:10.1523/JNEUROSCI.3922-11.2011

Seyfried, T.N., Glaser, G.H., 1985. A Review of Mouse Mutants as Genetic Models of Epilepsy. Epilepsia 26, 143–150. doi:10.1111/j.1528-1157.1985.tb05398.x

Shepherd, G.M. (Ed.), 2004. The Synaptic Organization of the Brain, 5th Edition, 5 edition. ed. Oxford University Press, Oxford ; New York.

Sloviter, R.S., 1983. “Epileptic” brain damage in rats induced by sustained electrical stimulation of the perforant path. I. Acute electrophysiological and light microscopic studies. Brain Res. Bull. 10, 675–697.

Sloviter, R.S., Damiano, B.P., 1981. Sustained electrical stimulation of the perforant path duplicates kainate-induced electrophysiological effects and hippocampal damage in rats. Neurosci. Lett. 24, 279–284.

Sloviter, R.S., Lømo, T., 2012. Updating the lamellar hypothesis of hippocampal organization. Front. Neural Circuits 6, 102. doi:10.3389/fncir.2012.00102

Spiers, H.J., 2012. Hippocampal Formation, in: Ramachandran, V.S. (Ed.), Encyclopedia of Human Behavior (Second Edition). Academic Press, San Diego, pp. 297–304.

Sun, H.-S., Jackson, M.F., Martin, L.J., Jansen, K., Teves, L., Cui, H., Kiyonaka, S., Mori, Y., Jones, M., Forder, J.P., Golde, T.E., Orser, B.A., Macdonald, J.F., Tymianski, M., 2009. Suppression of hippocampal TRPM7 protein prevents delayed neuronal death in brain ischemia. Nat. Neurosci. 12, 1300–1307. doi:10.1038/nn.2395

Swinkels, W.A.M., Kuyk, J., Dyck, R. van, Spinhoven, P., 2005. Psychiatric comorbidity in epilepsy. Epilepsy Behav. 7, 37–50. doi:10.1016/j.yebeh.2005.04.012

Tassi, L., Meroni, A., Deleo, F., Villani, F., Mai, R., Russo, G.L., Colombo, N., Avanzini, G., Falcone, C., Bramerio, M., Citterio, A., Garbelli, R., Spreafico, R., 2009. Temporal lobe epilepsy: neuropathological and clinical correlations in 243 surgically treated patients. Epileptic Disord. Int. Epilepsy J. Videotape 11, 281–292. doi:10.1684/epd.2009.0279

Téllez-Zenteno, J.F., Hernández-Ronquillo, L., Téllez-Zenteno, J.F., Hernández-Ronquillo, L., 2011. A Review of the Epidemiology of Temporal Lobe Epilepsy, A Review of the Epidemiology of Temporal Lobe Epilepsy. Epilepsy Res. Treat. Epilepsy Res. Treat. 2012, 2012, e630853. doi:10.1155/2012/630853, 10.1155/2012/630853

Theodore, W.H., Porter, R.J., 1995. Epilepsy: 100 elementary principles. Saunders.

Thom, M., 2014. Review: Hippocampal sclerosis in epilepsy: a neuropathology review. Neuropathol. Appl. Neurobiol. 40, 520–543. doi:10.1111/nan.12150

Thompson, P.J., Corcoran, R., 1992. Everyday memory failures in people with epilepsy. Epilepsia 33 Suppl 6, S18–20.

Tian, S.-L., Jiang, H., Zeng, Y., Li, L.-L., Shi, J., 2007. NGF-induced reduction of an outward-rectifying TRPM7-like current in rat CA1 hippocampal neurons. Neurosci. Lett. 419, 93–98. doi:10.1016/j.neulet.2007.04.020

Tisserand, R., Young, R., 2013. Essential Oil Safety: A Guide for Health Care Professionals. Elsevier Health Sciences.

Trinka, E., Höfler, J., Zerbs, A., 2012. Causes of status epilepticus. Epilepsia 53, 127–138. doi:10.1111/j.1528-1167.2012.03622.x

Tsien, J.Z., Huerta, P.T., Tonegawa, S., 1996. The Essential Role of Hippocampal CA1 NMDA Receptor–Dependent Synaptic Plasticity in Spatial Memory. Cell 87, 1327–1338. doi:10.1016/S0092-8674(00)81827-9

Ugawa, S., Ishida, Y., Ueda, T., Inoue, K., Nagao, M., Shimada, S., 2007. Nafamostat mesilate reversibly blocks acid-sensing ion channel

currents. Biochem. Biophys. Res. Commun. 363, 203–208. doi:10.1016/j.bbrc.2007.08.133

Vezzani, A., Friedman, A., Dingledine, R.J., 2013. The role of inflammation in epileptogenesis. Neuropharmacology 69, 16–24. doi:10.1016/j.neuropharm.2012.04.004

Vicedomini, J.P., Nadler, J.V., 1987. A model of status epilepticus based on electrical stimulation of hippocampal afferent pathways. Exp. Neurol. 96, 681–691.

Vorhees, C.V., Williams, M.T., 2014. Assessing Spatial Learning and Memory in Rodents. ILAR J. 55, 310–332. doi:10.1093/ilar/ilu013

Walker, M., 2007. Neuroprotection in epilepsy. Epilepsia 48 Suppl 8, 66–68.

Walker, M.C., 2009. Basic physiology of limbic status epilepticus. Epilepsia 50 Suppl 12, 5–6. doi:10.1111/j.1528-1167.2009.02373.x

Walker, M.C., Kovac, S., 2015. Seize the moment that is thine: how should we define seizures? Brain J. Neurol. 138, 1127–1128. doi:10.1093/brain/awv091

Walker, M.C., Perry, H., Scaravilli, F., Patsalos, P.N., Shorvon, S.D., Jefferys, J.G., 1999. Halothane as a neuroprotectant during constant stimulation of the perforant path. Epilepsia 40, 359–364.

Walker, M.C., White, H.S., Sander, J.W.A.S., 2002. Disease modification in partial epilepsy. Brain J. Neurol. 125, 1937–1950.

Worrell, G.A., Sencakova, D., Jack, C.R., Flemming, K.D., Fulgham, J.R., So, E.L., 2002. Rapidly progressive hippocampal atrophy: evidence for a seizure-induced mechanism. Neurology 58, 1553–1556.

Wykes, R.C., Heeroma, J.H., Mantoan, L., Zheng, K., MacDonald, D.C., Deisseroth, K., Hashemi, K.S., Walker, M.C., Schorge, S., Kullmann, D.M., 2012. Optogenetic and potassium channel gene therapy in a rodent model of focal neocortical epilepsy. Sci. Transl. Med. 4, 161ra152. doi:10.1126/scitranslmed.3004190

Wyllie, E., Cascino, G.D., Gidal, B.E., Goodkin, H.P., 2012. Wyllie's Treatment of Epilepsy: Principles and Practice. Lippincott Williams & Wilkins.

Wyllie's Treatment of Epilepsy: Principles and Practice by Elaine Wyllie | eBook on, n.d.

Xiong, Z.Q., Saggau, P., Stringer, J.L., 2000. Activity-dependent intracellular acidification correlates with the duration of seizure activity. J. Neurosci. Off. J. Soc. Neurosci. 20, 1290–1296.

Yamaguchi, S., Rogawski, M.A., 1992. Effects of anticonvulsant drugs on 4-aminopyridine-induced seizures in mice. Epilepsy Res. 11, 9–16.

Yin, J., Kuebler, W.M., 2010. Mechanotransduction by TRP channels: general concepts and specific role in the vasculature. Cell Biochem. Biophys. 56, 1–18. doi:10.1007/s12013-009-9067-2

Yu, H., Zhang, Z.-L., Chen, J., Pei, A., Hua, F., Qian, X., He, J., Liu, C.-F., Xu, X., 2012. Carvacrol, a food-additive, provides neuroprotection on focal cerebral ischemia/reperfusion injury in mice. PloS One 7, e33584. doi:10.1371/journal.pone.0033584

Zierler, S., Yao, G., Zhang, Z., Kuo, W.C., Pörzgen, P., Penner, R., Horgen, F.D., Fleig, A., 2011. Waixenicin A inhibits cell proliferation through magnesium-dependent block of transient receptor potential melastatin 7 (TRPM7) channels. J. Biol. Chem. 286, 39328–39335. doi:10.1074/jbc.M111.264341

Chapter 8. References